ADSORPTION OF Cs ON THE FRACTURE FILLING CLAY MINERALS OF THE LAC DU BONNET BATHOLITH, SOUTHEASTERN MANITOBA: IMPLICATIONS FOR NUCLEAR FUEL WASTE DISPOSAL

BY

REGINALD BELUOLISA EJECKAM

A Thesis
Submitted to the Faculty of Graduate Studies
In Partial Fulfillment of the Requirements for a Degree of

MASTER OF SCIENCE

Department of Geological Sciences
University of Manitoba
Winnipeg, Manitoba

2003

THE UNIVERSITY OF MANITOBA

FACULTY OF GRADUATE STUDIES

*****

COPYRIGHT PERMISSION PAGE

ADSORPTION OF Cs ON THE FRACTURE FILLING CLAY MINERALS OF THE LAC DU BONNET BATHOLITH, SOUTHEASTERN MANITOBA: IMPLICATIONS FOR NUCLEAR FUEL WASTE DISPOSAL

BY

REGINALD BELUOLISA EJECKAM

A Thesis/Practicum submitted to the Faculty of Graduate Studies of The University of Manitoba in partial fulfillment of the requirements of the degree of

Master of Science

ABSTRACT

A deep geological repository in stable plutonic rock is one of the approaches being considered for the long-term management of used nuclear fuel in Canada. This study examines the interaction of cesium, which contains ^{135}Cs, a long-lived radionuclide that is a component of nuclear waste, and adsorption of Cs onto a variety of clay minerals representing the materials that are likely to be used as engineered barriers in such a repository. Clay minerals are also likely to be associated with fracture zones in the crystalline rock hosting the repository. The Lac du Bonnet batholith in southeastern Manitoba is representative of plutonic rocks of the Canadian Shield. The batholith is sparsely fractured and of a large areal extent. The effect of a bacterial consortium from the Lac du Bonnet batholith on Cs adsorption was also evaluated.

Ion exchange experiments indicate that clay minerals adsorb cesium rapidly at various conditions of temperature and pressure. At room temperature and pressure, montmorillonite, a 2:1 layer clay mineral, adsorbed more Cs than all the other clay minerals. Vermiculite and illite, though 2:1 layer clay minerals, adsorbed much less Cs than montmorillonite. Bentonite (Wyoming bentonite and Kunigel bentonite), a multimineralic clay, adsorbed more Cs than vermiculite and illite but less than montmorillonite. Kaolinite, a 1:1 layer clay mineral, adsorbed very small amounts of Cs. Generally, 2:1 layer clays adsorbed more Cs than 1:1 layer clay because they have more available sites for Cs adsorption.

Under higher temperature and pressure, montmorillonite adsorbed more Cs than at room temperature and pressure. In the presence of a bacteria consortium montmorillonite adsorbed even more Cs while the bacteria on its own adsorbed 0.07 wt% of cesium. Elevated temperature and pressure affects environment for adsorbed Cs in clay but does not appear to affect the total amount of Cs adsorbed.

^{133}Cs MAS NMR spectral analysis indicates that Cs^+ is adsorbed on CS1 and CS2 sites of montmorillonite at the basal oxygen in the interlayer in two stages. The first stage is the rapid uptake of Cs in the outer sphere, which reaches capacity and remained same for the rest of adsorption time, and the second stage is the continued slower process, as Cs penetrates into the inner sphere of the interlayer. The Cs^+ at both CS1 and CS2 sites are affected by relative humidity.

The peaks in ^{29}Si MAS NMR spectra of clay minerals become more shielded with adsorption of Cs. The peaks in vermiculite are assigned to Q^3(2AL), Q^3(1AL) and Q^3(0AL), respectively. The systematic shift in the peak positions of ^{29}Si in montmorillonite at higher temperature and pressure as well as in kaolinite are assigned to Q^3(0Al).

ACKNOWLEDGMENTS

I wish to thank my supervisor, Dr. Barbara L. Sherriff, for her patience, guidance and for the numerous discussions that led to the completion of this thesis. I also would like to thank many others in the Department of Geological Sciences, University of Manitoba, including Greg Morden for analyses of the clay minerals for their chemistry and for the determination of cesium concentrations after ion exchange, and Neil Ball for his help in operating the X-ray difractometer. Also I extend my gratitude to Dr. Bill Last for the use of his laboratory to separate the clay minerals, and to Dr. Anne Brown for allowing me to use the bacterial culture that she grew in the laboratory and for providing instructions on the handling of bacterial cultures. To Terry Wolowiec (Department of Chemistry) for his tremendous help with running the NMR Instrument, and to Dr. Kirk Marat also in Department of Chemistry, University of Manitoba for allowing me to use Spinworks, a program he wrote to process NMR data.

I also express my gratitude to the following people at AECL, Whiteshell Laboratories, Pinawa, Manitoba: Dr. Anton Brown (retired) and Dr. Keith Nuttall for their encouragement and understanding. To Dr. Jude McMurry and Dr. Mel Gascoyne for their critical review and suggestions to improve this thesis, to Ms. Maureen Macdonald and Ms. Heather Worona for typing this thesis and to Ms. Janice Hawkins for her help with the graphics and most of all, to the late Dr. D. Choudary Kamineni, my mentor, who was like a big brother. Choudary passed away January 22 1993. "I know you would have been pleased".

A special appreciation goes to my wife, Chi Ejeckam and children, Chidozie (Big Bud), Chinedum (Bud Light) and Chukwuka (Little Bud) for their unconditional love, support, patience and understanding throughout the program, also for forgiving me for all the soccer and basketball games that I missed.

This research was funded by a National Science and Engineering Research Council (NSERC) research grant to Dr. Barbara L. Sherriff.

TABLE OF CONTENTS

Continued...

TABLE OF CONTENTS

Continued...

TABLE OF CONTENTS

LIST OF FIGURES

Pages

Continued...

LIST OF FIGURES

Pages

Continued...

LIST OF FIGURES

Pages

Continued...

LIST OF FIGURES

Pages

Continued...

LIST OF FIGURES

Pages

LIST OF TABLES

Continued...

LIST OF TABLES

Pages

LIST OF ABBREVIATIONS

AA	Atomic Absorption Spectroscopy
AC	Ammonium Citrate
AECL	Atomic Energy of Canada Limited
CEC	Cation Exchange Capacity
CMS	Clay Mineral Society
RT & P	Room Temperature and Pressure
CNFWMP	Canadian Nuclear Fuel Waste Management Program
EIS	Environmental Impact Statement
ICDD	International Centre for Diffraction Data
ICP	Inductively Coupled Plasma
LDB	Lac du Bonnet Batholith
MAS	Magic Angle Spinning
MIC	Microbial Induced Corrosion
NMR	Nuclear Magnetic Resonance
OES	Optical Emission Spectrometry
PDF	Powder Diffraction File
Q	Quadruple Moment
SEM	Scanning Electron Microscopy
TMS	Tetramethyl Silane
URL	Underground Research Laboratory
WRA	Whiteshell Research Area
XRD	X-Ray Diffraction

CHAPTER 1 INTRODUCTION

1.1 Purpose and Scope

The purpose of this study was to investigate the adsorption of cesium (Cs) onto a variety of clay minerals under ambient conditions, at elevated temperatures and pressure, and in the presence of a bacterial consortium. The sorption characteristics are studied by a number of ion exchange experiments involving cesium and clay minerals. Nuclear magnetic resonance spectroscopy (NMR) was used to observe the structure and the chemical environments of the sites at which the Cs^+ ions were adsorbed onto the clay mineral. The experiments were designed to provide information relevant to the migration of radioactive cesium through the clay-based sealant materials of a deep geological repository for used nuclear fuel waste, and through clay-filled fractures in crystalline rock that would be associated with such a repository. It was also designed to separate the biological effect of the active bacteria from any effect caused by the chemical effect of the ammonium citrate (AC) medium on the physical adsorption on the surface of the bacteria, as well as to determine the amount of cesium that would be adsorbed by clay minerals in the presence of active bacterial culture. This would indicate the effect of the bacterial culture on adsorption of Cs^+ by clay minerals.

This study is important to the deep geologic repository and long-term storage of radioactive waste because clay minerals are an important component of the buffer and backfill material in the design of the repository. Clay minerals also are always present in soils and are alteration products of many rock types.

Clay minerals have small sized particles, therefore they have large surface areas, and because of that, they have important surface chemical activities in the soil. Clay minerals can adsorb large amounts of cations in their interlayer due to negative charges resulting from substitutions. This study also provides information about the interaction of cesium cations with clay minerals, as Cs^+ is one of the components of nuclear waste material.

1.2 Deep Geologic Repositories and the Long-Term Management of Radioactive Waste

Approximately 15 percent of all electricity produced in Canada over the last fifty years has been generated by CANDU nuclear power reactors with almost half of the electricity in Ontario currently being produced by nuclear energy. CANDU reactors also operate in Quebec and New Brunswick. The by-products of the generation of electricity by nuclear power include a number of different radioactive elements, including cesium, that are produced either by nuclear fission inside the uranium oxide (UO_2) fuel pellets or by neutron activation of metals and impurities in the fuel assembly. Most radioactive isotopes of cesium have short half-lives and decay rapidly. Within 10 years after removal from a reactor, cesium represents less than 1 percent of the radioactive waste products in CANDU fuel (Johnson et al. 1994), which contains long-lived radionuclides of many other elements such as americium, plutonium, neptunium, thorium, strontium, technetium, cadmium, iodine, carbon, and chlorine (Tait et al. 1989, Stroes-Gascoyne et al. 1992). However, cesium is an element of concern

for long-term safety in radioactive waste management because ^{135}Cs, which is produced by the fission of ^{235}U, has a long half-life of 2.3 million years. Cesium is chemically similar to the more common elements sodium and potassium. It is relatively mobile in water (Comans et al. 1991, Maiti et al. 1989) and is easily adsorbed by plants.

When the used nuclear fuel comes out of the reactor, it is highly radioactive because it has many very short-lived emitters of gamma radiation. Within one hour of being removed from the reactor, however, the used fuel has lost more than 60 percent of its radioactive energy. The used fuel is stored at the reactor sites in water-filled pools for at least ten years. This provides a protective shielding and facilitates cooling while additional radioactive elements decay. After this time, the used fuel is transferred to reinforced concrete dry storage containers, in a waste management area at the reactor sites, where it remains shielded and can be monitored and kept secure indefinitely. After approximately 500 years, the gamma-emitting radionuclides will have decayed sufficiently that a person could enter a room containing an unshielded fuel bundle without hazard. However, some of the longer-lived alpha and beta emitters, such as ^{135}Cs, and also gamma emitters with long half-lives could be hazardous if ingested or inhaled. Therefore, it is necessary to isolate the used nuclear fuel from humans and from the environment for tens of thousands of years.

A deep geological repository is being considered for the long-term management of used nuclear fuel in Canada (AECL 1994). Research related to

this concept was formally initiated by the Federal Government and the Government of Ontario in 1978, at which time responsibility for "disposal in a deep underground repository in intrusive igneous rock" was assigned to Atomic Energy of Canada Limited (AECL). The concept has undergone continuous research and development since that time, as have similar programs for deep geologic repositories in granitic rock in other countries such as Sweden, Finland, and Japan. As the concept currently exists in Canada, used nuclear fuel would be sealed in durable thick-walled metal containers and placed in an engineered repository that would be constructed deep (nominally 500 to 1000m) in stable plutonic rock somewhere on the Canadian Shield (Davison et al. 1994a, b).

The layout of the repository would be a network of tunnels and emplacement rooms designed to accommodate the rock structure and stresses, the groundwater flow system, faults, and other subsurface conditions such as salinity and redox conditions at the site (Simmons and Baumgartner 1994). Clay and other natural materials would be used to enclose the containers of waste in order to slow the movement of groundwater, buffer the groundwater chemistry, and fill the remaining open spaces in the rooms when the repository is closed. If a defect in the containers eventually allowed water to contact the used fuel, some of the contaminants in the used fuel would be transported out of the containers and into the repository. An advantage of using clay minerals in the repository is that certain elements adsorb readily onto the surfaces of the clay minerals, which would impede the transport of these elements.

Figure 1 shows an example of one possible design for a deep geologic repository, in which the metal containers of used fuel would be emplaced individually in boreholes in the floor of an emplacement room. Each container would be surrounded by a compacted buffer mixture of bentonite and sand.

The emplacement rooms would be filled by a combination of lower and upper backfill (Figure 1). The lower backfill is a compacted mixture of crushed granite (from excavation of the repository), glacial clay, and some bentonite. The upper backfill is a mixture of bentonite and sand that would be emplaced pneumatically in the part of the rooms where it is impractical to compact the buffer material. Another design involves the placement of containers inside a form made of pre-compacted blocks of bentonite-based buffer material within emplacement rooms. Dense backfill would be added around the containers. The exact specifications, proportions, and components of the buffer and backfill materials in an actual repository will depend on the site-specific design requirements. It is very likely, however, on the basis of Canadian case studies and repository engineering concepts in other countries, that any design selected will include bentonite as an important repository component. Bentonite is a naturally occurring, soft sedimentary rock composed primarily of montmorillonite, a smectite clay mineral that has exceptional hydrophilic affinities and swelling properties. The low permeability and swelling capacity of saturated bentonite would slow groundwater movement near the waste container and would limit the

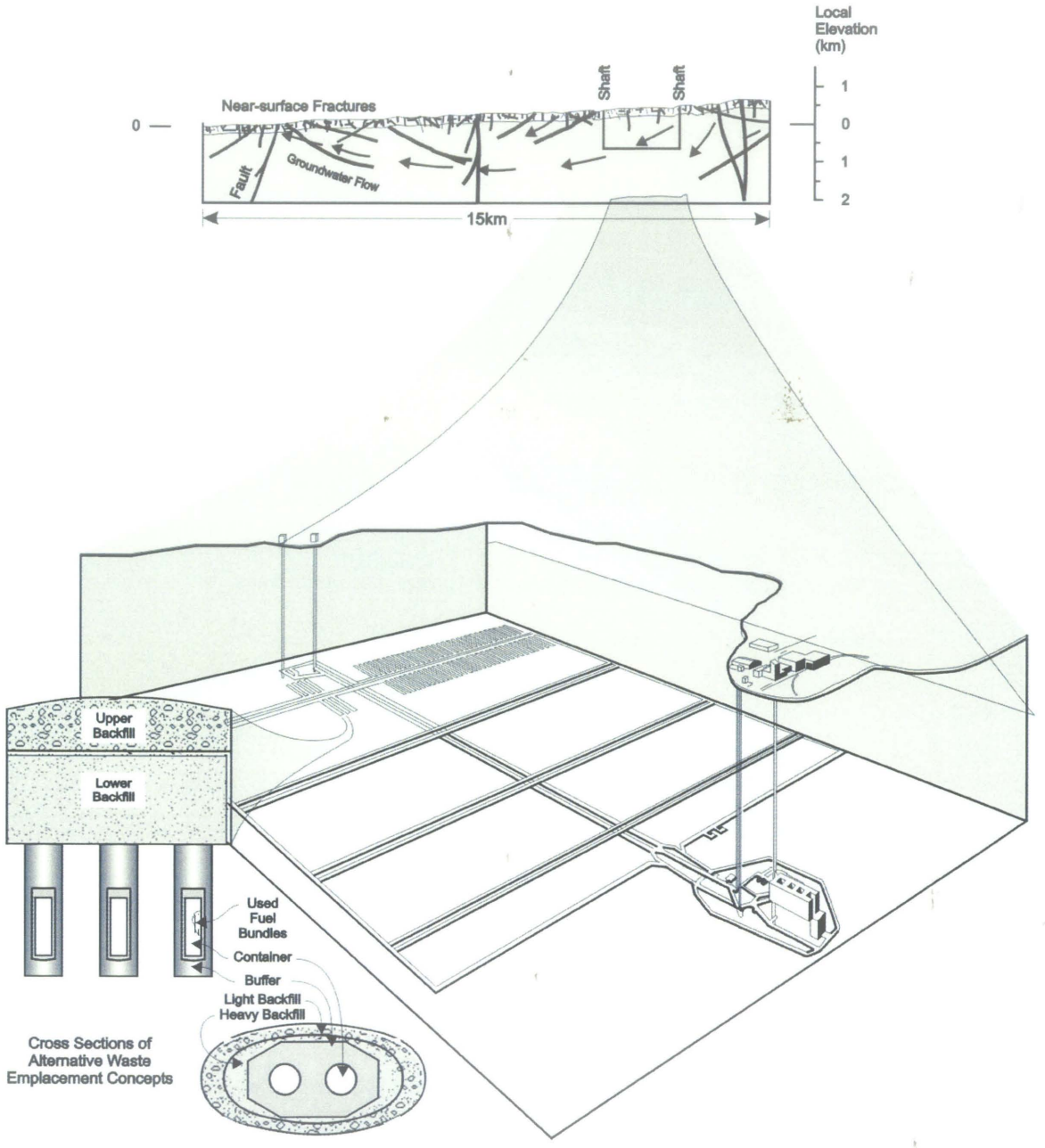

Figure 1: Design for a deep geologic repository in which containers of used fuel are emplaced in boreholes drilled in the floor of the emplacement room after which the boreholes and the rooms are sealed with backfill materials (from Davison et al. 1994a).

migration of radionuclides from the container by diffusion. The buffer would also adsorb the contaminants and maintain stable groundwater chemistry through ion exchange.

To a lesser extent, sorption by other clay minerals such as illite, vermiculite and kaolinite in fractures around the repository also will limit the migration of radionuclides. Locally available clay, such as sediment from a glacial deposit will probably be used for a repository as a component of the crushed granite and clay backfill. The sediment is likely to have some smectitic (swelling) clay, but will almost certainly have a high proportion of clay minerals such as illite, vermiculite or kaolinite. The addition of clay minerals such as illite in a Ca-Na ion exchange water treatment process for low-level radioactive waste has been determined to be effective in the reduction of aqueous radioactive cesium (Tamura and Jacobs 1960).

The components and proportions for the buffer and backfill materials in one possible repository design are listed in Table 1 with their density and hydraulic conductivity. Table 2 shows the predominant minerals in two kinds of bentonite and an illite-bearing shale proposed for use in repository. Wyoming bentonite is a commercially widely used bentonite that is mined in the western U.S.A. Kunigel bentonite is being considered as a clay-based buffer component for a deep geological repository in Japan, where it is locally mined. There is a high proportion of montmorillonite in these bentonite deposits. Sealbond illite is from the Dundas Shale Member of the Georgian Bay Formation in southern Ontario (Quigley 1984). It is a representative example of an illite-bearing shale from the Canadian Shield.

Table 1: Compacted Buffer and backfill characteristics for the disposal vault (from Davison et al. 1994a)

Vault Seal	Composition	Dry Density (Mg/m^3)	Hydraulic Conductivity (m/s)
Buffer	A mixture of 50% by weight sodium bentonite clay and 50% by weight silica sand	1.66	$<10^{-12}$
Lower Backfill	A mixture of 25% by weight glacial lake clay and 75% by weight crushed granite from the vault excavation	2.1	$<10^{-10}$
Upper Backfill	A mixture of 50% by weight sodium bentonite clay and 50% by weight silica sand	1.4	$<10^{-10}$

Table 2: Minerals in selected clay-rich rocks proposed for buffer materials (after Quigly 1984,Dixon 1994)

Wyoming MX-80 Bentonite	Kunigel VI Bentonite	Sealbond Illite
Montmorillonite (~90%)	Montmorillonite (~48%)	Illite (~40%)
Chlorite	Quartz	Quartz
Illite	Feldspar	Chlorite
Quartz	Carbonates	Vermiculite
Feldspar		Carbonates

Radionuclides that breach the engineered barriers and reach the edge of the repository may be transported in groundwater through fractures in the rock that hosts the repository and eventually to the surface environment. Therefore, the interactions of radionuclides with the minerals that occur in fractures have been studied.

In the late 1970s, AECL began field investigations in five research areas in the Canadian Shield to assess the concept of nuclear waste disposal in plutonic rocks. The objectives of the field investigations were to develop the methodology and instrumentation for screening and characterizing sites and to understand the field parameters that control fluid flow, mass transport, and geochemical response in plutonic rock. The most intensely studied of these five research areas was the Whiteshell Research Area (WRA) in southeastern Manitoba, which includes a large portion of the Lac du Bonnet batholith. Surface and airborne mapping of the Lac du Bonnet batholith were complemented by a major drilling program of more than 130 boreholes, most of them cored, to depths of up to 1100m to obtain a better understanding of the geology of the intrusion, and to develop and test a conceptual model of the groundwater flow system. Valuable detailed information about subsurface characteristics has been obtained from the detailed mapping (Everitt and Brown 1995) of the Underground Research Laboratory (URL), which was constructed by AECL in the 1980s to a depth of 443m below the surface to conduct in situ experiments in granitic rock (Everitt et al. 1998, Kozak et al. 1997). As a result, the subsurface

characteristics of the Lac du Bonnet batholith are among the best studied and documented of any granitic intrusion in Canada.

For the purposes of this study, it is assumed that the petrology and hydrogeology of the Lac du Bonnet batholith is representative of the types of properties in the Canadian Shield that would correspond to the location of an actual repository. Also, the bacteria that were used in these experiments were sampled from water-bearing fractures in the Lac du Bonnet batholith. Although no specific location has been selected for a deep geologic repository in Canada, the geological properties of the crystalline rock in which it is constructed are expected to be within the range of variation of numerous plutonic intrusions in the Canadian Shield. Therefore, the geology of the Lac du Bonnet batholith is described in detail in the following section.

1.3 Geology of the Lac du Bonnet Batholith

The granitic Lac du Bonnet batholith, located about 100 km NE of Winnipeg (Figure 2), is situated on the western margin of the Superior litho-tectonic province along the contact between the Bird River and Winnipeg River subprovinces. The batholith, intruded near the end of the 2760-2670 Ma Kenoran Orogeny (Davis et al. 1986) is one of the youngest plutons in the area. The age of the batholith has been determined as 2665 ± 20 Ma by U- Pb zircon method (Krogh et al. 1976, Davis et al. 1986), and as 2568 ± 23 Ma by whole Rb-Sr isochron method (Kamineni et al. 1990). It is tabular in shape, measuring about 70 x 20 x 10 km. The main phase of the batholith is porphyritic biotite

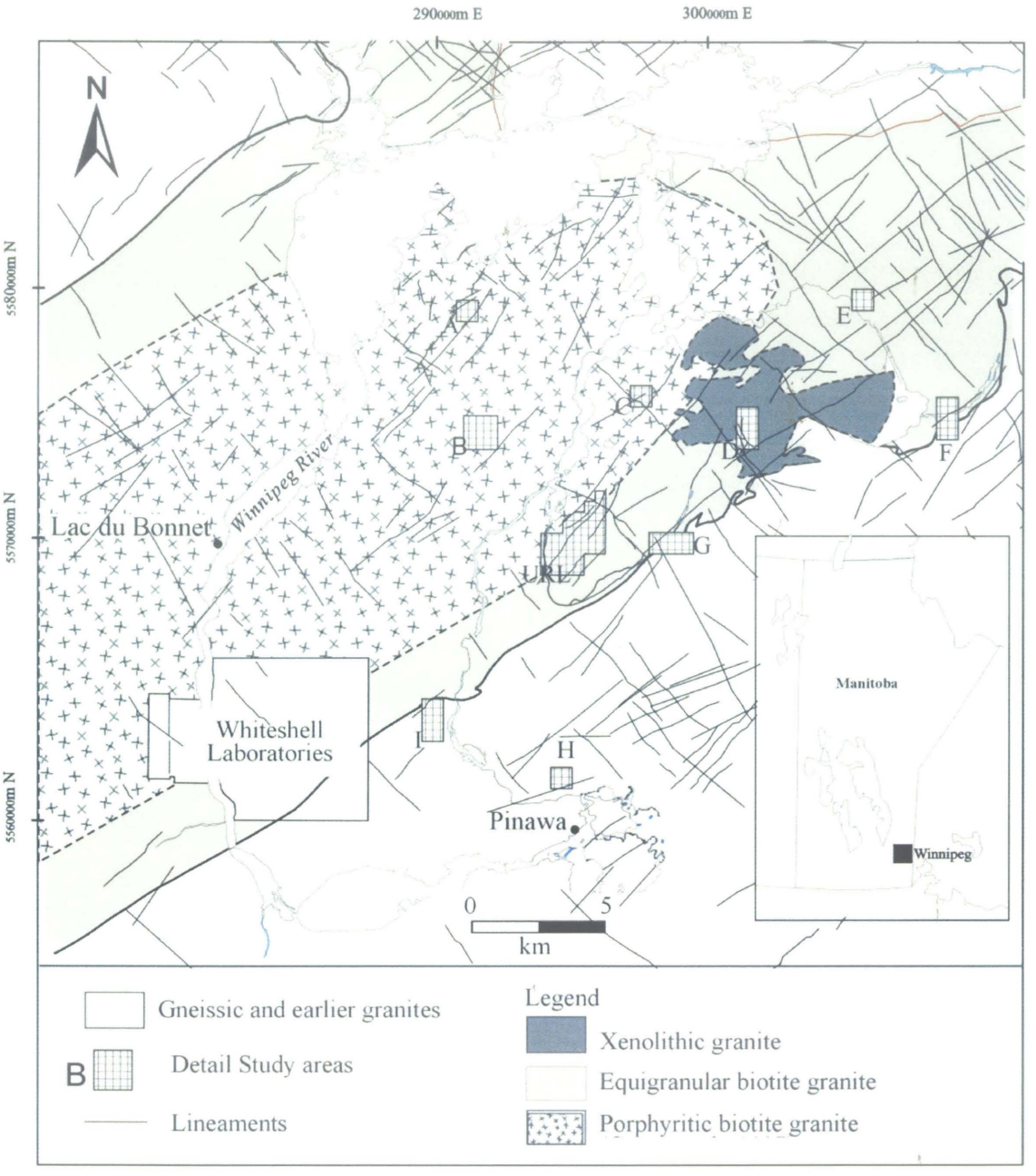

Figure 2: Geology of the Lac du Bonnet batholith, showing the different rock units, and the lineaments identified in the batholith. It also shows the location of the URL, and detailed study areas where some of the boreholes were drilled (after Everitt et al. 1998).

granite to granodiorite with a smaller phase of equigranular granite to quartz-monzonite. Xenolithic granite, interpreted to be the remnants of incompletely assimilated country rock, is present in the northeastern part of the batholith. The northern boundary of the Lac du Bonnet batholith is a sharp contact against the metavolcanic Bird River greenstone, and the southern boundary is gradational against the gneisses of the Winnipeg River Subprovince (Stone et al. 1984, Kamineni et al. 1990, Everitt et al. 1998, Ejeckam et al. 1990).

Figure 2 shows the major rock units of the Lac du Bonnet batholith, as well as the major lineaments that have been identified as faults either by surface mapping or geophysical methods (Stone et al. 1984, Kamineni et al. 1990, Brown et al. 1989, Everitt et al. 1998, Ejeckam et al. 1990). Figure 2 also shows the location of detailed study areas (A, B, C, etc.), where most of the cored boreholes were drilled from surface to study the batholith, and the location of the URL. A hydrogeological model for groundwater movement in the vicinity of the URL were developed from studies of fractures by geophysical surveys, data from the borehole and core logging, data acquired during the excavation of the URL shaft, and data from additional boreholes drilled into the batholith from depth inside the URL. There are two main water-bearing fracture types (Figure 3): a set of major low-dipping fractures that are part of ancient thrust fault zone, which can be traced from surface to depths of at least 300m, and a set of smaller near-vertical fractures that are abundant only in the upper 200m of the

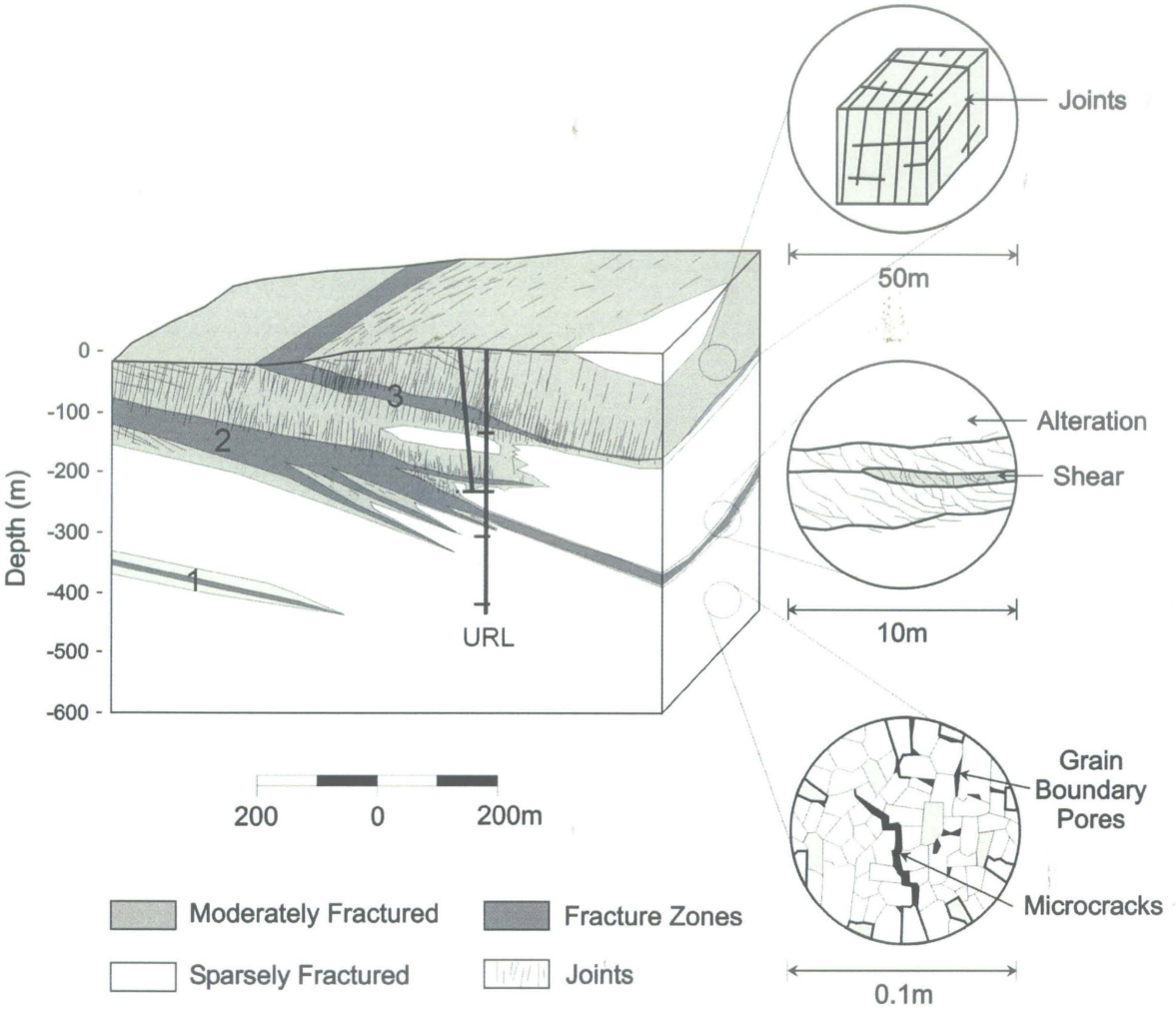

Figure 3: A block diagram showing the interpreted view of the three main fracture domains at the Underground Research Laboratory (URL), (from Davison et al. 1994a).

batholith (Brown et al. 1989, Davison et al. 1994a, Everitt et al. 1998). Few of the near-vertical fractures extend below their contact with the large, low-dipping fracture zones. The numerous minor near-surface fractures act as pathways for groundwater recharge, and discharge occurs along the large, low-dipping fracture zones. Three reverse faults (Fracture Zone (FZ) 1, 2, and 3, Figure 3) were encountered by drilling in the vicinity of the URL. These faults are important in controlling groundwater flow in the area. The upper 200-300m of the batholith is pink granite, within which most of the near-vertical fractures occur. The grey granite below 300m contains relatively few fractures of any kind and is referred to as sparsely fractured rock. Permeability and porosities in sparsely fractured granitic rock are extremely low, providing an additional barrier for the migration of radionuclides from depths of 500 to 1000m.

Water movement along the fracture system is the only credible method by which radioactive contaminants would be able to travel from the repository to the surface environment. The migration of contaminants in a fracture system would be controlled by hydrogeological parameters such as flow conditions, porosity, and permeability, and also by groundwater chemistry and by reactions with minerals encountered along the flow path including the secondary minerals that occur as coating on many fracture surfaces (Gascoyne and Cramer 1987, Gascoyne and Kamineni 1990, Ejeckam et al. 1990, Gascoyne et al. 1997). In the Lac du Bonnet batholith, fracture-lining minerals that have a high sorptive capacity include a variety of clay minerals and hematite (Figures 4 and 5). Other common fracture-lining minerals include calcite, chlorite, and primary minerals from the granite that are exposed on the fracture surfaces (Table 3).

Figure 4: Typical clay mineral infilling that coats the fracture surfaces encountered in Borehole URL6 in the URL. The infillings coating the sample have been identified as clay (yellowish) and hematite (red).

Figure 5: Typical example of hematite coating fracture surface in the Lac du Bonnet batholith. (Borehole WD-3).

Table 3: Modal volume % of fracture filling minerals in different fractures and depth intervals in boreholes drilled in the Lac du Bonnet batholith (from Gascoyne and Kamineni 1990)

	Volume %		
Mineral	**A**	**B**	**C**
Chlorite	12	14	25
Muscovite/Sericite	2	3	-
Illite	21	19	2
Iron Oxide	20	15	30
Calcite	5	3	30
Biotite	5	5	-
Plagioclase	8	11	5
Microcline	12	15	3
Quartz	15	15	5

A - low dip fracture zone (0-150m)

B - low dip fracture zone (150-500m)

C - subvertical fractures (0-150m)

Clay minerals are among the most abundant fracture lining minerals in open (water-bearing) fractures of the Lac du Bonnet granite (Kamineni 1992, McMurry and Ejeckam 2002). Preferential adsorption on negatively charged clay minerals has been demonstrated to retard the movements of radionuclides (Kim et al. 1996a, Oscarson et al. 1994, Ticknor et al. 1989 1991, Kamineni et al. 1986). X-ray diffraction studies of the clay minerals lining fractures in the Lac du Bonnet batholith have identified illite as the most abundant clay mineral, although kaolinite and vermiculite also have been noted (Griffault et al. 1992, Gascoyne and Kamineni 1990, McMurry and Ejeckam 2002).

Movement along the major fracture zones in the batholith has caused the rock in these zones to be brecciated and hydrothermally altered (Figure 6). As the major fracture zones are the main pathways for water movement in the batholith, the rubble in these zones is exposed to large volumes of water, causing the rock to become severely altered and friable (Figure 7) and capable of adsorbing contaminants from groundwater. In this study, three samples of altered rubble were analyzed by X-ray diffraction to identify the clay mineral present in the rubbles zones.

In the Lac du Bonnet batholith, near surface conditions are oxidizing because of abundance of oxygen, however, the condition changes to reducing as oxygen is depleted. Dissolved oxygen in meteoric water is removed by reacting with surficial organic matter in the system. In places, oxygen penetrates only a few metres into the subsurface. Within the depths where dissolved oxygen is present, the chemical environment is oxidizing, however,

Figure 6: Core from a fracture zone intersected in Borehole URL-4 at ~64.5m below the surface. The first two rows of core show discrete fractures in the core (sparsely fractured rock) whereas the bottom two rows show intensely fractured and highly altered core (rubble) in the main part of the fracture zone.

Figure 7: Example of friable, clay-bearing rubble from highly altered granite core sample from Borehole URL-7.

concentrations of dissolved oxygen diminishes to below detection limits in most groundwaters below 100m. Along fracture zones the depth of oxygen penetration is deeper, but continued reaction with organics and fracture filling minerals along the path, further lowers the redox potential such that most deep groundwaters in the Canadian Shield greater than 400m are reducing (McMurry and Ejeckam 2002, Gascoyne 2001). The groundwater of the Lac du Bonnet batholith, like that of many other localities on the Canadian Shield, generally becomes more saline with depth (Gascoyne 2000). Interactions with clay-rich overburden at the surface in the Lac du Bonnet batholith cause high concentrations of bicarbonate and sulfate in some shallow waters, but usually the shallow bedrock groundwaters have a fairly low concentration of total dissolved solids (TDS). Concentrations of TDS increases with depth, with Ca, Na, and Cl being the most abundant elements in the saline water (Figure 8), such that waters in fracture zones below about 400m are reducing and have TDS > 10 g/L. The saline, Ca-Na-Cl groundwater is representative of the composition of groundwater that is likely to be in contact with the buffer and backfill materials of a deep geologic repository in granitic rock in the Canadian Shield. Groundwaters that seep into open boreholes at depth that are not part of a fracture system are extremely saline (TDS > 90 g/L) and are thought to be derived from brine-filled fluid inclusions and intergranular pore spaces in the sparsely-fractured rock (Gascoyne 2000).

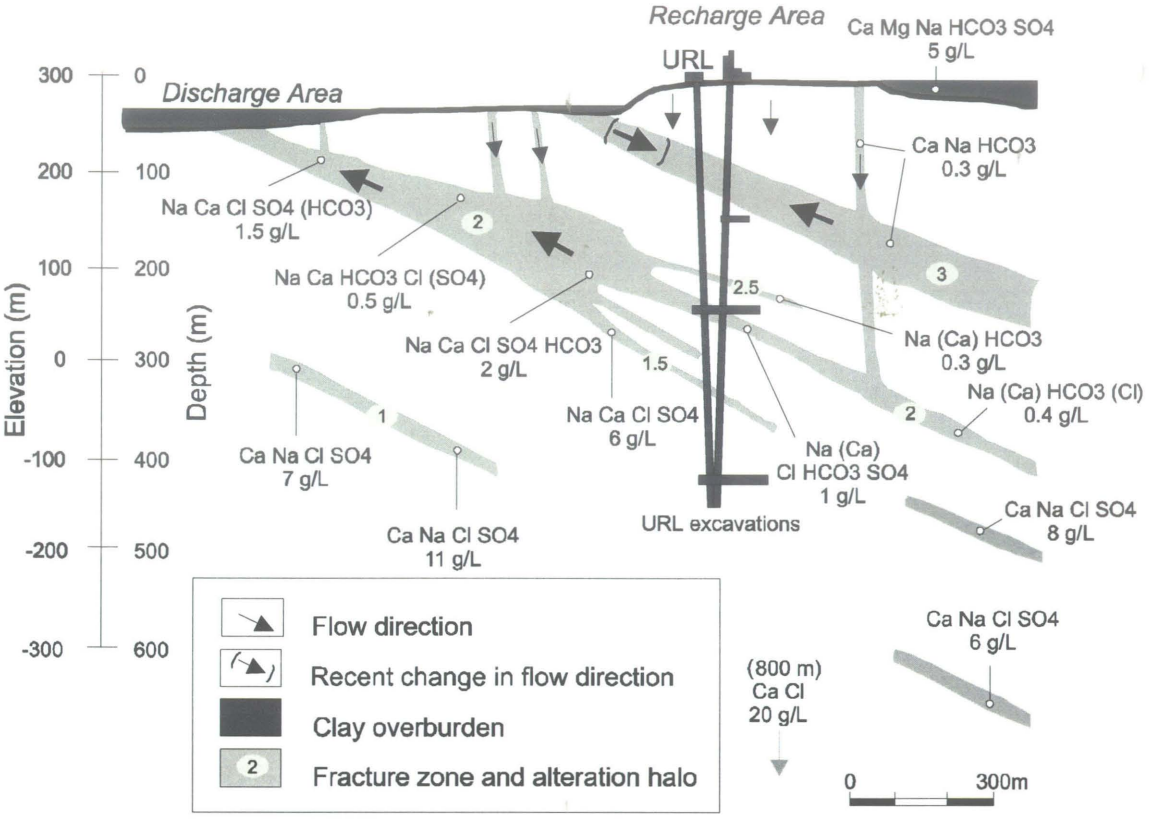

Figure 8: Variation of groundwater chemistry with depth in the vicinity of the URL, based on a schematic cross-section of groundwater flow paths (after Gascoyne 2000). Arrows in parentheses indicate recent changes in flow direction due to excavation of the URL. Groundwater salinities are from Total Dissolved Solids.

1.4 Role of Bacteria in Sorption of Contaminants

Naturally-occurring bacteria in the repository environment may have an impact on the migration of radionuclides. Studies have shown that microbes are present under a wide range of conditions in the subsurface, even in the relatively nutrient-poor environment of a granitic batholith (Stroes-Gascoyne et al. 1992, Brown et al. 1994, Stroes-Gascoyne and West 1996 and 1997, Stroes-Gascoyne and Sargent 1998, Brown et al. 1998, Brown and Sherriff 1999, Motamedi 1999). Microbes may also affect the migration of contaminants like cesium by changing the acidity and redox conditions of the groundwater through a series of biochemical reactions (Brown and Sherriff 1999). The presence of microbes may buffer the water in a repository to an alkaline condition, so that the uranium in the used fuel would remain insoluble and hence immobile in a reduced state as U(IV) (Brown et al. 1995, Brown and Sherriff 1999). Radionuclides may also adsorb on biofilms, which are slimy polymers produced by bacteria. Biofilms with negative surface charges can become sorption sites for positively charged ions (Brown and Sherriff 1999) such as Cs^+. In the presence of iron oxides, biofilms may grow rapidly, clogging open pore spaces and preventing the free movement of groundwater while acting as a sorptive "sponge" or storage site for radionuclides (Stroes-Gascoyne and West 1997). Accumulation of microbes may have a negative effect on conditions in or near a repository as acidic conditions caused by microbes may enhance microbial influenced corrosion (MIC), resulting in damage to the metal containers for waste (Stroes-Gascoyne and Sargent 1998). Because bacteria can play a number of roles with respect to

the migration of contaminants in a repository, one component of this study was to investigate ion exchange of cesium in clay minerals in the presence of microbes or bacterial cultures.

CHAPTER 2 CESIUM AND CLAY MINERALS

2.1 Chemistry and Properties of Cesium (Cs)

Cesium has an atomic number of 55, and an atomic weight of 132.9055g. An alkaline metal, it belongs to the Group 1A elements in the Periodic Table and as such it has chemical properties similar to the alkaline metals potassium (K) and rubidium (Rb). Cesium has one of the lowest melting points of all metals, 28.5 ^{o}C, so that it is liquid at warm room temperatures. It has a boiling point of 670^{o}C, a valence of 1, density of 1.90g/cm^{3}, atomic radius of 2.35 Å, and an ionic radius of 1.69 Å. The electronic configuration of Cesium is $1s^2 2s^2 2p^6 3s^2 3p^6 3d^{10} 4s^2 4p^6 4d^{10} 5s^2 5p^6 6s^1$ (Mortimer 1975).

Cesium has 32 isotopes, with masses ranging from ^{114}Cs to ^{145}Cs (CRC Handbook 1992-1993), most of which are unstable with very short half-lives. Stable cesium exists as ^{133}Cs. ^{135}Cs with a half-life of 2.3 million years, is produced by the fission of ^{235}U (Table 4).

Although pure cesium can be made by electrolysis of fused cesium cyanide in an inert atmosphere, and it can be stored under an inert liquid or gas in a vacuum to prevent contact with air or water, cesium is one of the most reactive elements in the Periodic Table. It is always found combined with other elements in nature. Cesium reacts readily with oxygen (O_2) to form cesium oxide (Cs_2O). It reacts explosively with water (H_2O) to form a strong base, cesium hydroxide (CsOH), and hydrogen (H_2) gas. Cesium also reacts with halogens to form cesium fluoride, cesium chloride, cesium bromide, and cesium iodide as

well as sulfates, carbonates and nitrates. The following are some common chemical reactions with cesium:

$$4Cs_{(s)} + O_{2(g)} \rightarrow 2Cs_2O_{(s)} \quad \textbf{(1)}$$

$$2Cs_{(s)} + 2H_2O \rightarrow 2CsOH_{(aq)} + H_{2(g)} \quad \textbf{(2)}$$

$$2Cs_{(s)} + Cl_{2(g)} \rightarrow 2CsCl_{(s)} \quad \textbf{(3)}$$

Table 4: Radioactive properties of selected Cs isotopes

			Radioactive Energy (MeV)		
Isotopes	**Half-life (yrs)**	**Decay Mode**	**Alpha (α)**	**Beta (β)**	**Gamma (γ)**
Cs-133	-	-	-	-	-
Cs-134	2.1	β		0.16	1.6
Cs-135	2.3×10^6	β	-	0.067	-
Cs-137	30	β	-	0.19	-

Modified from http://riskcentre.doee.gov/doc/cre/factsheet/cesium.pdf

The only mineral in which cesium occurs abundantly is the zeolite pollucite, $(Cs,Na)_2Al_2Si_4O_{12}\cdot H_2O$. Approximately two-thirds of the world's known reserves of pollucite are found at Bernic Lake, Manitoba (Hammond, 1993), where the pollucite is found in the Tanco pegmatite, which intruded the Bird River greenstone belt adjacent to the Lac du Bonnet batholith. Other pollucite localities include South West Africa and the United States.

Cesium compounds are used in the production of ceramics and glass. Cesium chloride is used in photoelectric cells, in optical instruments and in electron tubes. Cesium is also used to remove traces of gas from vacuum tubes to protect them from air and water, and it is used industrially to produce a dense biodegradable drilling fluid, cesium formate, which is used as a lubricating agent for large-scale drilling projects. The radioactive isotope ^{137}Cs, which has a half-life of 30 years, is a powerful emitter of beta radiation (Table 4) and is used for cancer treatment and for other types of medical and industrial research.

2.2 Ion Exchange Theory

Ion exchange involves the substitution of one ionic species by another without changing the structure of the mineral. In some cases there may be some distortion of the crystal lattice but the basic structure does not change and the mineral is still recognizable. Ion exchange in soils and sediments is one of the main processes that affect the chemical composition of groundwater in aquifers (Karger et al. 1973). The ability of soil colloids to reversibly adsorb cations from solution was known long before the chemical structure of clay minerals was

found to be the origin of the negative charge of soils. Ion exchange is also important in the replacement or the transportation of ions in living cells.

Clay minerals have varying capacities to adsorb cations, as a result of different charges, mineral structures, and surface areas. Cation exchange capacity (CEC) is defined as the quantity of cations reversibly adsorbed per unit weight of mineral (McBride 1994) and is commonly expressed as centimoles per kilogram (cmoles/kg). Clay minerals, such as kaolinite, with little or no permanent charge have a relatively low CEC (Table 5). Other clay minerals have a higher CEC, ranging from 70-120 cmoles/kg for montmorillonite and 100-150 cmoles/kg for vermiculite. The unit surface areas of montmorillonite and vermiculate are also substantially greater than for kaolinite (Table 5).

Table 5: Surface areas and CEC of common clay minerals (from McBride 1994)

Clay Minerals	Specific Surface Area m^2/g	CEC (cmoles/kg)
Kaolinite	5 - 20	1 - 15
Illite	80 - 150	10 - 40
Vermiculite	300 - 500	100 - 150
Montmorillonite	700 - 800	70 - 120

Exchange between two ions in aqueous state is controlled by the size and charge of the exchanging ions. If the sizes of the ionic radii differ by less than 15%, substitution is possible. Ions with a charge difference ≤ 1 can substitute for each other. However, ions with different electronegativity or different types of bonds may not substitute for each other (Faure 1998). When two different ions can occupy the same position in a crystal, the ion with a higher ionic potential forms the stronger bonds with the surrounding anions and hence is the preferred choice.

The active mass or activity of exchangeable ions is measured not by the quantity of these ions in the adsorbed state but rather by the fraction of exchange sites that they occupy (McBride 1994). The exchange between Cs^+ in solution and Ca^{2+} ions in a clay mineral is expressed as

$$2CsCl(aq) + CaX_2(s) = CaCl_2(aq) + 2CsX\ (s) \qquad \textbf{(4)}$$

where (aq) and (s) refer to the aqueous and solid phases, respectively,
Cs and Ca are the exchanged cations, Cl denotes the chloride anion in solution, and X denotes the negative exchange site on the mineral surface.
The equilibrium constant K_{eq} for the reaction above is expressed as (McBride 1994):

$$K_{eq} = \frac{(CaCl_2) * (2CsX)}{(2CsCl) * (CaX_2)} \qquad \textbf{(5)}$$

The electrostatic attraction energy (E_{att}) also plays a role in the ion exchange between two ions. The electrostatic attraction energy between an

adsorbed cation, Cs^+, and the surface charge site is inversely proportional to the sum of the effective radius (r_s) of the charge site and the radius (r_{cs}) of the Cs^+ cation. Where e is the electronic charge unit, this is expressed as (McBride 1994):

$$E_{att} \propto e^2/(r_s + r_{Cs}) \quad \textbf{(6)}$$

Other properties that limit ideal cation substitutions include unequal charge of the ions, effective radius of the charge site, radius of the cation, charge of the cation, concentration of the cation in solution, and structural charge. When ion exchange sites have dimensions that are nearly equal to the size of the hydrated exchanging ion, ions may still be excluded from the site on the basis of their hydrated size. When the charge difference in the substituting ion is greater than one, the substitution may not take place because the electrical neutrality cannot be maintained. In some minerals such as clay minerals, the deficiencies could be accommodated by adsorption of ion on the charged surface of the crystal. In general, ions with higher ionic potential (charge/radius ratio) form stronger bonds than those with lower ionic potential. For example, Ca^{2+} is effective as a competitor for clay exchange sites in a low salt concentration solution, however, it is less effective in competing for clay exchange sites with ions with higher ionic potential, such as Al^{3+}.

2.3 Structure and Chemistry of Clay Minerals

Clay minerals are generally formed as a result of rock-water interactions with pre-existing minerals. For example, potassium feldspar reacts with water to form kaolinite. The reaction is expressed as (Faure 1998):

$$2KAlSi_3O_8 + 9H_2O + 2H^+ \rightarrow Al_2S_2O_5(OH)_4 + 2K^+ + 4H_4SiO_4 \quad \textbf{(7)}$$

For this reaction to run to completion there must be a sufficient supply of water acidity to remove the reaction products formed and to provide H^+. Clay minerals generally occur as platy or fibrous particles in fine-grained aggregates that have various degrees of plasticity when mixed with water. They vary in size from colloidal to just above the limits of resolution of an optical microscope. When heated, they lose their water component.

Clay minerals are phyllosilicates (sheet silicates) and consist of tetrahedral (T) layers and octahedral (O) layers. A tetrahedral layer is formed by linkage of SiO_4 tetrahedral bases in a hexagonal array. The bases of the tetrahedra are in an approximately co-planar arrangement with their vertices all pointing in the same direction (Figure 9). The linked tetrahedra share oxygen atoms at three of the four corners of the tetrahedra.

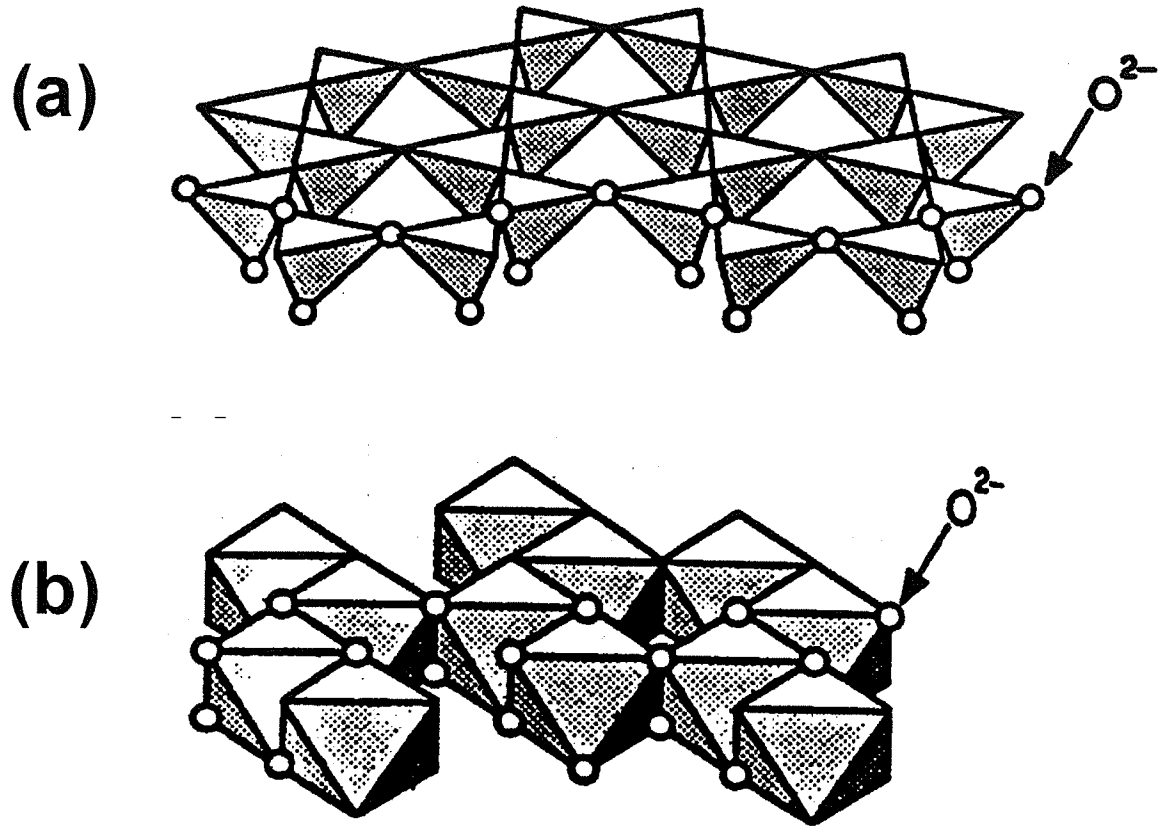

Figure 9: Structure of 1:1 and 2:1 layer clay minerals: a) SiO_2 tetrahedra linked to form the tetrahedral sheet, and b) MO_6 octahedra linked to form the octahedral sheet (modified after Sposito 1984).

The octahedral layer (Figure 9) consists of aluminum hydroxide, in which an Al^{3+} ion is located in the centre of the octahedron with six hydroxyl ions located at the corners. In a dioctahedral layer Al^{3+} or Fe^{3+} occupies only two of every three available sites in the structure. In cases where another trivalent element such as Fe^{3+} replaces Al^{3+}, the octahedral layer remains dioctahedral because as with Al^{3+}, only two of every three available sites are occupied. If Al^{3+} is replaced by three divalent ions such as Fe^{2+} or Mg^{2+}, then all sites in the octahedral layer are occupied, giving a trioctahedral layer (Sposito 1984, Faure 1998).

Clay minerals are classified on the basis of the number and types of layer types that they contain. The 1:1 layer structure, which is represented by kaolinite ($Al_4[Si_4O_{10}](OH)_8$), is formed by one tetrahedral and one octahedral layer (Figure 9). The 2:1 layer type structure, which is represented by montmorillonite ($(Ca,Na)_x(Al,Mg,Fe)_4[(Si,Al)_8O_{20}](OH)_4.nH_2O$), illite ($K_xAl_4[(Si,Al)_8O_{20}](OH)_4$), and vermiculite ($(Mg,Ca)_x(Mg,Al,Fe)_6[(Si,Al)_8O_{20}](OH)4.n(H_2O)$), is formed by joining one tetrahedral layer and two octahedral layers (Figure 9). The structure is such that one octahedral layer is sandwiched between two tetrahedral layers.

The different compositions of clay minerals result from partial or complete substitutions for Al^{3+} in the octahedral layer. This substitution can occur by the replacement of Al^{3+} by Fe^{3+}, Fe^{2+}, Mg^{2+} and other trivalent and divalent cations. Al^{3+} can also partially replace Si^{4+} in the tetrahedral layer causing an excess of negative charge, which is balanced by the adsorption of a cation. Substitution in both the tetrahedral and octahedral layers occurs mainly in the 2:1 layer

structure whereas in the 1:1 layer type structure, very little substitution is permitted (Faure 1998). These substitutions cause permanent structural charges on the composite layer (Sposito 1984). Fe^{3+}, Fe^{2+}, Mg^{2+}, Zn^{2+}, Li^{+} and Cr^{3+} can replace Al^{3+} in the octahedral layer. In a 2:1 layer clay, the excess layer charge caused by incomplete substitution in its tetrahedral layer could be partially compensated by excess charge in the octahedral layer. Any excess after this compensation is neutralized by adsorption of a cation in the interlayer or on the surface of the tetrahedral layer bonding the clay mineral together. The layers are held together loosely by exchangeable cations (Figure 10). The types of cation between the layers depend on the net charge and the substitution allowed in the layers. The number of interlayer ions varies in different clay minerals and depends on the charge density of the layer. Also the layer separations vary because of swelling and shrinkage that may occur from hydration or dehydration (Sposito 1984).

2.3.1 Kaolinite $Al_4[Si_4O_{10}](OH)_8$

Kaolinite is a 1:1 layer type clay mineral. It has a low cation exchange capacity compared to the other clay minerals. Because it is a 1:1 layer mineral, it does not have exchangeable interlayer cations. Therefore, very little substitution can take place. A distorted hexagonal structure in kaolinite results from the presence of both vacant and occupied octahedral sites.

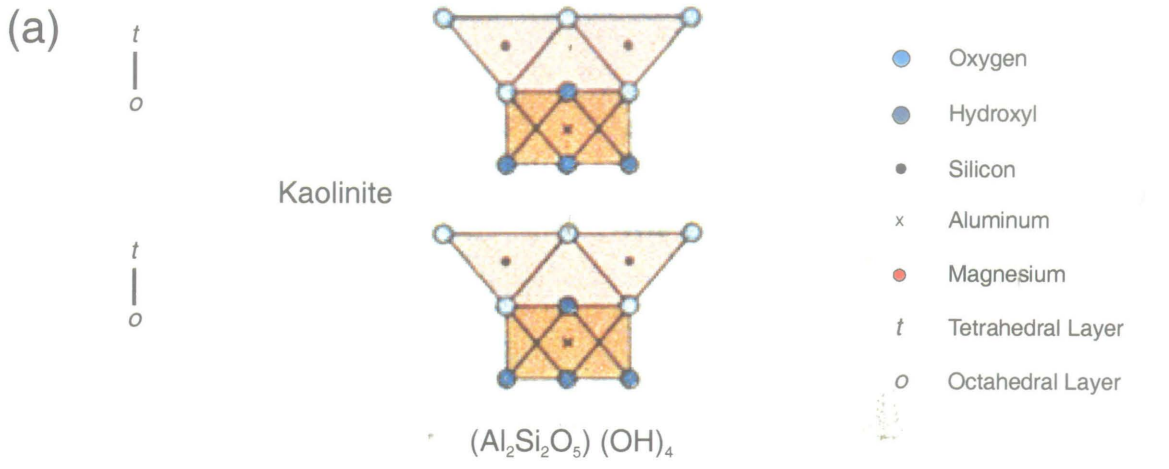

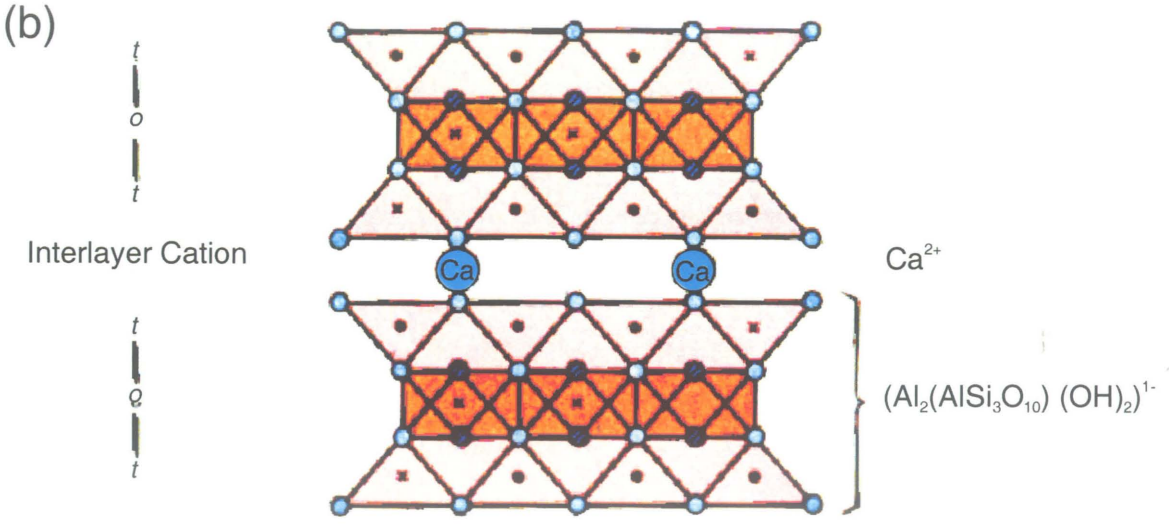

Figure 10: Configuration of the 1:1 and 2:1 layer clay structure: (a) shows the single tetrahedral layer attached to the single octahedral layer with no interlayers, and (b) shows one octahedral sheet sandwiched between two tetrahedral sheets. It also shows the interlayer cation between layers (after Klein and Hurlbut 1985).

In this arrangement, six smaller occupied sites surround one large vacant site. The vacant site is enlarged because of the mutual repulsion of surrounding Al^{3+} cations and the lack of a cation in the cavity to pull the anions towards the centre (Bailey 1980). Silicon is present in the tetrahedral site whereas Al occurs in the octahedral site (Figure 10a). Kaolinite is formed primarily by hydrothermal alteration or weathering of feldspar, feldspathoids and other silicates (Equation 7) (Deer et al. 1998).

2.3.2 Illite $K_xAl_4[(Si,Al)_8O_{20}](OH)_4$

Illite is a 2:1 layer clay whose structure has an octahedral layer sandwiched between two inward pointing sheets of linked $(Si,Al)O_4$ tetrahedra (Figure 10b). Illite belongs to the group of clay minerals with non-expanding lattices because the spacing of the interlayer is fixed. It may, however, interlayer with other expandable clays (Faure 1998). It may also be dioctahedral when two Al^{3+} or Fe^{3+} cations substitute in the octahedral layer or trioctahedral when three Mg^{2+} cations substitute. The negative layer charge in the tetrahedral layer is neutralized by K^+ that fits into the hexagonal hole formed by the linked silica tetrahedral. The K^+ that fits into the hexagonal hole is non-exchangeable. Si occurs in the tetrahedral site and Al can occur in both tetrahedral and octahedral sites. Illite clay results from the alteration of silicate minerals, feldspar in particular. It also results from alteration of muscovite. It can be derived from a hydrothermal origin in an alteration zone or diagenetic through alteration of other clays (Deer et al. 1998).

2.3.3 Montmorillonite $(Ca,Na)_x(Al,Mg,Fe)_4[(Si,Al)_8O_{20}](OH)_4.nH_2O$

Montmorillonite is a 2:1 layer type clay mineral similar to illite (Figure 10b) which belongs to the smectite group of expandable clay minerals. Montmorillonite is a dioctahedral clay due to Mg^{2+} in the octahedral layer. In the tetrahedral layer, Si^{4+} is partially substituted by Al^{3+} creating an excess charge of -0.26. The incomplete substitution in both the tetrahedral and octahedral layers creates a net excess negative charge -0.26 and -0.20, respectively, that can be neutralized by surface adsorption of cations such as Ca^{2+}, Na^{+}, and Mg^{2+}. The adsorbed cations do not provide enough positive charge to completely neutralize the negative charge, therefore, these substitutions create an imperfect substitution and as such are susceptible to either a partial or a complete exchange. Any of these cations (Ca^{2+}, Na^{+}, and Mg^{2+}) can be replaced by other cations of similar size or charge or can be replaced by a water molecule (Faure 1998).

The characteristic swelling property of the smectite group is one of the identifying properties of montmorillonite. When it is immersed in water, water molecules replace the interlayer cations. Because the net positive charge of the water molecule is small, it requires a large amount of water molecules in order to neutralize the excess charge. This prompts water molecules to fill the interlayer, increasing the interlayer distance and expanding the clay. If montmorillonite is heated at 300°C for one hour, the interlayer distance decreases from 15Å to about 10Å after the adsorbed water has been expelled. The distance expands

back to the original separation distance when the mineral is re-hydrated (Bailey, 1980, Faure 1998).

Montmorillonite has a high cation exchange capacity and differs from illite in that it has more of the exchangeable cations (Ca^{+}, Na^{2+} and Mg^{2+}). Montmorillonite is formed by alteration of volcanic ash, hence a major component of bentonite clay. It can also be formed by alteration of basic igneous rocks (Deer at al. 1998).

2.3.4 Vermiculite $(Mg,Ca)_x(Mg,Al,Fe)_6[(Si,Al)_8O_{20}](OH)_4.n(H_2O)$

Vermiculite is also a 2:1 clay, which is composed of macroscopic particles that resemble mica. Like other 2:1 layer type clays, it has an octahedral layer that is sandwiched between two inward pointing sheets of linked $(Si,Al)O_4$ tetrahedra. Vermiculite occurs as both dioctahedral and trioctahedral clay subgroups. The partial or incomplete substitution in the octahedral layer creates an excess (+0.22) positive charge, which is compensated by excess (-1.30) negative charge that results from the extensive substitution of Si^{4+} by Al^{3+} in the tetrahedral layer. The remaining negative charge is neutralized by adsorption of Mg^{2+} and Ca^{2+} in the interlayer. K^{+}, Na^{2+}, Rb^{+}, Cs^{+} and Li^{+} can also replace the interlayer cations. As in montmorillonite, the expandable property of vermiculite is created by the presence of water molecules in the interlayer. Heating vermiculite at 500°C decreases the interlayer distance from about 14Å to 10Å by expelling the interlayer water molecules. On re-hydration, the interlayer distance

of Mg^{2+} saturated, low charge vermiculite, expands again to the original separation distance (Bailey, 1980). Faure (1998) noted that when vermiculite is treated with a solution of potassium chloride, the K^+ replaces the Mg^{2+} in the clay and it becomes non-expandable.

Vermiculite is different from the smectite group of clays because it has a higher negative charge in the tetrahedral layer and also by the dominant presence of Mg^{2+} as the exchangeable cation in the interlayer. Another difference is that it loses its expandable property after the substitution of Mg^{2+} by K^+ in the interlayer. The structure of vermiculite can range from a 3-dimensional ordered structure to an almost completely disordered structure (Bailey 1980, de la Calle and Suquet 1988). In vermiculite clay, Al^{3+} replaces Si^{4+}, in an isomorphic substitution causing a negative charge that is partially compensated by the substitution of Mg^{2+} by Al^{3+} or Fe^{3+} in the central layer. What is left after the partial compensation is then balanced by the interlayer cation that can easily be exchanged. The most common interlayer cation is Mg^{2+} rather than K^+, though in some cases, Ca^{2+} and Na^+ are found. These interlayer cations can be replaced by cations such as K^+, Ca^{2+}, Na^+, Rb^+, Cs^+, Li^+, and NH_4^+. One of the characteristics of vermiculite is its swelling property with different liquids especially, glycerol, and ethylene glycol which is used to identify vermiculite (de la Calle and Suquet 1988). Vermiculite is formed by weathering or hydrothermal alteration of biotite or other micas (Deer et al. 1998).

2.4 Cs Exchange in Clay Minerals

Adsorption is a set of complex formation reactions between dissolved solutes and surface functional groups (Sposito 1984). The functional groups control stoichiometry of adsorption reaction, variation in adsorption with solution chemistry, electrical properties of the interface and the adsorption capacity. Cation adsorption on clay minerals occurs on the surface of the mineral, at the frayed edges resulting from mineral alteration, and in the interlayer (Kim et al. 1996a, b). Sawhney (1972) observed that sorption of K^+ or Cs^+ by montmorillonite or vermiculite produces a collapse in the inter-layers when Mg^{2+} is replaced by K^+. Montmorillonite collapses to a 12Å c-axis spacing on saturation with K^+ or Cs^+ substituting for Na^+, whereas vermiculite shows a 10.8 Å spacing on saturation with Cs^+ (Sawhney 1972). In vermiculite, the collapse is in alternate layers that produce regular interstratified 10Å and 14Å layer sequences. Random collapses occur in montmorillonite when large amounts of these cations are adsorbed. The collapses in the layers of vermiculite or montmorillonite are caused by vertical and horizontal forces resulting from the attraction to K^+ or Cs^+ in the interlayer position near the frayed edges, and negative layer charge that exists in the tetrahedral layer. The approaching K^+ or Cs^+ increases the attraction between the negative layer charge and the K^+ or Cs^+ eventually collapsing the edge to produce the stable structure similar to the central core (Sawhney 1972).

At lower concentrations of K^+ and Cs^+ ions in solution, illite and mica have a larger selectivity than vermiculite and montmorillonite. This is probably because the frayed-edge sites in illite and mica are more likely to be the first site of adsorption than the interlayer sites. Another reason could be that K^+ fits into the hexagonal ring of the silica tetrahedra that make up the tetrahedral layer. However, as the concentration increases, selectivity of illite and mica become less important than in vermiculite.

In a comparative study of the sorption capacity of fracture filling minerals encountered in fracture zones, for radionuclides representing alkaline earth elements, Kamineni et al (1983,1986) concluded that increased K^+ content in the mineral significantly increased Cs^+ sorption. This is probably due to the fact that Cs^+ can replace K^+ in an ion exchange reaction because their ionic sizes are comparable. This exchange reaction was confirmed by Oscarson et al. (1987,1994), and Ticknor et al. (1989), where Cs^+ is adsorbed preferentially on K-bearing minerals such as sericite and illite clay. Ticknor et al. (1991) also observed that the presence of organic material in the groundwater solution did not affect the sorption of Cs^+ in clay materials, especially where the concentration of organic material was low.

2.5 Study of Clays With Nuclear Magnetic Resonance Spectrometry

High field, solid state, nuclear magnetic resonance spectrometry (NMR) has been successfully used in the study of phyllosilicates (Kirkpartick 1988, Weiss et al. 1990a, b, Kim et al. 1996a, b, Kim and Kirkpatrick 1998, Sullivan et

al. 1998) and in the case of nuclear waste, it has been used to study clay mineral interactions with ^{133}Cs. Westrich et al. (1998) studied the sorption isotherms for Cs^{+}, Sr^{2+} and Ba^{2+} (as an analog for Ra^{2+}) onto kaolinite and smectite clays. This study, conducted at temperatures of 25°, 50° and 70°C over a wide range of pH values (2-12), confirmed the observation by Kim et al. (1996b) that Cs^{+} is adsorbed at mineral surfaces and at interlayer sites of smectite clays, and on edge and basal sites of kaolinite.

The studies by Kim et al. (1995, 1996a) and Weiss et al. (1990b) showed that that Cs^{+} adsorption in non-expandable clay minerals (kaolinite and hydrothermal illite) occurs in two locations called the Stern layer (CS1-near surface adsorption) and the Gouy layer (CS2 adsorption in the interlayer). In the CS1 layer, the Cs^{+} is tightly bonded to the surface. In the CS2 layer the Cs^{+} is loosely bonded. In the clays with expandable layers, the Cs^{+} adsorption occurs at the broken edges, frayed edges, basal or planar surfaces. Other studies (Kim et al. 1996b) showed that Cs^{+} adsorbed on crystalline tops and bottoms of kaolinite clay, which are probably the same sites referred to as planar or basal sites. The chemical shift of Cs^{+} in the CS1 layer changes with surface composition, becoming more shielded (i.e., more negative) with increasing Si/Al ratio. The chemical shift of Cs^{+} in the CS2 layer on the other hand, does not show a systematic change with the changing Si/Al ratio, though it is more sensitive to changes in relative humidity and surface density. The CS1 layer peaks are noted to be more negative and are narrower compared to those peaks

from the CS2 layer, as well as having larger spinning side bands indicating that the Cs^+ is more tightly bonded in the CS1 layer sites.

Higher pH values also cause the Cs^+ to undergo motional averaging between CS1 and CS2 at sites with frequencies greater than 100 kHz, producing only one observable peak. The temperature effect on the CS1 layer adsorption is similar to the effect of relative humidity. At lower concentrations of CsCl, and lower temperatures (-60°C), their results point to a preferential adsorption on the CS1 layer.

A study of the expandable clays shows that when montmorillonite is highly hydrated, cations are adsorbed in the interlayer. The adsorbed cations present in the interlayer are separated from the clay surfaces by water molecules and are able to move freely throughout the interlayer and may exchange rapidly between a surface -bonded and hydrated species (Sullivan et al. 1998). Weiss et al. (1990a, b) confirmed the mobility of these cations in all samples containing interlayer water.

A ditrigonal cavity that occurred in montmorillonite from six corner-sharing silica tetrahedra is also a site for Cs^+ adsorption. The Cs^+ adsorbed in expandable clay tends to be in a more disordered environment (Kemner et al. 1997). This is equivalent to Cs^+ ions being loosely bonded to a single ditrigonal cavity at the clay surface. Kemner et al. (1997) concluded that the relative intensities of the NMR peaks reported in their study suggested that majority of Cs^+ ions reside within the collapsed layers of mica and illite clay structures.

The three isotopes examined by NMR in this study are ^{29}Si, ^{27}Al and ^{133}Cs. ^{27}Al has a natural abundance of 100%, a spin number (I) of 5/2 and a rapid relaxation time. Its relative sensitivity at constant field is 0.206, and its electric quadrupole moment (Q) is 0.149×10^{-24} cm^2. Similarly, ^{133}C has a natural abundance of 100%, a spin number (I) of 7/2 and a rapid relaxation time. It has a very small electric quadrupole moment (Q). ^{29}Si has a natural abundance of 4.7%, a spin number (I) of ½ and a slow relaxation time. Its relative sensitivity at constant field is 7.84×10^{-3}. It has no electric quadrupole moment (Q). ^{133}Cs has a chemical shift that is very sensitive to the local structural environment. The chemical shift for ^{133}Cs ranges from +100 to -500 ppm relative to a 0.1M aqueous solution of CsCl. The chemical shifts for ^{29}Si ranges from -60 to -130 ppm relative to tetramethyl silane (TMS), while the isotropic chemical shifts for ^{27}Al ranges from +50 to +80 ppm when in tetrahedral site, and between -10 and +20 ppm when in octahedral site relative to 1M aqueous solution of aluminum chloride (Liang 1992). Hartman et al. (1998) found other chemical shifts for ^{27}Al outside this range due to unpaired cesium electron density.

CHAPTER 3 MATERIALS, ANALYTICAL METHODS AND EXPERIMENTAL PROCEDURES

3.1 Materials

The clay minerals in samples of the altered rubble from fracture zones in the Lac du Bonnet batholith were analysed by XRD. Clay minerals selected for ion exchange experiments are representative of clays found in fracture zones and likely to be used as buffer and backfill materials in the deep geological repository.

The materials that were selected for the ion exchange experiments were montmorillonite (the main constituent of bentonite), illite, kaolinite, two types of vermiculite, and two types of bentonite clay (Wyoming bentonite and Kunigel,(Japanese bentonite)). Kaolinite (KGa-1), one sample of vermiculite (VTx-1), and montmorillonite (STx-1) were obtained from the Source Clay Repository of the Clay Mineral Society (CMS), Missouri, USA. Samples of Wyoming bentonite, Sealbond-illite and Kunigel bentonite were obtained from AECL, Whiteshell Laboratories, Pinawa, MB., Canada. A second vermiculite, sample Ver 46-E, was obtained from Ward Scientific, NY, USA, after XRD analysis of the vermiculite sample VTx-1 indicated that it was inpure and contained a number of other minerals.

The kaolinite sample (KGa-1), used in the quantitative ion exchange experiments and in MAS NMR spectroscopy, was analyzed by X-ray diffraction and gave an X-ray pattern that is consistent with known examples of kaolinite

(Brindley 1980). Montmorillonite sample STx-1 was found to contain a trace amount of a silica phase, which was identified by Liang (1992) to be cristobalite. However, the montmorillonite was considered to be pure enough to be used in the ion exchange experiments. It was used in the ion exchange experiments under (a) ambient conditions, (b) at 80°C, (c) at 107°C and 1.5 bars, and (d) in the presence of bacterial cultures. These were analysed by MAS NMR spectroscopy. Wyoming Bentonite and Kunigel Bentonite were included in the ion exchange experiment because bentonite is likely to be a major constituent of the clay-based sealing systems that would be used as buffer and backfill in a deep geologic repository.

To avoid some of the additional minerals in the vermiculite sample VTx-1, grains of vermiculite were handpicked from the sample and were ground to about 0.1mm with a mortar and pestle. The handpicked grains were analyzed by XRD and were consistent with known examples of pure vermiculite (Brindley, 1980). This sample was used in a quantitative ion exchange experiment and in MAS NMR spectroscopy. The other vermiculite sample (Ver 46-E) was very coarse-grained (up to 1 cm in diameter) and was ground to 0.1mm using a coffee grinder. It was used in quantitative ion exchange experiments but it was not included in the MAS NMR spectroscopy because of its high content of iron (e.g. see Table 7 in chapter 4). The presence of paramagnetic ions in naturally-occurring mineral affects the collection of NMR spectra. Clay minerals with 0.5% iron (Fe_2O_3) causes broadening of the spectrum, and 20% or more will

prevent the rotor from spinning and no spectrum will be collected (Thompson, 1984).

3.2 Analytical Methods

3.2.1 Inductively Coupled Plasma (ICP) Optical Emission Spectrometry (OES) and Atomic Absorption (AA) Analysis

Chemical analyses were conducted at the Department of Geological Sciences of the University of Manitoba, Winnipeg, to determine the amount of cesium in the clay mineral. The powdered samples were dried at 110°C overnight, after which 0.1g of each sample was weighed into a 50mL centrifuge tube, and 8.5mL of nitric acid and 1.5mL of hydrofluoric acid was added to digest the sample. After mixing, the sample was heated in a CEM model MDS 2100 microwave for one hour. After the liquid had cooled, 20mL of the acid mixture was added and the solution was heated in the microwave for another hour. The resulting sample was then diluted with distilled water to 50mL (500-fold dilution). Aliquots of each sample were analyzed for cesium concentration using a Varian Spectra Atomic Absorption Spectrometer Model 300.

A Varian Liberty 200 ICP-OES machine was used to determine the major elements of the clay minerals, which are reported as weight percent oxides (SiO_2, Al_2O_3, Fe_2O_3, MnO, MgO, Na_2O, TiO_2, K_2O, P_2O_5). The clay mineral samples were analyzed before and after ion exchange to verify gain or loss of

cations. The software FORMULA, was used to calculate the structural formula of each sample (see Table 7).

Wyoming bentonite, Kunigel and Sealbond illite were not analyzed because they are composite materials that contain more than one type of mineral.

3.2.2 X-Ray Diffraction Technique

X-ray diffraction was conducted at the Department of Geological Sciences of the University of Manitoba, Winnipeg. Some highly altered rock samples collected from fractures zones in the Underground Research Laboratory in the Lac du Bonnet batholith were crushed with a mortar and pestle, glycol saturated and then analyzed by XRD. Glycolation is used to determine the different types of clay minerals present in the specimen because ethylene glycol causes the d-spacing in the swelling clays to change. This change will then cause a shift in the XRD pattern that can be related to a specific clay mineral (Last 2001, Dixon 1995).

Continuous scan X-ray diffraction data were collected on a Philips automated diffractometer system PW1710 Bragg-Brentano goniometer equipped with incident- and diffracted-beam Soller slits, 1.0^{o} divergence and anti-scatter slits, a 0.2mm receiving slit and a curved graphite diffracted-beam monochromator. For the clay minerals, the normal focus Cu X-ray tube was

operated at 40kV and 40mA, using a take-off angle of 6°. The profiles were collected from 4-64° 2θ at a scan rate of 6° 2θ /min.

Fein-Marquart's micro-Powder Diffraction Search-Match software (μPDSM) was used for the identification of the phases present, based on a search of the minerals subfile of the Powder Diffraction File (PDF) database leased from the International Centre for Diffraction Data (ICDD).

3.2.3 Nuclear Magnetic Resonance Spectroscopy

Magic Angle Spinning (MAS) Nuclear Magnetic Resonance (NMR) spectra were collected using a Bruker AMX500 spectrometer with a 11.7 Tesla magnet. The solid state NMR principles are described in Appendix A. Powdered samples were packed in 5mm diameter zirconia rotors which were spun at a magic angle of 54.7° to the external magnetic field (βo) at speeds ranging from 5 kHz to 8 kHz in a MAS probe manufactured by Doty Scientific Inc. All spectra were collected at room temperature and pressure.

The ^{27}Al spectra were obtained at a frequency of 130.3 MHz, with a pulse width of 0.4 μs and a relaxation delay of 0.5 second. The number of scans varied from 900 to 6000 scans. The spectra are referenced to ^{27}Al in a 1M solution of aqueous aluminum chloride.

The ^{29}Si spectra were obtained at a frequency of 99.3 MHz, and a pulse width of 4μs, with a relaxation delay of 5 seconds. The number of scans varied from 150 to about 7000. The spectra were referenced to ^{29}Si in TMS.

The ^{133}Cs spectra were obtained at a frequency of 65.6 MHz, and a pulse width of 1μs, with a relaxation delay of 1 second. The number of scans varied from 700 to 8000 scans. The spectra were referenced to ^{133}Cs in 0.1M aqueous solution of CsCl. Spectrum of solid cesium chloride was obtained by grinding the CsCl crystals in a mortar and packing in the rotor. It was spun at 5.8 KHz, collecting only 26 scans. The relative peak intensities of ^{133}Cs spectra were obtained by cutting out the peaks and associated sidebands and weighing them. These values were converted to wt % by using the analytical results.

3.3 Experimental Procedures

3.3.1 Ion Exchange Experiments

Ion exchange experiments were conducted using cesium chloride solution and clay minerals. Most of the experiments were conducted under ambient conditions, but two set of experiments were performed at elevated temperatures and/or pressure in order to simulate conditions that might be encountered in a deep geological repository. One set of experiments examined the effect on adsorption due to a bacterial consortium, which originally had been isolated from groundwater in the Lac du Bonnet batholith (Brown et al. 1994).

3.3.2 First Adsorption Experiment at Ambient Conditions

The initial ion exchange experiment was conducted at room temperature and pressure with kaolinite (KGa-1), Ca-montmorillonite (STX-1), vermiculite (VTx-1 and Ver-46-E), Sealbond illite, Wyoming bentonite, and Kunigel bentonite. A 0.1M solution of CsCl was prepared by dissolving 16.84 g of CsCl in 1000mL of distilled water. For each sample, 6g of clay was weighed into a 100mL glass beaker, and mixed with 50mL of the 0.1M solution of CsCl using a mechanical mixer for one minute. The sample was then left to stand for 6 hours with occasional stirring. At the end of this time, the clay particles were allowed to settle and the liquid was decanted. The clay was then washed three times with distilled water and dried in the oven at 80°C for 12 hours prior to analysis by ICP-OES and AA.

3.3.3 Second Exchange Rate Experiments at Ambient Conditions

Montmorillonite (STx-1) was selected for use in this experiment because the initial ion exchange trial showed that montmorillonite adsorbed more cesium than other clay minerals. Two sets of rate experiments were conducted to determine the rate of adsorption of Cs^+ on clay minerals.

In the first experiment, 30g of montmorillonite (STx-1) was weighed and poured into a 500mL glass beaker and 350mL of 0.1M CsCl solution was added (this amounts to 0.9g of clay in 10mL of CsCl solution). The clay was completely

mixed to form a slurry. 20mL (STx-1-1m) of the slurry was decanted into a 100mL beaker and 50mL of distilled water was immediately added; it was allowed to settle, then clear liquid was decanted. The clay residue was washed two more times with 50mL of distilled water each and then dried in the oven at 80°C for 12 hours. When the clay slurry was decanted, it was not separated immediately from the CsCl solution, so the clay particles were still in contact with the CsCl solution while it settled before decanting though it has been diluted. The second sample (STx-1-30m) was poured out after 30 minutes, washed and dried in the same way as the first sample. Subsequently other sample portions about 20mL each (Stx-1-1h, Stx-1-2h, Stx-1-3h, Stx-1-4h, Stx-1-5h, STx-1-6h and STx-1-24h) were poured out and into 100mL glass beakers after each hour for 6 hours, and the last sample (STx-1-24h) was left for 24 hours. All samples were washed and dried in the same way as the first sample (STx-1-1m).

In the second set of exchange rate experiments, the sample size was reduced to conserve clay. Exactly 1.2g of montmorillonite (STx-1) clay were weighed into each of the 57 separate glass vials used for this experiment. In each, 10mL of 0.1M CsCl was added. The first set of triplicate samples (M1-1, M2-1 and M3-1) were shaken to mix and then filtered immediately using a Buchner vacuum filter system fitted with 10-micron filter paper. After filtration, 10mL of distilled water was poured into the sample holder to wash the sample and filtered again with the filter system. The clay sample was left on the bench to air dry for 20 minutes before it was scraped off the filter paper into another glass vial. The filtrate was preserved for analysis. A triplicate set of samples

were filtered and washed at 10-minute intervals for the first hour, each hour for the next six hours, and then each day for the next seven days. The triplicate set samples are designated as M1, M2 and M3 series.

In total, there were nineteen sets of triplicate samples for a total of 57 samples. All the samples were filtered and washed using the same Buchner vacuum filter system and air-dried in the same way. After each washing and filtration, the Buchner vacuum filter system was completely washed with a generous amount of distilled water to prevent contamination. All the samples were dried in the oven for 6 hours at 80°C.

3.3.4 Ion Exchange at 80°C

Three portions of 6g of montmorillonite (STx-1) were weighed into 500mL glass beakers and 200mL of 0.1M CsCl solution were added and mixed with a mechanical mixer to form a slurry (i.e., 0.3g montmorillonite per 10mL of CsCl solution). After mixing, the open beakers containing the clay suspension were put in the oven at 80°C for 6 hours. In this experiment, 200mL of 0.1M CsCl solution was used for ion exchange at high temperature and pressure so that any evaporation in the 6-hour period that the beakers stayed in the oven would not dry out the sample. After 6 hours, the sample beakers were removed from the oven and set on the bench to cool down for 30 minutes. The clear liquid was decanted. The clay residue was washed as described in section 3.3.3 and dried in the oven at 80°C for 6 hours.

3.3.5 Ion Exchange at 107°C and 1.5 Bars

Three portions of 6g of montmorillonite (STx-1) were weighed into three 500mL beakers and 150mL of 0.1M CsCl aqueous solution was added to each beaker (i.e. 0.5g of montmorillonite clay per 10mL of CsCl solution). The pH of the montmorillonite suspension in CsCl solution was measured, after which the three beakers were placed inside a pressure cooker. The pressure cooker was sealed, and placed on a hotplate. There was no opportunity to stir the sample inside the cooker. The temperature and pressure inside the pressure cooker were monitored through a temperature and pressure gauge attached to the cover of the pressure cooker. The temperature and pressure inside the pressure cooker were recorded each hour for the next 6 hours after which the experiment was terminated. The pressure cooker was removed from the hotplate and allowed to cool down for one hour before it was opened. The samples were washed three times in each case with 50mL of distilled water and dried in the oven at 80°C for 6 hours prior to analysis by ICP-OES and AA.

3.3.6 Ion Exchange in a Bacterial Culture

The bacteria consortium that was used in this experiment was initially extracted from the infillings and groundwater from fracture zone 2 in the Underground Research Laboratory in the Lac du Bonnet batholith. The

consortium was subsequently cultured in the lab in a glass vessel filled with granite chips from the URL (Brown et al. 1994, 1998).

In order to conduct this experiment in a sterile condition, all the materials used for the experiment including the growth medium (ammonium citrate), beakers, flasks, and stirring rods, as well as the clay minerals used in the experiment and also some of the bacteria-containing solution was sterilized in an autoclave. Ammonium citrate (AC) medium was prepared by dissolving 5g of ammonium citrate ($(NH_4)_3C_6H_5O_7$), 0.5g of potassium phosphate diabase (K_2HPO_4), 0.2g of magnesium sulfate ($MgSO_4.7H_2O$) and 0.01 of calcium chloride ($CaCl_2.2H_2O$) in 1L of distilled water. 10mL of the bacterial culture from the glass vessel was used to inoculate 100mL of AC medium and left on the rocker (shaker) for three days in order to allow the bacteria in the culture to grow to full population density.

Five sets of ion exchange experiments were conducted in triplicate using both montmorillonite (STx-1) and kaolinite (KGa-1), which represented the 2:1 and 1:1 layer clay types, respectively. The first set of experiments was conducted with 6g of clay mixed with 50mL of 0.1M CsCl aqueous solution and 50mL AC medium without active bacteria. This first set of experiments was done as a control to determine the amount of cesium that would be adsorbed by the clay mineral in the absence of bacterial culture.

The second set of experiments was conducted using the same materials and proportions that were used in the control, except that 5mL of active bacterial culture was added.

The third set of experiments was conducted using 50mL of 0.1M CsCl aqueous solution, 50mL of AC medium, and 5mL of active bacterial culture, but without clay minerals. This particular experiment was conducted using only bacterial culture to determine whether the bacteria alone would adsorb Cs^+. To set up this experiment, 5mL of active bacteria was added to 50mL of AC medium and left on the rocker for three days, after which 50mL of 0.1M CsCl solution was added. This was then left on the rocker for 7 days.

The fourth set of experiments was conducted with 6g of sterilized clay mineral mixed with 50mL AC medium plus 50mL 0.1M CsCl and 5mL of active bacterial culture. The clay mineral was sterilized in this experiment to ensure that there were no residual bacteria in the clay mineral that might affect adsorption.

The fifth set of experiments was conducted with 6g of clay mineral mixed with 50mL of 0.1M CsCl aqueous solution plus 50mL of AC medium and 5mL of sterilized bacterial culture. The bacterial culture was sterilized in this particular experiment to determine whether physical adsorption on bacterial surfaces or on biofilm would still affect adsorption of cesium on clay minerals.

Each set of experiments was done in triplicate for a total of 30 experiments. The glass flasks used in the experiments were covered with rubber or foam stoppers, and each time any of the flasks were opened to either add or remove any solution, the neck and opening of the flask was held over a Bunsen burner flame for about 30 seconds to reduce the likelihood of contamination of the sterilized material and equipment. All the experiments were

left on the rocker for 5 days except the third experiment conducted with only active bacterial culture, which was left for 7 days to allow enough time for the bacteria consortium to grow biofilms that may adsorb cesium.

At the end of the scheduled time for each experiment, the samples with clay minerals were decanted, washed three times with distilled water and dried in the oven at 80°C for 6 hours. For the sample without clay minerals, the mixture was centrifuged to separate the bacterial pellets from the supernatant. These were refrigerated until they were analyzed for cesium.

CHAPTER 4 RESULTS AND EVALUATION OF ANALYTICAL DATA

4.1 Ion Exchange in Clay Minerals

The results of the ion exchange are presented in this section. In the first ion exchange experiments under ambient conditions, montmorillonite (STx-1) adsorbed the most cesium (6.1 wt %), followed by vermiculite (Ver 46-E (4.9 wt %) and VTx-1 (3.8 wt %)). Kaolinite (KGa-1) adsorbed the least amount of cesium (0.8 wt %).

There is slight increase in the amount of cesium adsorbed in montmorillonite after ion exchange at 80°C (6.6 ± 0.3 wt%) and after exchange at 107°C and 1.5 bars (6.2 ± 0.2 wt%), compared to the experiments conducted at room temperature and pressure (6.1 ± 0.2 wt%), (Table 6 and Figure 11). Kunigel bentonite and Wyoming bentonite, both of which contain montmorillonite, adsorbed 6.3 wt% and 4.9 wt% cesium respectively. Sealbond illite adsorbed 0.9wt%.

The chemical compositions of montmorillonite, kaolinite, and vermiculite samples before and after ion exchange at ambient conditions are given in Table 7. The triplicate data are given in Appendix C, Table AP-C2.

Table 6: Summary of cesium concentration adsorbed by clay minerals under different temperature and pressure conditions (Triplicate data in Appendix C, Table AP-C1)

Mineral	Sample No.	Conditions	Cs Concentration	Std Dev
			(wt%)	
Montmorillonite	Stx-1	RT & P	6.1	0.24
Montmorillonite	Stx-1-Cst	80°C	6.6	0.03
Montmorillonite	Stx-1-Cstp	107°C & 1.5 bars	6.2	0.2
Kunigel Bentonite	JP-Kn-Cs	RT & P	6.3	0.3
Wyoming Bentonite	WYOB-1-Cs	RT & P	4.9	0.1
Vermiculite (CMS)	VTx-1-HPCs	RT & P	3.8	0.0
Vermiculite (WARD)	ver-46-ECs	RT & P	4.9	0.02
SealBond Illite	Ill-SB-ECs	RT & P	0.9	0.13
Kaolinite	KGa-1-Cs	RT & P	0.8	0.0

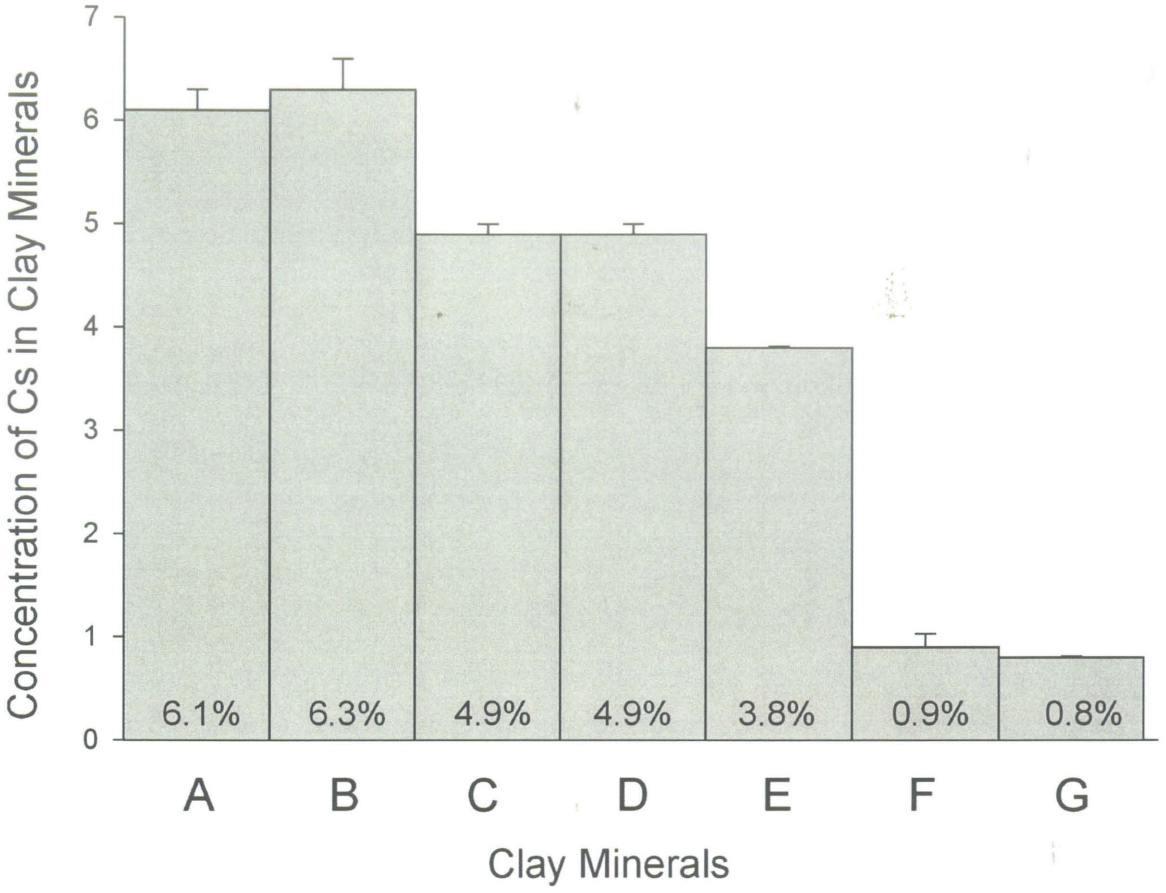

A Montmorillonite
B Kunigel (Japanese bentonite)
C Wyoming Bentonite
D Vermiculite (WARD)
E Vermiculite (CMS)
F Sealbond illite
G Kaolinite

Figure 11: Summary of amount of cesium adsorbed by different types of clay minerals and by bentonite at room temperature and pressure.

Table 7: Whole rock analysis results and structural formula of clay minerals before (A) and after (B) cesium ion exchange, (triplicate data are given in Appendix C, Table AP-C2)

	1A	1B	2A	2B	3A	3B	4A	4B
SiO_2	35.59	40.29	35.3	35.3	34.28	35.87	51.38	50.71
Al_2O_3	5.80	5.37	14.3	14.3	42.61	43.45	15.75	15.03
TiO_2	0.89	0.91	0.248	0.248	n/d	n/d	n/d	n/d
Fe_2O_3	5.77	5.58	0.08	0.08	0.04	0.05	0.53	0.41
MnO	0.04	0.03	0.03	0.03	0.00	0.00	n/d	n/d
MgO	21.01	17.09	27.8	27.8	0.02	0.0	2.46	1.99
CaO	0.22	0.42	0.19	0.19	0.02	0.01	1.49	0.11
Na_2O	0.36	0.01	0.09	0.09	0.09	0.07	0.37	0.11
K_2O	5.43	5.22	0.01	0.01	0.04	0.03	0.10	0.08
CsO_2	0.00	4.87	0.00	3.81	0.00	0.81	0.00	6.10
H2O*	-	-	-	-	-	-	-	-
Sum	**76.11**	**80.51**	**78.05**	**81.86**	**81.05**	**80.28**	**72.09**	**74.53**

Contintued...

Table 7 (Concluded): Structural formula

	1A		1B		2A		2B		3A		3B		4A		4B	
Si^{4+}	5.79	**6.9**	6.37	**7.37**	5.113	**7.554**	5.083	**7.51**	3.81	**4.00**	3.86	**4.00**	7.52	**8.00**	7.64	**8.00**
Al^{3+}	1.11		1.00		2.441		2.427		0.19		0.14		0.48		0.37	
Al^{3+}	-	**5.99**	0.11	**4.88**	-	**6.04**	-	**6.01**	5.39	**5.39**	5.36	**5.36**	2.24	**2.83**	2.30	**2.80**
Ti^{4+}	0.11		0.11		0.027		0.027		0.00		0.00		n/d		n/d	
Fe^{3+}	0.78		0.74		0.009		0.009		0.00		0.00		0.05		0.05	
Mg^{2+}	5.09		4.03		6.003		5.968		0.00		0.00		0.54		0.45	
Mn^{2+}	0.01		0.00		0.004		0.004		0.00		0.00		n/d		n/d	
Cs^{+}	0	**1.28**	0.33	**1.45**	0.00	**0.57**	0.234	**0.29**	0.00	**0.03**	0.04	**0.02**	0	**0.36**	0.39	**0.46**
Ca^{2+}	0.04		0.07		0.029		0.029		0.00		0.00		0.23		0.02	
Na^{+}	0.11		0.00		0.025		0.025		0.02		0.02		0.11		0.03	
K^{+}	1.13		1.05		0.002		0.002		0.01		0.00		0.02		0.02	
H^{+}	4.00		4.00		4.00		4.00		4.00		4.00		4.00		4.00	
CATSUM	14.17		13.71		13.653		13.807		9.42		9.42		11.18		11.25	
O	22.00		22.00		22.00		22.00		18.00		18.00		22.00		22.00	

Notes:

- n/d = not detected
- VERMICULITE (WARD)
- 1A = sample Ver 46-E before adsorption
- 1B = sample Ver 46-E-Cs after Cs adsorption
-
- VERMICULITE (CMS)
- 2A =sample VTx-1HP before adsorption (Liang 1992)
- 2B = sample VTx-1-HP-Cs after adsorption (Liang 1992)
- KAOLINITE
- 3A = sample KGa-1-1 before adsorption
- 3B = sample KGa-1-1-Cs after adsorption
- MONTMORILLONITE
- 4A = sample STx-1-1 before adsorption
- 4B = sample STx-1-1-Cs after adsorption

From Table 7, it can be noted that there is a loss of Mg^{2+}, K^{+} and Na^{2+} from montmorillonite after ion exchange. Vermiculite (ver-46-E, ver-46-E-Cs) showed the greatest losses in concentration for Na^{+} (0.11 apfu) and Mg^{2+} (1.1 apfu), but CMS vermiculite showed no such loss.

Kaolinite (KGa-1-1, KGa-1-1-Cs) adsorbed very little cesium (0.04 apfu) and does not show much variation in its overall composition before and after ion exchange, however, there is no difference in the measured amount of Na^{+} (i.e. 0.02 apfu). Montmorillonite (STx-1-1, STx-1-1-Cs), the sample that adsorbed the highest (0.4 apfu) amount of cesium, showed reductions in the following cations: Ca^{2+} from 0.23 to 0.02 apfu; Mg^{2+} from 0.54 to 0.45 apfu, and Na^{+} from 0.11 to 0.03 apfu. As Ca^{2+} and Na^{+} are the exchangeable cations, in montmorillonite, it can be inferred that Ca^{2+} and Na^{+} are the cations being replaced by Cs^{+}, loosing 91% and 75%, respectively, of their initial concentration after Cs exchange. Together, these cations accounted for 0.3 apfu of the 0.4 apfu adsorbed Cs^{+}.

Montmorillonite adsorbed about 55% of the cesium that was dissolved in 0.1M CsCl solution (Table 8), with a slight increase in Cs adsorption to 58% at 80°C and 57% at 107°C and 1.5 bars. Wyoming bentonite and Kunigel bentonite, because of their high content of montmorillonite, adsorbed 44% and 56%, respectively. Vermiculite adsorbed 34% (CMS) and 43% (WARD) with sealbond illite and kaolinite adsorbing the least amount at 8% and 5%.

Table 8: Percentage of cesium adsorbed by clay minerals

Minerals	Condition	Total Wt of Cs (g)*	Cs Adsorbed by Clay	Percent Cs Adsorbed by Clay
Montmorillonite	RT & P	0.67g	0.37g	55%
Montmorillonite	80°C	0.67g	0.39g	58%
Montmorillonite	107°C & 1.5bar	0.67g	0.38g	57%
Kunigel Bentonite	RT & P	0.67g	0.38g	56%
Wyoming Bentonite	RT & P	0.67g	0.29g	44%
Vermiculite (CMS)	RT & P	0.67g	0.23g	34%
Vermiculite (WARD)	RT & P	0.67g	0.29g	43%
Sealbond illite	RT & P	0.67g	0.05g	8
Kaolinite	RT & P	0.67g	0.05g	5%

* in 50mL of 0.1M CsCl solution

4.2 Ion Exchange Rate Experiments

The results of the first ion exchange experiment are given in Table 9, and the second in Table 10 with both sets of data plotted in Figure 12. In the first timed experiment, the adsorption of cesium onto montmorillonite appears to have been almost instantaneous because the sample that was withdrawn immediately after mixing contained 5.9 wt% of Cs, whereas the sample that was

decanted after 6 hours had adsorbed up to 6.1 wt% Cs. One sample (STx-1-24h) which was left for 24 hours, showed a slight drop in concentration of adsorption of Cs to 4.6 wt%.

Table 9: Cesium concentration in the first set of exchange rate experiments using montmorillonite

Sample Number	Time of Adsorption (hrs)	Wt % Cs Adsorbed
STx-1-1m	0.02	5.9
STx-1-30m	0.5	6.3
STx-1-1h	1	6.4
Stx-1-2h	2	6.4
STx-1-3h	3	5.9
STx-1-4h	4	6.0
STx-1-5h	5	5.9
STx-1-6h	6	6.1
STx-1-24h	24	4.6

Table 10: Cesium concentrations in the second set of ion exchange rate experiments using montmorillonite, (triplicate data are in Appendix C, Table AP-C3)

Sample#	Time of adsorption Time (hours)	Clay (Avg wt% Cs)	Solution (Avg wt% Cs)
M1	0.02	4.4±0.3	0.02±0.004
M10	0.2	3.8±0.2	0.01±0.002
M20	0.3	4.0±0.3	0.02±0.002
M30	0.5	4.0±0.3	0.02±0.004
M40	0.7	4.1±0.2	0.01±0.002
M50	0.8	3.5±0.2	0.01±0.002
M60	1	4.0±0.3	0.01±0.008
M2h	2	6.2±0.3	0.06±0.001
M3h	3	6.1±0.5	0.05±0.003
M4h	4	5.6±0.2	0.04±0.01
M5h	5	6.2±0.4	0.05±0.01
M6h	6	6.3±0.5	0.08±0.03
M1d	24	5.7±0.3	0.05±0.006
M2d	48	6.3±0.5	0.05±0.002
M3d	72	6.2±0.2	0.05±0.002
M4d	96	6.0±0.6	0.05±0.002
M5d	120	5.9±0.1	0.05±0.007
M6d	144	5.8±0.2	0.05±0.006
M7d	168	6.3±0.2	0.06±0.01

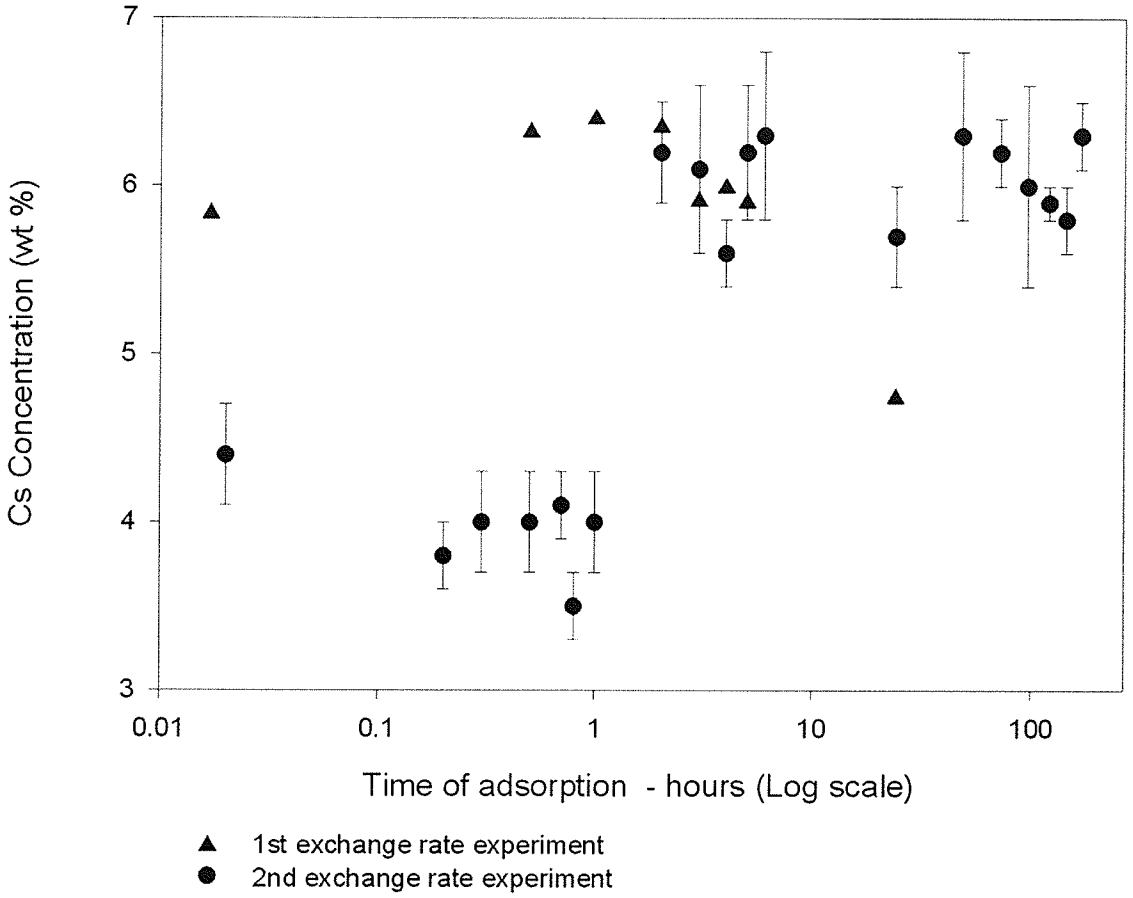

Figure 12: Cs adsorption in both sets of Cs exchange rate experiments using montmorillonite.

In the second exchange rate experiment, the initial sample, (M1) adsorbed 4.4 wt% of cesium after only a minute of adsorption time. In contrast to the first exchange rate experiment, this value remained constant for one hour. After two hours, the cesium content of the montmorillonite had increased to 6.2 wt% and remained at or near this level for the remainder of the experiment (Figure 12, Table 10). It is not readily obvious why the values of the Cs concentration in montmorillonite are different in the first hour of both exchange rate experiments. However, in the second exchange rate experiment, triplicate samples were used. Therefore, the results are believed to give more reliable data.

4.3 Ion Exchange in a Bacterial Culture

The amount of cesium adsorbed by montmorillonite increased from 6.9 ± 0.2 wt% to 7.5 ± 0.4 wt% when adsorption took place in the presence of bacterial culture (Table 11). For kaolinite, the amount of Cs adsorbed is 0.4 wt% compared with 0.8 wt% in the absence of bacteria. When the bacterial culture was mixed with cesium chloride without clay minerals, the amount of cesium adsorbed by the bacteria was 0.07 wt%.

Table 11: Cesium concentrations in montmorillonite and kaolinite after ion exchange in bacterial culture, at room temperature and pressure. Time of adsorption is 6 hours, (triplicate data are in Appendix C, Table AP-C4).

	Average Cesium Concentration	
Experiment	**Montmorillonite**	**Kaolinite**
Cs + Cy	6.9±0.2	0.4±0.4
Cs + Cy + B	7.5±0.4	0.4±0.1
B + Cs	0.07±0.01	0.07±0.01
Cs + Cy + Bst	7.0±0.3	0.3±0.1

Cs: 0.1M CsCl Solution
Cy: Clay Mineral
B: Bacterial Culture
Bst: Bacterial Culture Sterilized

4.4 Experimental and Measurement Errors

Any measurement or analytical results, no matter how careful the experiment is conducted, contains some degree of uncertainty. The averages of triplicate results are calculated with the standard deviation to show the degree of variability and the significance. Some of these uncertainties are introduced in the experimental design. Other sources of error are variations in environmental conditions such as temperature, pressure and relative humidity. Errors can also be introduced by the precision or detection limits of the analytical instruments. In many cases, the difference in the values is within the experimental error. The

ion exchange experiments were all done in triplicate and the average values were used in some places, (e.g. Table 10), whereas in others one value of the experiment was used (Table 7). All the experimental data are included in the appendices.

One source of error in this study came from washing the samples after ion exchange. Although the same amount of water was used to wash the samples, the vigour of washing may have differed. This could lead to some samples being washed more thoroughly than the others. In the preliminary experiments, after mixing the clay samples with CsCl, the mixtures were stirred to ensure homogeneity. They were also placed on the rocker and shaken occasionally. The variation in mixing techniques may have led to some samples adsorbing more than others due to differences in surface area of the grains exposed to the cesium chloride solution. This could have contributed to a variation of about 10% in the adsorption of Cs by montmorillonite under similar conditions. Some cesium may have been adsorbed on the surface of the glassware and filter paper causing a difference in Cs concentration. Another source of error is the analytical error generated from the detection limits of the analytical instruments used for the analysis of the clay minerals. Limits of determination are estimates of the accuracy of the determination depending upon the dilution needed. For the 10 major oxides analysed in this study, the limit of determination for ICP was about 0.025%.

CHAPTER 5 NMR RESULTS AND INTERPRETATIONS

5.1 ^{27}Al MAS-NMR Spectra in Clay Minerals

The ^{27}Al and ^{29}Si results of MAS NMR spectroscopy are summarized in Tables 12 and 13. Table 12 lists the peak positions and the peak widths of ^{27}Al, and Table 13 list the peak positions and peak widths of ^{29} Si. Depending on the width of the NMR spectra, the uncertainties in the measured peak position are estimated to be about 0.5 ppm for ^{27}Al and ^{133}Cs. For ^{29}Si the uncertainty is 0.1 ppm. The position of broad peaks may also vary slightly by the phasing technique.

^{27}Al resonance is assigned to the tetrahedral site when it is about 60 ppm, and to an octahedral environment when it occurs near 0 ppm (Thompson 1984, Sullivan et al. 1998). In the ^{27}Al MAS NMR spectrum of kaolinite, there is one prominent octahedral peak that shifts from 2.9 ppm to 3.1 ppm with cesium adsorption (Table 12, Figure 13). This shift may be within experimental error given the width of the peak. There is no clear evidence of a tetrahedral adsorption though a small tetrahedral peak is barely visible at 60 ppm in the spectrum of kaolinite before adsorption.

Table 12: ^{27}Al MAS NMR peak positions of spectra of montmorillonite, kaolinite and vermiculite at room temperature and pressure before and after ion exchange, including Peak Assignment

Mineral	Before Exchange	Peak width (Hz)	After Exchange	Peak width (Hz)	Site of adsorption
Kaolinite (KGa-1)	2.9 ppm	957Hz	3.1 ppm	1017Hz	O
Montmorillonite (STx-1)	2.3 ppm	1322Hz	1.5 ppm	1572Hz	O
Montmorillonite at 80°C	2.3 ppm	-	1.9 ppm		O
Montmorillonite at 107°C, 1.5 bar	2.3 ppm	-	1.9 ppm		O
Vermiculite (VTx-1)	66.4 ppm	1364 Hz	66.6 ppm	1169Hz	T
	8.6 ppm	-	8.0 ppm	242Hz	O

Table 13: ^{29}Si MAS NMR peak assignment of clay minerals before and after ion exchange

Mineral	^{29}Si (ppm)			
	Before	After	Shift	Assignment
Montmorillonite RTP	-93.5 ppm	-93.7 ppm	-0.2 ppm	Q^3(0Al)
Montmorillonite at 80°C	-93.5 ppm	-94.0 ppm	-0.5 ppm	Q^3(0Al)
Montmorillonite at 107°C, 1.5 bars	-93.5 ppm	-94.1 ppm	-0.6 ppm	Q^3(0Al)
Kaolinite	-91.4 ppm	-91.1 ppm	+0.3 ppm	Q^3(0Al)
Vermiculite	-84.4 ppm	-85.6 ppm	-1.2 ppm	Q^3(2Al)
	-88.4 ppm	-88.7 ppm	-0.3 ppm	Q^3(1Al)
	-92.8 ppm	-92.8 ppm	0.0 ppm	Q^3(0Al)

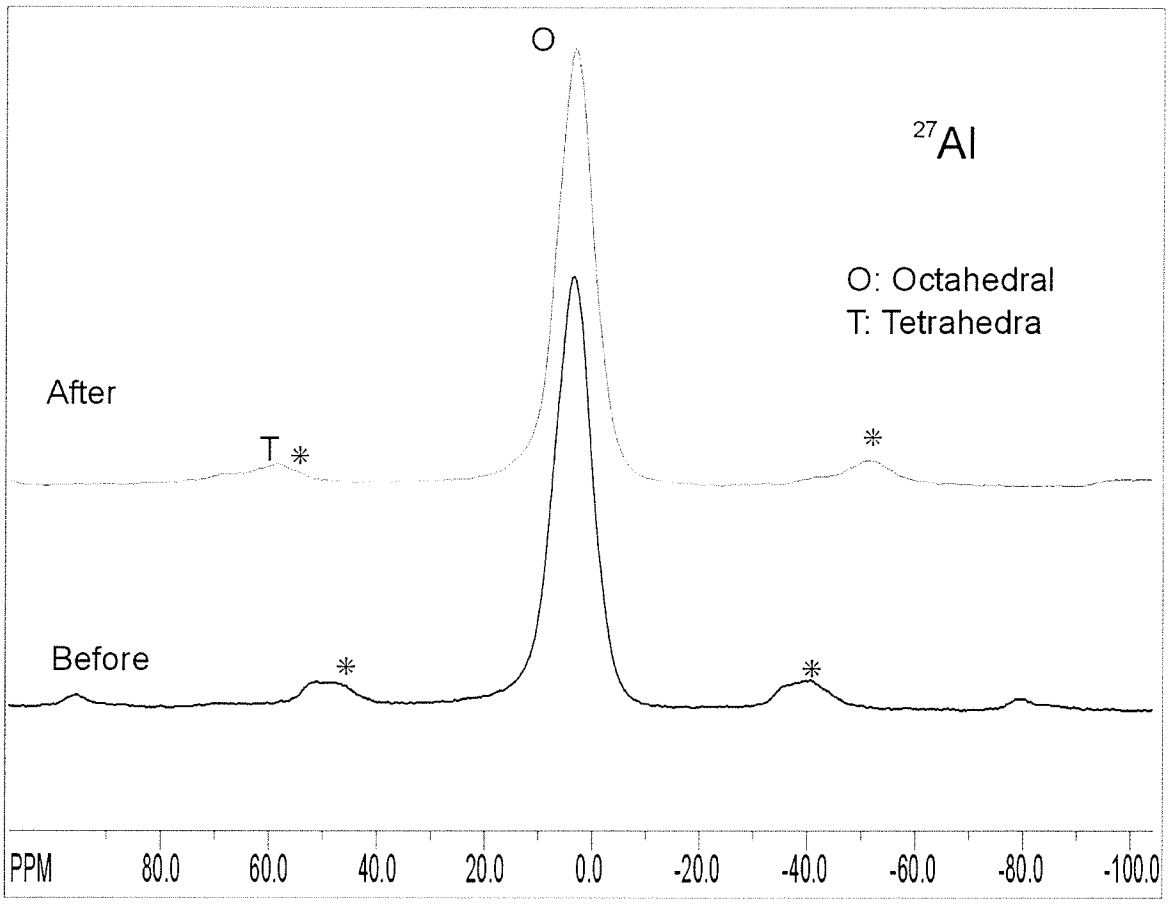

Figure 13: ^{27}Al MAS NMR spectrum of kaolinite at room temperature and pressure before and after ion exchange. The major peak positions occur at 2.9 and 3.1 ppm, respectively. * Indicates spinning sidebands.

The ^{27}Al MAS NMR spectrum of montmorillonite before ion exchange has a peak at 2.3 ppm with a peak width of 1322 Hz, which shifted to 1.5 ppm with a peak width of 1572 Hz after cesium adsorption (Table 12, Figure 14). The peak position after exchange at 80°C and at 107°C and 1.5 bars occurred at 1.9 ppm (Table 12, Figure 14). A small tetrahedral peak could have occurred at about 60 ppm as 0.5 apfu Al was calculated to be in the tetrahedral site from the structural formula. This tetrahedral peak would be hidden under the spinning side band that occupies the same location. A small peak was observed by Fyfe et al. (1986) in the tetrahedral site in a ^{27}Al spectrum of montmorillonite.

For vermiculite, there is no difference in the tetrahedral peak position, which occurred at 66.4 ppm (PW = 1364 Hz) before and at 66.6 ppm (PW = 1169 Hz) after ion exchange as the shift is within error of measurement. There is a small octahedral peak at 8.6 ppm that remained after exchange at 8.0 ppm (Table 12, Figure 15).

5.2 ^{29}Si MAS-NMR Spectra in Clay Minerals

The ^{29}Si results of MAS NMR spectroscopy are given in Table 13. The ^{29}Si MAS NMR peak positions listed for kaolinite, montmorillonite and vermiculite before and after the cesium ion exchange. The ^{29}Si MAS NMR chemical shifts are most sensitive to the number of Al ions occupying adjacent tetrahedral sites. The designation for full Al^{3+} substitution for Si^{4+} would be $Q^3(3Al)$, where Q^3 refers to the layer silicates and the (3Al) represents the number of Al^{3+} tetrahedra sharing oxygen with the SiO_4 tetrahedron (Lippmaa et al. 1981). With more Al substitution, the ^{29}Si spectrum will become deshielded (less negative).

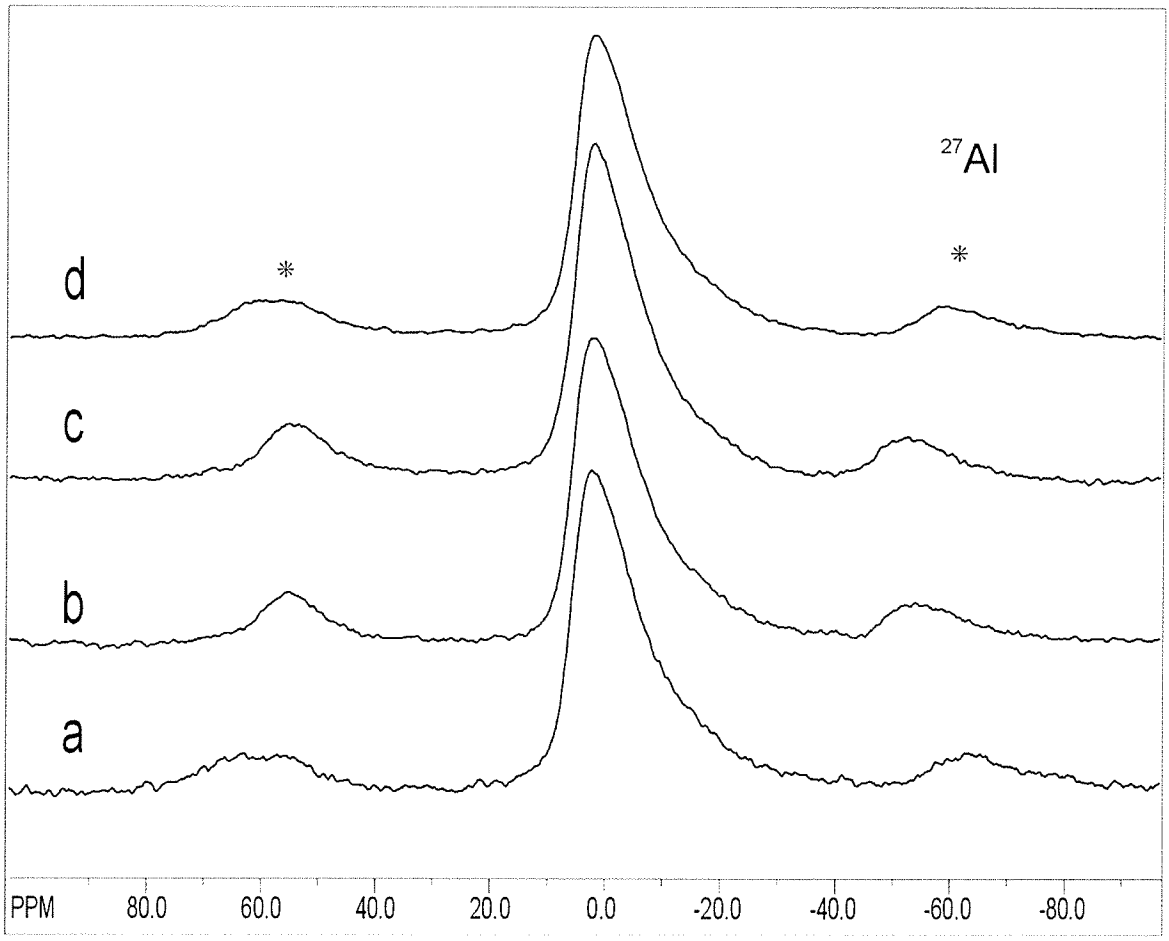

Figure 14: ^{27}Al MAS NMR spectra of montmorillonite: (a) before ion exchange, (b) after ion exchange at room temperature and pressure, (c) after exchange at 80°C, and (d) after exchange at 107°C and 1.5 bars pressure. * Indicates spinning sidebands.

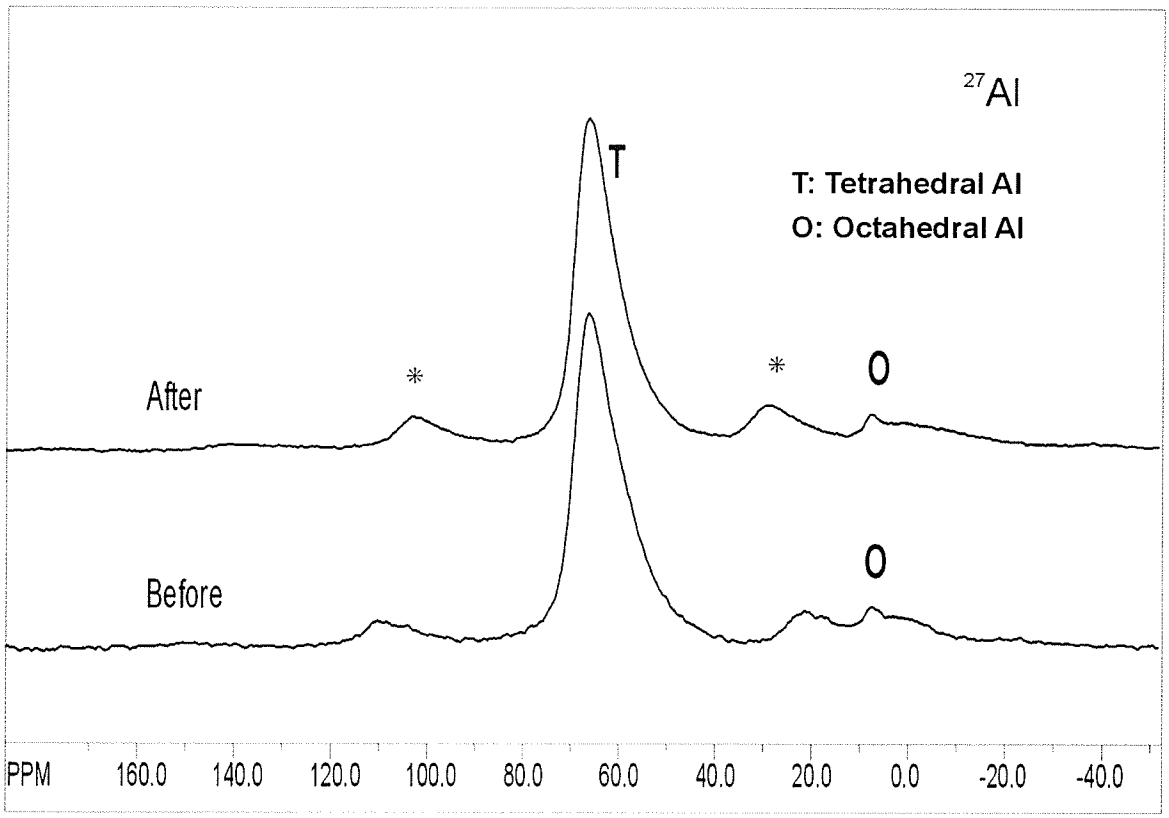

Figure 15: ^{27}Al MAS NMR spectrum of vermiculite at room temperature and pressure before and after ion exchange. The major tetrahedral peak positions before and after exchange occur at 66.4 ppm and at 66.6 ppm, respectively. * Indicates spinning sidebands.

The spectrum of kaolinite before ion exchange has a single peak at -91.4 ppm with a peak width of 182 Hz, which shifted by 0.3 ppm to -91.1 ppm after cesium adsorption (Table 13, Figure 16).

For montmorillonite at room temperature and pressure, the ^{29}Si MAS NMR peak shifted from -93.5 ppm (PW = 404 Hz) to -93.7 ppm (PW = 357 Hz) after cesium adsorption (Table 13, Figure 17) becoming more shielded. These peaks can be assigned to $Q^3(0Al)$ sites (Table 13). After ion exchange at elevated temperature and pressure (80°C and at 107°C and 1.5 bars) this montmorillonite peak becomes more shielded at -94.0 ppm (PW = 381 Hz) and at -94.1 ppm (PW = 415 Hz), respectively (Table 13, Figure 17). A peak at -111 ppm is due to impurities of cristobalite (Liang 1992). The shift of montmorillonite central peaks by -0.2 to -0.6 ppm (Table 13) indicates increased shielding with increasing temperature and pressure. The systematic shift is a result of the shielding caused by Cs^+ in the interlayer site in the clay structure.

Vermiculite showed three resonances before ion exchange at -84.4 ppm (PW= 373 Hz), -88.4 ppm (PW= 342 Hz) and at -92.8 ppm (PW=220 Hz). After ion exchange, the peaks shifted to -85.6, -88.7 and -92.8 ppm. (Table 13, Figure 18). The three peaks can be assigned to $Q^3(2Al)$, $Q^3(1Al)$ and $Q^3(0Al)$ respectively, in agreement with Thompson (1984), Engelhardt and Michel (1987) who assigned ^{29}Si resonances of vermiculite at -84.6 to $Q^3(2Al)$, at -88.7 ppm to $Q^3(1Al)$ and -92.9 ppm to $Q^3(0Al)$. The presence of three peak environments in vermiculite was interpreted by Thompson (1984) as a disordered vermiculite

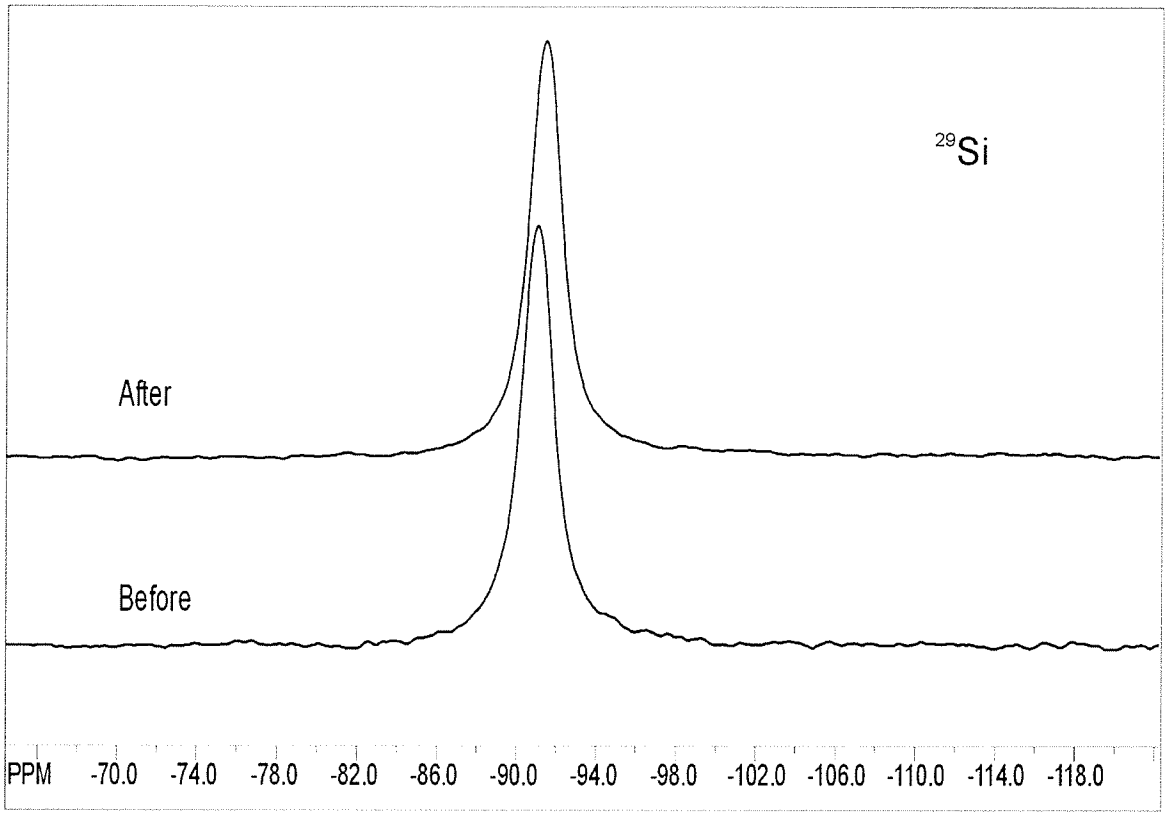

Figure 16: ^{29}Si MAS NMR spectrum of kaolinite before and after ion exchange. Peak at -91.4 and -91.1 ppm, respectively.

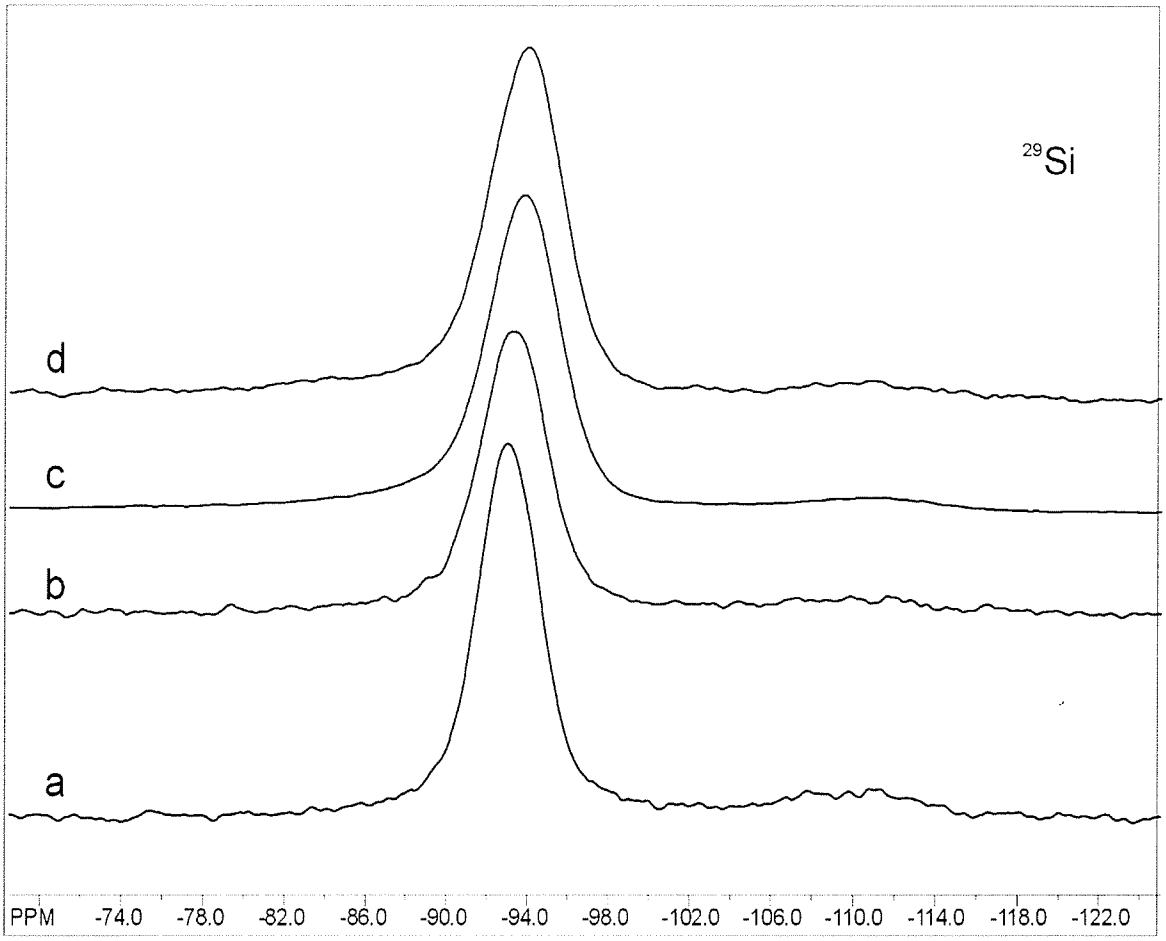

Figure 17: ^{29}Si MAS NMR spectra of montmorillonite: (a) before ion exchange, (b) after exchange at room temperature and pressure, (c) after exchange at 80°C, and (d) after exchange at 107°C and 1.5 bars pressure. Peaks occur at -93.5, -93.7, -94.0 and -94.1 ppm, respectively.

structure. He observed that regular ordering of 3Si:1Al in the tetrahedral site by maximizing the Al-Al distance would generate a single peak at -88.7 ppm. As three peaks were observed in this study, it can be interpreted that the vermiculite (CMS) sample used is disordered. Also in the ^{29}Si MAS NMR spectrum of vermiculite, the site giving the peak at -84.4 ppm has two Al adjacent with the substitution of Si^{4+} by Al^{3+}. This substitution produces less positive charge compared to the other sites, therefore more Cs^{+} is likely to be adsorbed at this site compared to the other site that has one adjacent Al. These two sites showed more shielding after Cs ion exchange indicating that the Cs cation is adsorbed close to the Al site to balance the overall negative charge. The site giving the peak at -92.8 ppm has no adjacent Al, has no charge and no Cs^{+} adsorption at the site, resulting in no change in peak position before and after Cs exchange.

5.3 ^{133}Cs MAS-NMR Spectra in Clay Minerals

The following sections describe the ^{133}Cs MAS NMR spectra of the clay minerals and some of the conditions that affected the presence or absence of peaks as well as changes in peak positions. The ^{133}Cs spectra of kaolinite, montmorillonite, and vermiculite were obtained both during the winter and summer after exchange at room temperature and pressure and for montmorillonite after exchange at high temperature and pressure. One spectrum was also obtained of montmorillonite after the sample was saturated to 100% relative humidity (RH).

5.3.1 Effect of Humidity on ^{133}Cs Spectra Peak Position

In colder months of the year, even air that is fully saturated with water vapour does not have as much moisture, hence the dryness and static electricity (Tarbuck and Lutgens 2000). In Winnipeg, at a temperature of -30°C only 0.3g of water vapour are required to saturate 1kg of air, whereas at 30°C, 26.5g of water vapour are required to saturate 1kg of air (Appendix B). In the winter when the cold air is warmed to 25°C within a building, there is very little moisture in the air compared to the amount of water vapour in the air during the summer.

The first ^{133}Cs MAS NMR spectra were obtained in March, when winter conditions still prevailed. The ^{133}Cs peaks for montmorillonite after ion exchange were -37.8 ppm and at 13.5 ppm. A second set of ^{133}Cs MAS NMR spectra were obtained in July when summer conditions prevailed. In this set, the peak positions changed to -28.4 and 23.5 ppm (Figure 19). The spectra obtained during the summer appear narrower, with better signal to noise ratio, and in general better resolved. Some M1 series samples that were run in winter were re-run during the summer, and the peak positions of these winter and summer re-runs (Table 14) were plotted in scatter plot diagram for comparison (Figure 20). Similar peak shifts between winter and summer data were observed for spectra of montmorillonite after exchange at high temperature and pressure (STx-1-Cst, and STx-1-Cstp) (Figure 21).

Table 14: ^{133}Cs MAS NMR spectra peak positions obtained from montmorillonite used in ion exchange rate experiment. Peaks 1A and 2A refer to peak positions of M1 series obtained in winter, whereas Peaks 1B and 2B refer to the peak positions of the same M1 series samples re-run in the summer.

Time of Adsorption (Hours)	Sample Series	Peak Positions (ppm) M1 Series			
		Peak 1A	Peak 2A	Peak 1B	Peak 2B
0.02	M-1	-37.4	42.7	-28.5	18.2
0.3	M-20	-40.9	34.2	-26.1	23.1
0.5	M-30	-42.5	30.4	-27.6	23.6
0.8	M-50	-29.2	29.0	-28.7	22.2
1	M-60	-43.1	30.0	-27.6	25.4
3	M-3h	-50.0	31.4	-28.5	24.7
6	STx-1-Cst	-50.0	-	-26.5	24.5
6	STx-1-Cstp	-77.0	-	-24.7	29.3

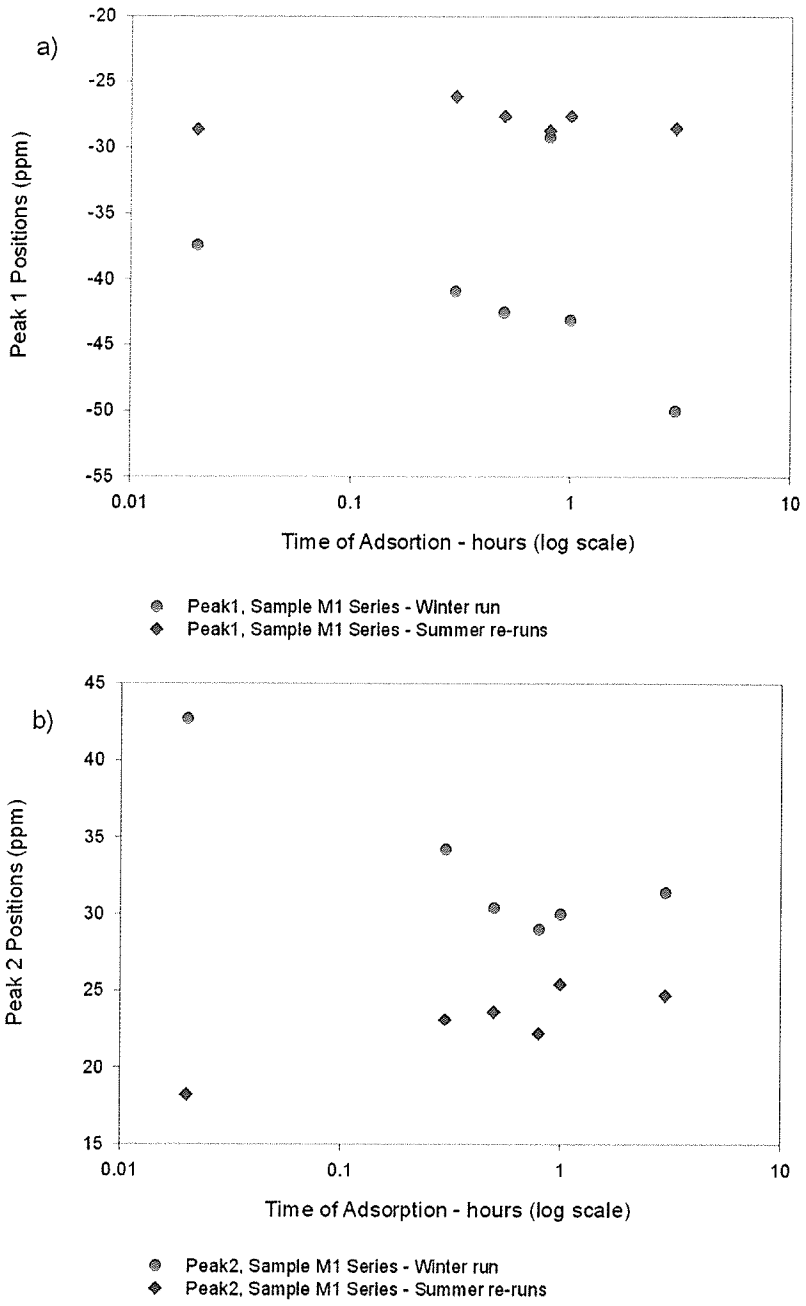

Figure 20: Scatter plot of peak positions (a) peak 1, and (b) peak 2 versus time of adsorption of Cs in montmorillonite for M1 sample series obtained in the winter (red circle) and re-run in the summer (blue diamond).

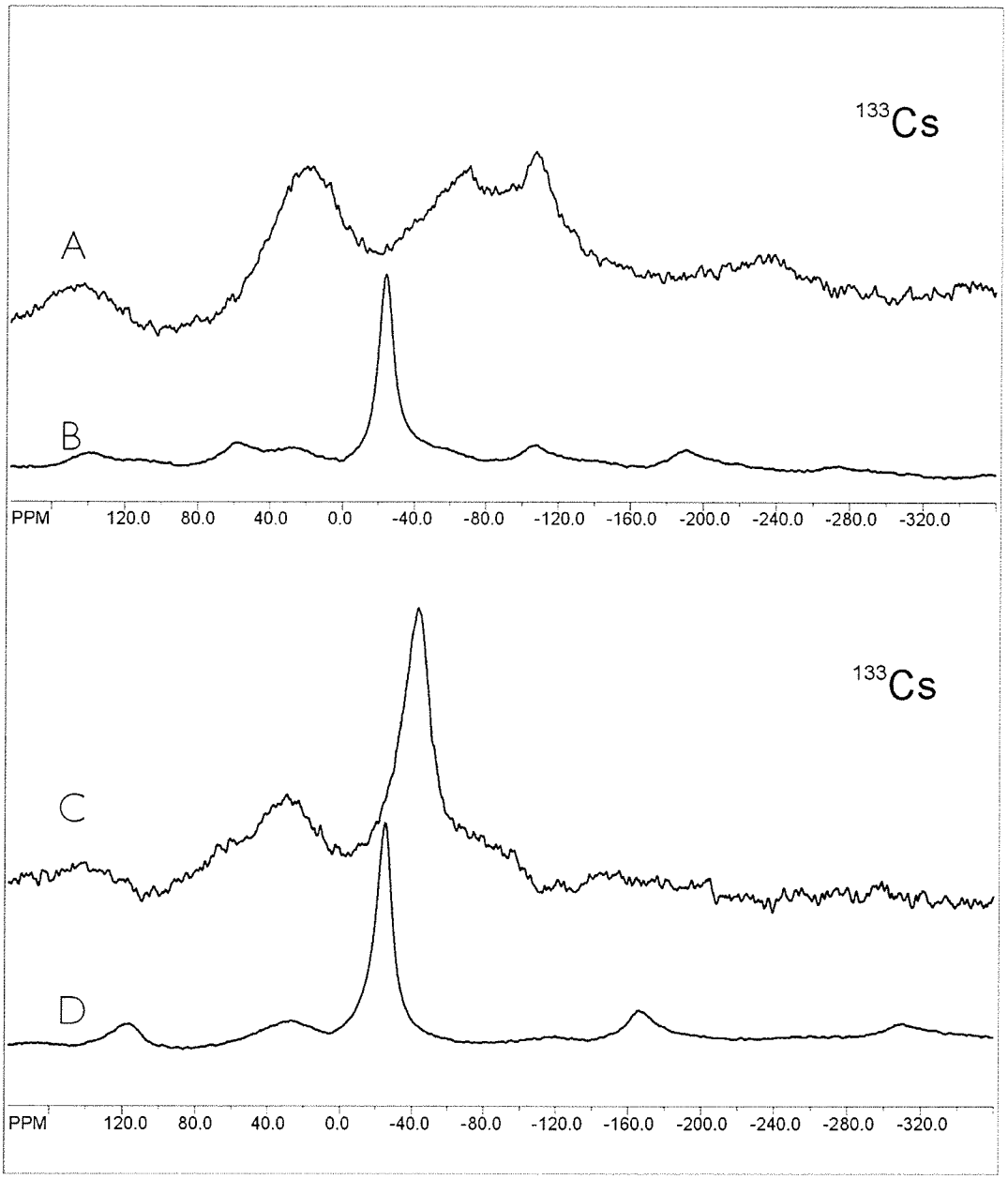

Figure 21: Winter and summer ^{133}Cs MAS NMR spectra of montmorillonite after exchange at 107°C and 1.5 bars: (A) winter, and (B) summer; and at 80°C, (C) winter and (D) summer.

The ^{133}Cs MAS NMR spectrum for montmorillonite after ion exchange obtained in the winter produced three peaks at -37.8 ppm, 13.5 ppm, and at 210.0 ppm compared to the peak positions obtained in the summer runs (Figure 19). Also montmorillonite exchange at 80°C produced three peaks in its winter run spectrum, at 22.9 ppm, 16.7 ppm and -50.0 ppm, and ion exchange at 107°C and 1.5 bars also produced the three peaks in winter run at 10.0 ppm, -77.0 ppm, and at -115.0 ppm. These are compared to spectra of the same samples spectra obtained during the summer that show better-resolved peaks. They also produced only two peaks (Figure 21). Again these differences are attributed to increased relative humidity during the summer months when the MAS NMR experiments were conducted. Both peaks tends towards 0 ppm which would be the peak location if the Cs cation is completely surrounded by water molecules.

The winter MAS NMR runs were conducted when there was very little amount of water vapour in the air even at room temperature, therefore the samples were drier because there was no moisture in the air for clay minerals to adsorb. Conversely, the little water in the clay minerals evaporated into the dry warm air in the laboratory. During the summer, however, the clay minerals were able to retain water and even adsorb more moisture from the air, increasing the amount of water molecules in the clay samples thereby remaining wet, and causing the Cs^+ to become mobile. Sullivan et al. (1998) observed that when montmorillonite is highly hydrated, the cation adsorbed in the interlayer move freely because of the increased amount of water molecules. This observation confirms the conclusion that Cs^+ becomes mobile due to the increased amount

of water molecule. Several authors (Kim et al. 1995, 1996a, b, Weiss et al. 1990a) observed that the ^{133}Cs chemical shift is very sensitive to local structure, composition and local environment. The increased amount of water molecules resulting from higher relative humidity in this case changes the local environment.

This interpretation is consistent with the observation by Kim et al. (1996b) that as the RH increases, additional water is adsorbed by hydrogen-bonding to other water molecules and making a continuous film of water in which the adsorbed Cs^+ can move. They also observed that the motion of the Cs is closely related to the mobility of surface water. For instance, Cs adsorbed by a clay mineral would be closer to the mineral surface in a thin layer of water and would be likely to be less mobile because of the thin layer. In a thick layer of water molecules, the Cs adsorbed will be further away from the mineral surface. With this increased space, it becomes more mobile as the water molecules move. This, as they suggested, would cause motional averaging and a chemical shift. Some samples were run after they had been saturated to 100% RH and in each case the samples generated only one sharp peak that shifted from -27.4 ppm at ambient RH to -24.8 ppm (M3-d7-Cs) at 100% RH whereas the second peak at 26.7 ppm at ambient RH disappeared completely (Figure 22). The single peak at 100% RH is most likely due to motional averaging of the two peaks that occurred at room RH.

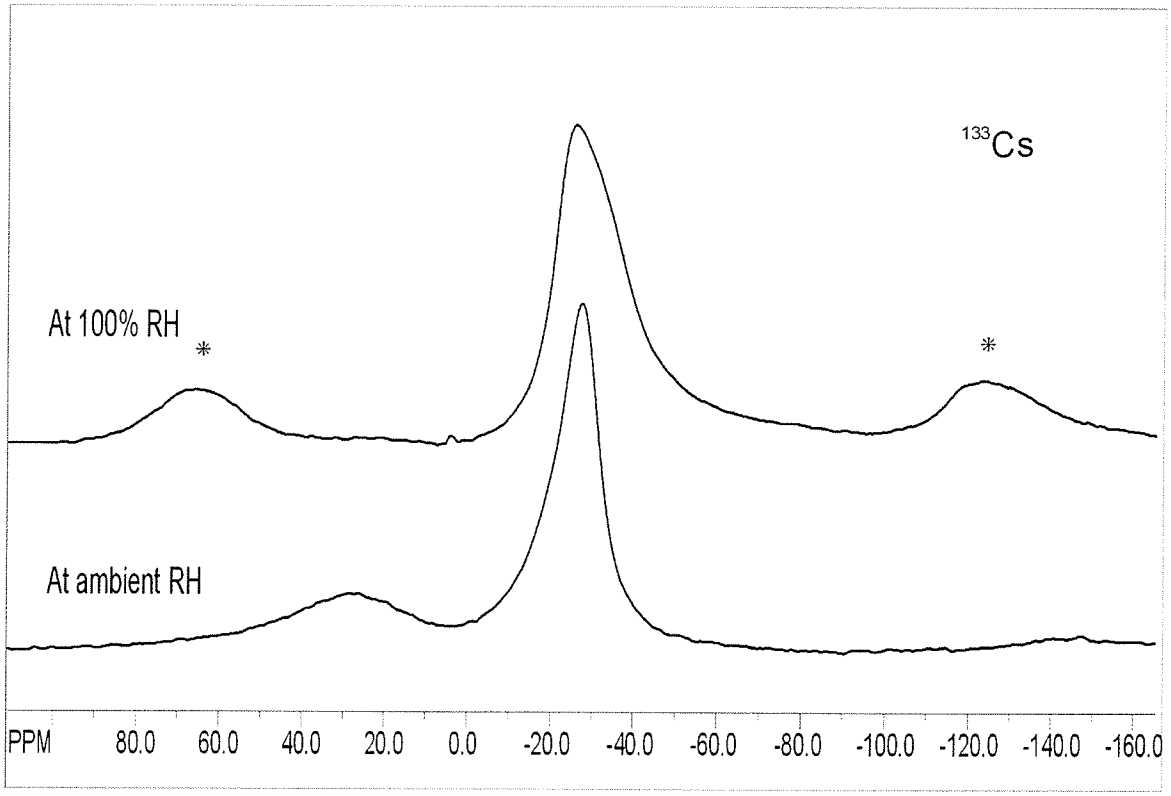

Figure 22: ^{133}Cs MAS NMR spectrum of montmorillonite (M3-d7-Cs): (a) at ambient RH, and (b) at 100% RH. Note single peak occurs at -24.8 ppm 100% RH, and two peaks -27.4 and 26.7 ppm at ambient RH. * Indicates spinning sidebands.

All the ^{133}Cs MAS NMR for M1 series of montmorillonite results reported in this section were obtained in winter and summer months of the year (Table 14), however, MAS NMR spectra of M2 and M3 series of the same mineral were obtained during the summer months. There is a distinct difference in peak positions between the winter and summer obtained spectra.

The ^{133}Cs MAS NMR spectra obtained during the summer has the following peak positions: For exchange at room temperature and pressure the peak occurs at -28.4 ppm, at 80°C the peak occurs at -26.5 ppm, and at 24.5 ppm whereas for the exchange, at 107°C and 1.5 bars, the peak occurs at -24.7 ppm and 29.3 ppm (Figure 21). This difference in peak position between the experiments is due to the effect of relative humidity. This conclusion agrees with the observation made by Kim et al. (1995), in their experiment in which they concluded that relative humidity affects the peak position of Cs^+ adsorbed in clay minerals.

5.3.2 ^{133}Cs MAS NMR of Kaolinite and Vermiculite

The ^{133}Cs MAS NMR spectrum of kaolinite consists of three peaks at 213 ppm, -21.4 ppm and -50.7 ppm which all disappeared after the sample was re-washed with distilled water (Figure 23). The peak at 213 ppm is assigned to CsCl on the surface. Kim et al (1995) obtained peaks at -24.4 ppm and -7.2 ppm, which they interpreted as being in an expandable site. Therefore their -24.4 ppm peak may correlate with the peak at -21.4 ppm.

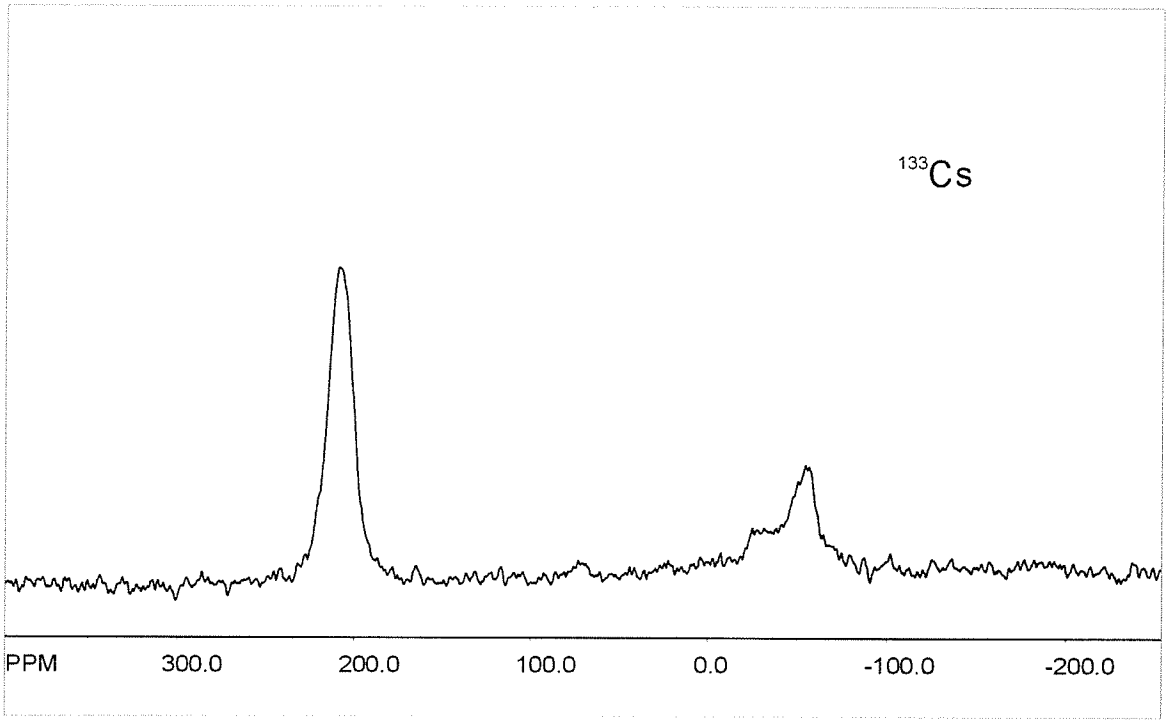

Figure 23: ^{133}Cs MAS NMR spectrum of kaolinite at room temperature and pressure after ion exchange.

The ^{133}Cs spectrum of vermiculite has a broad peak centered at 42.5 ppm with large spinning sideband (Figure 24). This is similar to the results obtained by Weiss et al. (1990a) of a peak centered at 55.1ppm with large spinning sidebands, which they assigned to dehydrated Cs in the interlayer sites. They argued that Cs in the vermiculite interlayer site is expected to be dehydrated and tightly bound to the basal oxygen because of the large negative tetrahedral layer charge. Therefore the peak observed in the ^{133}Cs of vermiculite sample is assigned to the vermiculite interlayer. The difference in peak position between this study and the values of Weiss et al (1990a) may be due to the problem of humidity discussed in section 5.3.1.

5.3.3 Surficial Adsorption of Cs

This section describes surface adsorption of cesium on kaolinite and the effect of re-washing the clay mineral. The spectral ^{133}Cs MAS NMR peak at about 213 ppm is interpreted as surface precipitation of solid CsCl as the spectrum of solid CsCl has a single peak at 217.7 ppm (Figure 25). Weiss et al. (1990a) observed a similar surface precipitation peak at 229 ppm, whereas Kim et al. (1995) observed the same effect at 200 ppm. Again, the variation in the peak position may be related to the absolute humidity.

The peak at 213 ppm in the ^{133}Cs MAS NMR spectrum of kaolinite disappeared after re-washing the sample as described in section 3.3.3. Similarly, the peak disappeared in the montmorillonite spectrum obtained at

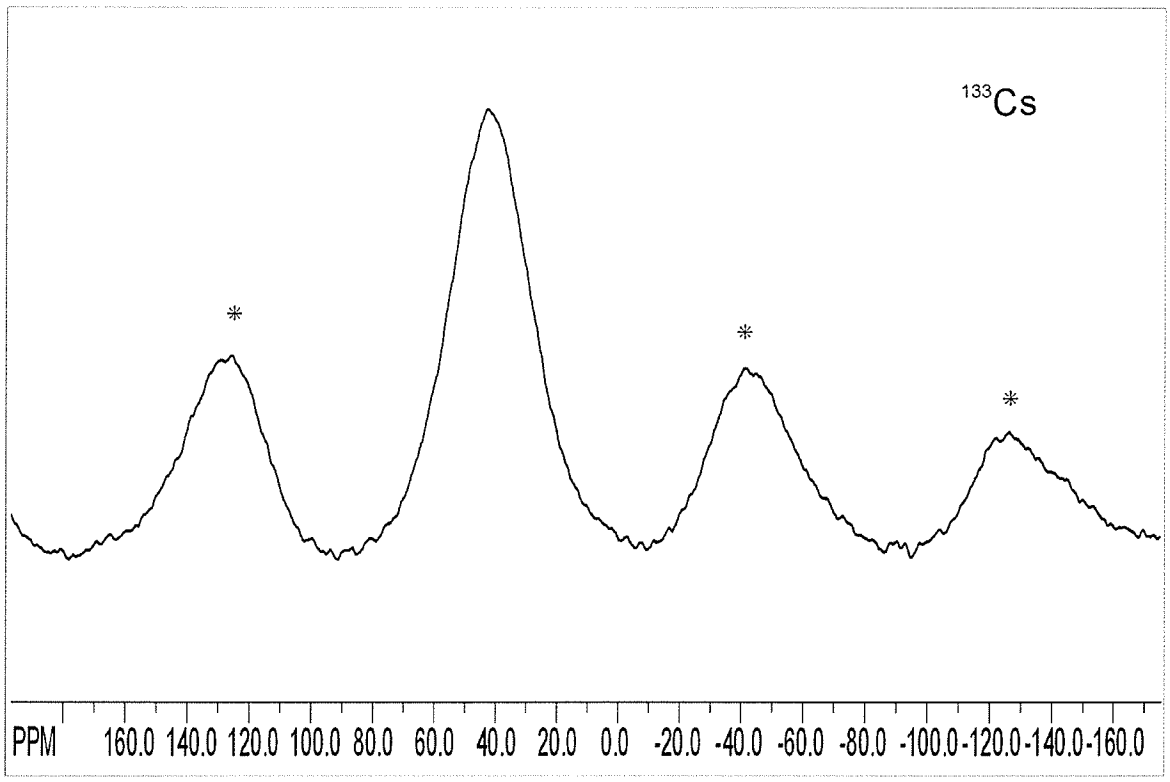

Figure 24: ^{133}Cs MAS NMR spectrum of vermiculite after exchange at room temperature and pressure. The centre band is at 42.5 ppm. All other peaks (*) are spinning sidebands (SSB).

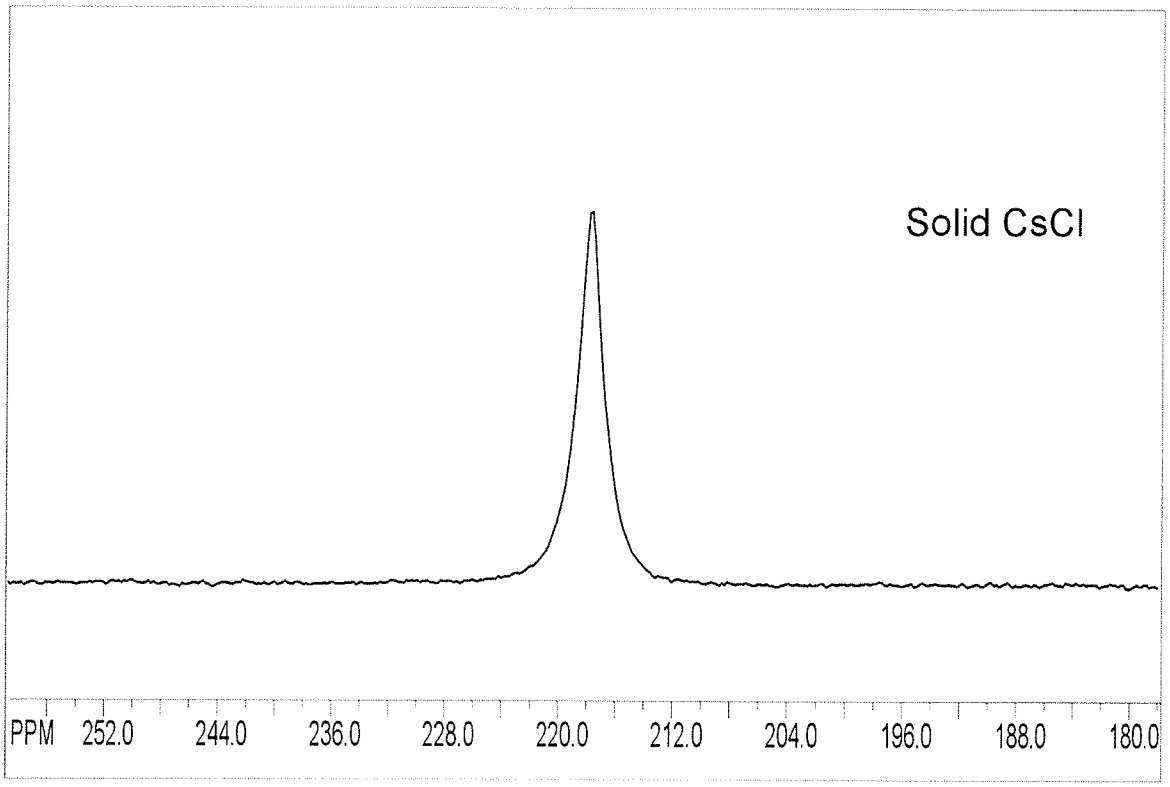

Figure 25: ^{133}Cs MAS NMR spectrum of solid CsCl. The peak occurs at 217.7 ppm.

higher humidity in the summer because the surface precipitation has been washed away. This confirms the interpretation of the peak at 213 ppm being due to precipitation of solid CsCl on the surface of kaolinite and montmorillonite.

The ^{133}Cs MAS NMR spectra of montmorillonite exchanged at 80°C and at 107°C and 1.5 bars did not show a CsCl peak probably because these samples were washed more thoroughly than the others.

Kim and Kirkpatrick (1998) reported some difference in the peak positions of ^{133}Cs NMR when they compared the results obtained after using different amounts of water to wash the clay samples compared to unwashed samples. They also noted a reduction in the intensity of the kaolinite spectra. In their study, they used small amounts of water (ranging from 1mL to 5mL) to wash the samples, which showed no difference in concentration of Cs among these samples. It should be noted that the amount of water they used to wash the samples was very small and may not have effectively washed the samples well. Washing the samples in this study with 50 mL of distilled water removed the entire solid surface CsCl precipitation. Therefore washing the samples three times with 50mL of distilled water in each case washed away the Cs^+ that was attached to the surface of the clay mineral as shown by the disappearance of the peak at about 213 ppm. The same amount of water was used to wash all samples, but some of the samples may have been washed (shaken) more vigorously or for a longer time than others.

5.3.4 ^{133}Cs MAS NMR of Montmorillonite

The ^{133}Cs MAS NMR spectra of montmorillonite obtained on samples ion exchanged at room temperature and pressure, at 80°C, and at 107°C and 1.5 bars have two peaks (Figure 26). The major peak for montmorillonite ion exchanged at room temperature and pressure occurred at -28.4 ppm (referred to as Peak 1), for the exchange at 80°C, at -26.5 ppm and for exchange at 107°C and 1.5 bars at -24.5 ppm. There is a second very broad peak at about 26 ppm (referred to as Peak 2) in all three spectra.

The positions of the two peaks in the second exchange-rate experiment with montmorillonite at room temperature and pressure (Table 15) do not seem to show any systematic changes in peak position. The differences observed are not significant because of the effects of humidity.

A trend was noted when the amounts of cesium adsorbed at the different sites was calculated as weight percent (Table 16). Similar proportions between peak 1 and peak 2 were observed for exchange rates at 80°C (CST-Cs2,3) and at 107°C & 1.5 bars (CSTP-Cs2,3) (Table 16). The amount of cesium in peak 2 remained relatively the same at about 1 wt % even after several days of adsorption time, while the amount of cesium going into peak 1 increased after 1 hour of adsorption time from 2.5 to 5.5 wt % (Figure 27).

The ^{133}Cs MAS NMR prominent peak of montmorillonite spectra -28.4 ppm, (Peak 1), is assigned to Cs^+ adsorption in the inner sphere of the interlayer (CS1) (Figure 28). Although the Cs^+ is tightly bonded to the basal oxygen of the inner sphere, it is affected by the increased amount of water molecules within the interlayer becoming less shielded resulting from increased

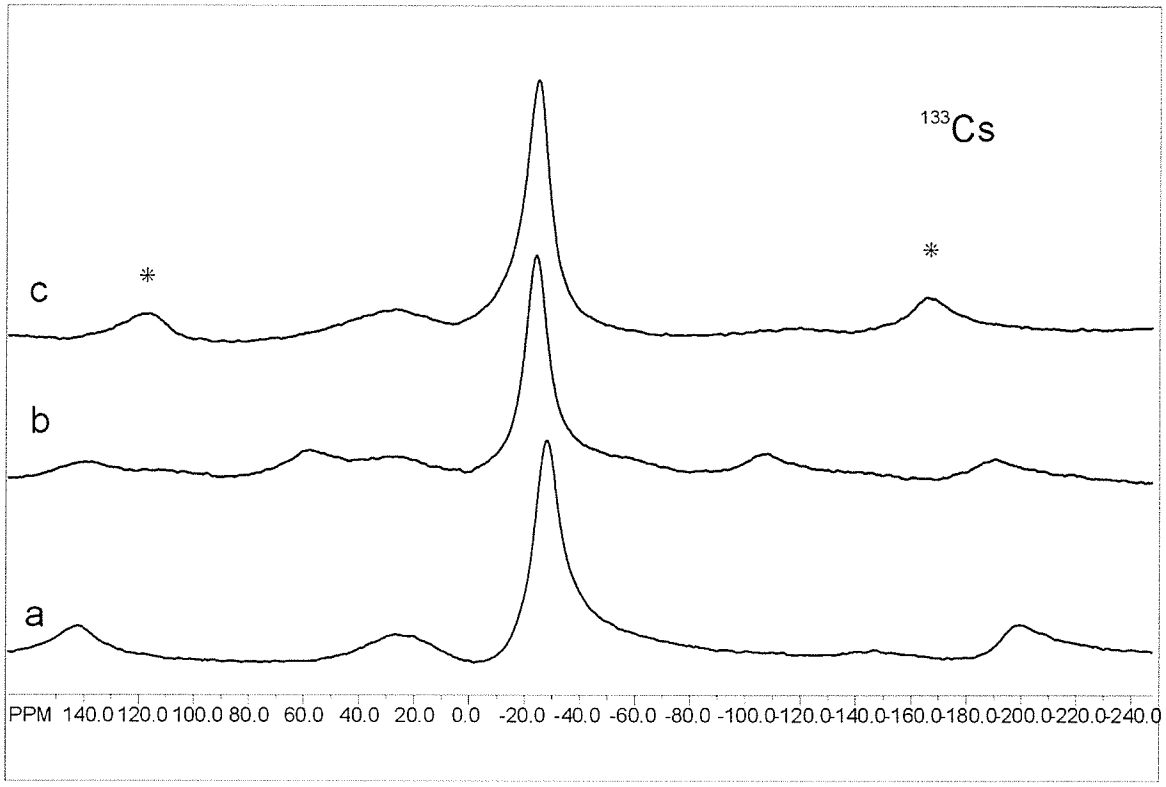

Figure 26: ^{133}Cs MAS NMR spectrum of montmorillonite: (a) after ion exchange at room temperature and pressure, (b) after ion exchange at 80°C, and (c) after ion exchange at 107°C and 1.5 bars. * Indicates spinning sidebands.

Table 15: ^{133}Cs MAS NMR spectra peak positions obtained from montmorillonite used in the second ion exchange rate experiment (M2 and M3) obtained in July, 2002

Time of Adsorption (Hours)	Sample Series	M2 series		M3 series	
		Peak 1 (ppm)	Peak 2 (ppm)	Peak 1 (ppm)	Peak 2 (ppm)
0.02	M-1	-28.4	23.5	-28.5	22.7
0.2	M-10	-29.2	26.3	-29.7	19.7
0.3	M-20	-28.0	28.8	-29.3	18.5
0.5	M-30	-	-	-	-
0.7	M-40	-27.5	27.3	-28.7	22.1
0.8	M-50	-27.0	28.1	-21.2	37.3
1	M-60	-	-	-	-
2	M-2h	-	28.2	-24.2	-
3	M-3h	-30.0	24.0	-24.3	29.1
4	M-4h	-28.7	26.6	-22.2	30.1
5	M-5h	-30.5	21.8	-	-
6	M-6h	-31.8	29.4	-25.1	27.2
24	M-1d	-28.8	22.0	-26.5	30.0
48	M-2d	-29.4	20.8	-	-
72	M-3d	-		-26.0	30.5
96	M-4d	-	-	-25.2	29.2
120	M-5d	-25.9	25.0	-	-
144	M-6d	-29.9	24.0	-22.8	29.8
168	M-7d	-		-27.4	26.7

Table 16: Calculated amount of Cs adsorbed at different sites in montmorillonite for M2 and M3 series (see more detailed table in Appendix C, Table AP-C5)

Sample	Weight Peak 1 (g)	Weight Peak 2 (g)	Cs Adsorbed wt%	Wt% of Cs in Peak 1	Wt% of Cs in Peak 2
M2-1-cs	0.1066	0.0482	4.42	3.04	0.09
M2-10-cs	0.3568	0.1968	4.03	2.60	1.43
M2-20-cs	0.3449	0.1969	4.11	2.62	1.49
M2-30-cs	-	*	3.77	-	-
M2-40-cs	0.3684	0.1294	4.31	3.19	1.12
M2-50-cs	0.2651	0.1056	3.60	2.57	1.03
M2-60-cs	*	*	4.19		
M2-2h-cs	*	*	6.41		
M2-3h-cs	0.1839	0.0332	6.39	5.41	0.98
M2-4h-cs	0.1402	0.0168	5.46	4.88	0.58
M2-5h-cs	0.1121	0.0167	6.34	5.52	0.82
M2-6h-cs	0.2851	0.092	6.88	5.21	1.68
M2-d1-cs	0.1434	0.0491	6.02	4.48	1.53
M2-d2-cs	0.12	0.0187	5.88	5.08	0.79
M2-d3-cs	-	-	6.29		
M2-d4-cs	*	*	5.32		
M2-d5-cs	*	*	5.92		
M2-d6-cs	*	*	5.62		
M2-d7-cs	0.2706	0.1991	6.45	3.71	2.73

Continued...

Table 16 (Concluded): Calculated amount of Cs adsorbed at different sites in montmorillonite

Sample	Weight Peak 1 (g)	Weight Peak 2 (g)	Cs Adsorbed wt%	Wt% of Cs in Peak 1	Wt% of Cs in Peak 2
M3-1-cs	0.1316	0.0422	4.59	3.47	1.11
M3-10-cs	0.2604	0.1418	3.81	2.47	1.34
M3-20-cs	0.1529	0.0883	4.11	2.60	1.50
M3-30-cs	*	*	4.31		
M3-40-cs	*	*	3.82		
M3-50-cs	0.3766	0.1697	3.20	2.21	0.99
M3-60-cs	*		3.61		
M3-2h-cs	0.3461	0.0641	6.40	5.40	1.00
M3-3h-cs	0.236	0.0351	5.52	4.81	0.71
M3-4h-cs	0.1658	0.0348	5.64	4.66	0.98
M3-5h-cs	*		5.84		
M3-6h-cs	0.339	0.0542	5.86	5.06	0.81
M3-d1-cs	0.1827	0.039	5.48	4.51	0.96
M3-d2-cs			6.79		
M3-d3-cs	0.3426	0.0555	6.31	5.43	0.88
M3-d4-cs	0.309	0.0471	6.52	5.66	0.86
M3-d5-cs			5.95		
M3-d6-cs	0.2643	0.055	5.62	4.65	0.97
M3-d7-cs	0.3136	0.0623	6.46	5.39	1.07
CST-Cs2	0.9444	0.1585	6.54	5.60	0.94
CST-Cs3	0.8674	0.1239	6.60	5.78	0.82
CSTP-Cs2	0.7853	0.2177	6.37	4.99	1.38
CSTP-Cs3	0.6408	0.089	6.05	5.31	0.74

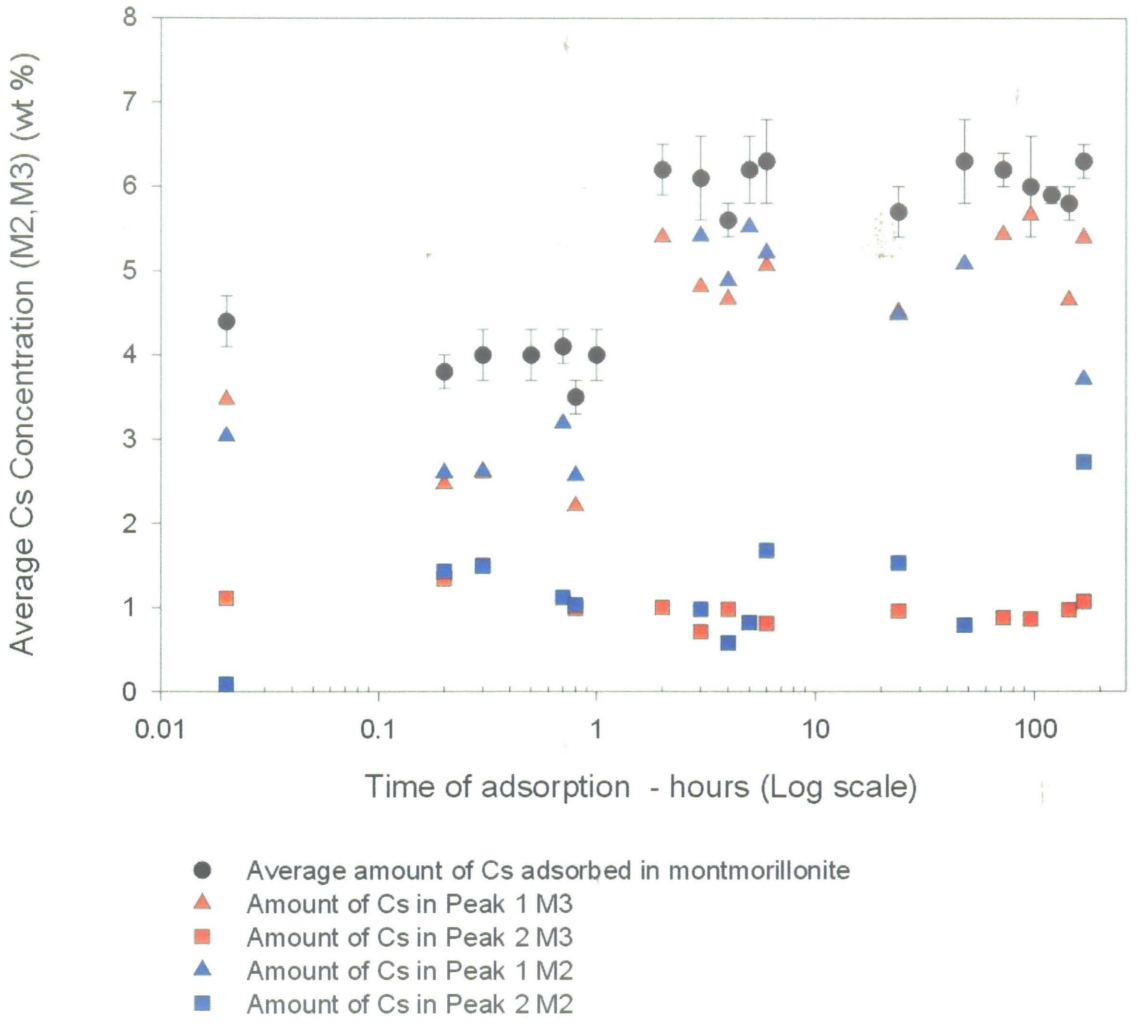

Figure 27: Cs adsorption in the second set of ion exchange rate experiments using montmorillonite, and the amounts of Cs adsorbed in ^{133}Cs MAS NMR Peaks 1 (triangles) and 2 (squares).

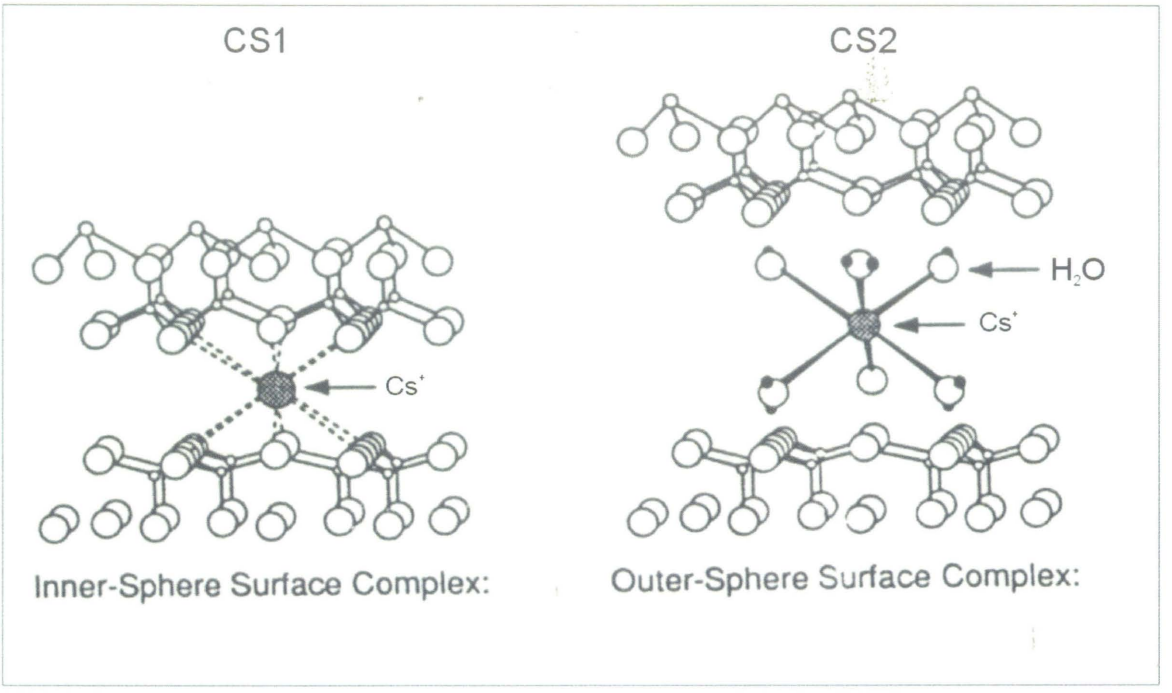

Figure 28: Inner and outer sphere surface complexes between cation and siloxane ditrigonal cavity in 2:1 clay structures (modified from Sposito 1984).

humidity that made the cesium cation mobile. Peak 2, at 23.5 ppm is due to Cs adsorbed in the interlayer (CS2) but less tightly bonded because it is bonded to water molecules of the outer sphere. These assignments correspond to those of Kim et al. (1996a&b, 1995) and Weiss et al. (1990a), in the same range to CS1 (Stern layer) and CS2 (Gouy layer) respectively.

The multi-site adsorption model proposed by Comans et al. (1991) is used to explain the variable rate of adsorption of Cs at the CS1 and CS2 sites. The rapid uptake occurs at the basal oxygens of the outer sphere of the interlayer by first attaching to the interlayer water molecules, and the slow up take continues as Cs penetrates into the inner sphere of the interlayer. With this model, it is expected that over an extended period of adsorption time, the amount of Cs adsorbed on the basal oxygen of the inner sphere (CS1) of the interlayer will increase and exceed the amount of Cs adsorbed on the oxygen of the outer sphere also in the interlayer (CS2) (Figure 28).

The amount of cesium adsorbed in the interlayer (Peak 1) increased from about 3.04 wt % of cesium in the first minute of adsorption to 5.41 wt % of cesium after 1 hour (Table 16) and then stayed about the same till end of seven days adsorption time. Conversely, the amount of cesium adsorbed on the site represented by peak 2 that is on water molecule of the outer sphere also in the interlayer stayed constant at about 1.0 wt % of cesium throughout the adsorption experiment (Table 16). Also there is a noticeable difference in the properties of the peaks from samples that have longer adsorption time compared to samples with shorter adsorption time. The peaks of samples with longer adsorption time are sharper and better resolved (Figure 19).

CHAPTER 6 DISCUSSION

The adsorption of Cs^+ onto clay minerals is influenced by a number of factors, including concentration of CsCl in solution. In non-selective exchange, the concentration of the cations with large hydration energies such as Mg^{2+}, Na^+, Ca^{2+}, or Sr^{2+} are equal to the amount of cation adsorbed by the clay mineral. In selective exchange, cations with smaller hydration energies such as K^+, NH_4^+ and Cs^+ are preferentially adsorbed by clay from solution. These preferentially adsorbed cations are usually held tightly and generally are not easily replaced. This process is called fixation. Cation fixation is caused by the force of attraction of the cation for a hydration shell of water (hydration energy), and the electrostatic attraction between the cation and the clay. Generally, large monovalent cations such as Cs^+ have small hydration energies, hence there is a large electrostatic attraction between the cation and the clay mineral. This causes the preferential adsorption of cations with low hydration energies (Weiss et al. 1990a).

The layer charge of the clay mineral may also affect the amount of Cs adsorbed because the cation is adsorbed to balance the negative charge created by isomorphic substitutions of a lower charged cation (Al^{3+}) for a higher charged cation (Si^{4+}) in the tetrahedral layer or the substitution of Al^{3+} or Fe^{3+} in octahedral sites by ions of lower charge such as Fe^{2+} and Mg^{2+}. Clays with lower layer charge, such as kaolinite, have a lower CEC, whereas those with larger layer charge, such as montmorillonite, have higher CEC as well as possible

adsorption in the interlayer. Because of the low layer charge on kaolinite, most sites on kaolinite surfaces are un-reactive and the only reactive sites are located along the edges of the sheets (Sposito 1984). Smectite and vermiculite all have significant permanent charge and have reactive sites. Besides the presence of surface hydroxyl groups in clays with permanent charge, they also have rings of siloxane groups that occur on the basal planes of the interlayer region. The type and size of the interlayer exchangeable cation and the type of clay (1:1 versus 2:1 layer) may also affect adsorption (Weiss et al. 1990a, Sawhney 1972).

An outer sphere is formed between the exchangeable cations and the ditrigonal cavity. The outer sphere is the complex in which there is at least one layer of water molecules between the complexing ion and the functional group (Davis and Kent 1990, Sposito 1984). Substitution in the tetrahedral layer leads to a larger layer charge, a higher charge density, and higher permanent charge on the ditrigonal cavity. This higher permanent charge in ditrigonal cavity favours formation of inner sphere complex between interlayer cations and ditrigonal cavities, which means that there is no water (solvent) molecule layer between the cation and the site of adsorption. The configurations of both the inner and outer sphere (Figure 28) make them likely sites for cation attachment at the interlayer. Therefore the presence of both the inner and outer spheres in clay minerals has some influence on the cation adsorption. The attachment in the inner sphere is tightly bound, whereas the cation on the outer sphere is loosely held.

In the Cs adsorption experiments, montmorillonite adsorbed cesium more effectively than illite, kaolinite, and vermiculite. Bentonites, which contain

montmorillonite as their main constituent, also adsorbed cesium effectively. These results appear to be related to the structural properties of the various clay minerals because montmorillonite has a larger layer charge, higher CEC and more sites for Cs adsorption.

When clay particles are suspended in 0.1M CsCl solutions, Cs^+ has access to the whole surface area of the clay mineral particle and to the sorption sites that exist in that mineral. Kim et al. (1996b) reported several possible sites where adsorption can take place: crystalline tops and bottoms of the grain, broken crystal edges, frayed edges, and interlayer sites. The interlayer sites are limited to the 2:1 layer clays that have exchangeable cations.

Kaolinite has no exchangeable cation, and it also has a very low layer charge hence it adsorbed only 0.8 wt% Cs^+ (0.018 Cs apfu). The Cs^+ is likely to be adsorbed on the expandable layers, broken edges, tops and bottoms of the grain. McBride (1994) suggested that the silonol group is the most probable edge site in kaolinite to adsorb cations at pH < 7. The ^{133}Cs MAS NMR spectrum of kaolinite suggests that there is precipitation of solid CsCl on the surface of the grain indicated by the prominent peak at 213 ppm. After re-washing as described in section 3.3.3, and repeating the MAS NMR analysis during the summer, the peaks at 213 ppm, -21.4 and at -50.7 ppm disappeared, leaving only a small peak at 4.0 ppm. This suggested that the 213 ppm peak which is a surface precipitation has been washed away. This was confirmed by the CsCl spectrum, which gave a strong prominent peak at 217.7 ppm (Figure 25).

In contrast to kaolinite, montmorillonite is 2:1 layer clay and possesses more adsorption sites and adsorbed most cesium, 0.40 apfu. Vermiculite, also a 2:1 layer mineral, also had relatively high Cs adsorption, at 0.34 apfu for vermiculite (WARD) and 0.23 apfu for vermiculite (CMS) samples.

McBride (1994) suggested that the less hydrated cations such as Cs^+ and K^+ are expected to come in contact with the sample surface by pushing aside the water molecule to make contact with oxygen atoms on the crystal basal surface. This direct contact with surface oxygen causes the nearest and the next nearest neighbouring environment and chemical shift to be different from those of the loosely bonded Cs, resulting in two peaks, one of which is loosely bonded and the other tightly bonded (Kim et al. 1996a). Montmorillonite spectra of samples with ion exchange at room temperature and at higher temperature and pressure also have two peaks indicating adsorption of cesium at two sites in the montmorillonite clay. The Cs^+ adsorption in the interlayer of a 2:1 clay may not be easily removed by washing the sample, however, increased amount of water molecules in the interlayer may make the cations more mobile changing its local environment. Therefore, washing does affect the shape, intensity or peak location due to the mobility of Cs^+ with introduction of more water molecules in the interlayer. The change in peak location and shape may also be related to the collapse of the structure of the clay mineral after substitution or the increased amount of water molecule (Sawhney 1972).

Kim et al. (1996b) observed that the presence of low hydration energy cations such as K^+ or Cs^+ in the interlayer tends to draw together the negatively

charged frayed edges. The cation presence increases the force of attraction between the two edges, which continue to move closer together until they collapse inward to create a stable structure. The collapse in montmorillonite is random when cesium is adsorbed, and in vermiculite the collapse is in alternate layers (Sawhney 1972). These collapses in clay mineral structures may be useful for the disposal of the used nuclear fuel waste program because in trapping the Cs^+ cation within the interlayer, they prevent the cations from any chance of desorption or being carried away by groundwater. These may also have some negative effect if the clays in the buffer are dry because collapsing of in clay mineral structures in the buffer zone can lead to formation of fissures or fractures and therefore creating more open conduits in the zone.

The results of the first exchange rate experiment indicated that the adsorption of Cs^+ in montmorillonite was instantaneous because the amount of cesium adsorbed by the clay sample that was withdrawn within one minute of mixing with 0.1M CsCl was 5.9 wt%. This amount increased slightly to 6.4 wt% after two hours of adsorption, after which the concentration remained fairly stable, even after six hours of adsorption time. One montmorillonite sample was left for 24 hours, and the amount of Cs adsorbed was 4.6 wt %. By the end of 24 hours, there was little CsCl left in the solution, so there is a possibility that Cs migrated out into the solution given the lower concentration of Cs in the clay.

In the second exchange rate experiment the concentration of cesium that was adsorbed in the first hour, when samples were washed every ten minutes, ranged from an average of 4.4 wt% in the first minute to an average of 4.0 wt%

in the first hour (Appendix C, Table AP-C3). However, at the end of the second hour when the samples were being washed every hour, the cesium concentration increased dramatically to 6.2 wt%. At the end of seven days, when samples were washed every day for seven days, the concentration of cesium remained at 6.3 wt% not changing much from the concentration adsorbed at the end of second hour. The experimental condition in the second exchange rate experiment is very different from the first exchange rate experiment, and it is possible that the difference between the designs of the two experiments is the source of the difference in the amount of Cs adsorbed. It is uncertain what caused the sharp increase after the first hour. It could be due to cesium cation penetrating into the inner sphere of the interlayer. The initial rapid uptake may have started at both sites in the interlayer, and CS2 site (peak 2) reached maximum capacity rather quickly (within 1 minute) such that the amount of Cs going into the site remained stable for the rest of the adsorption time. In the case of CS1 site (peak 1), the amount of Cs going into this site continued to increase from the initial concentration to capacity at the end of the second hour of adsorption time. It remained at this level for the rest of the seven days of adsorption time. The amount (~0.9 wt %) of Cs in CS2 site (peak 2) remained relatively the same, however, with increased temperature and pressure, the amount of Cs in CS1 site (peak 1) of the clay mineral (M3-6h-cs) increased from 5.06 wt% after exchange at room temperature and pressure to 5.69 wt% after exchange at 80°C and to 5.2wt % after exchange at 107°C and 1.5 bars. This increase indicates that as the clay mineral is heated up, the Cs is more tightly

bound. It also suggests that even as the CS2 is saturated, the CS1 site continues to adsorb Cs until it reached saturation (Figure 27)

In general, only about 52% of the cesium in solution was adsorbed by the clay minerals, and about 0.03% remained in the solution (Table 10). The rest of the cesium may have been lost to adsorption to the glassware or filter paper. Montmorillonite adsorbed 6.6 wt% of cesium when the ion exchange experiment was conducted at 80°C and 6.2 wt % at 107°C and 1.5 bars. Therefore higher temperatures and pressure do not appear to enhance adsorption of cesium.

The presence of active bacteria contributed to the sorption of cesium. In the ion exchange experiment in the presence of active bacteria, montmorillonite adsorbed 7.5 wt% cesium, the most adsorbed by any of the clay minerals. This is in agreement with the results of the study by Stroes-Gascoyne et al. (2000) that showed that radionuclides can adsorb on biofilms produced by bacteria. The ion exchange experiment with only active bacteria (no clay) shows Cs adsorption of 0.07 wt% (Table 11). Therefore out of the 7.5 wt% cesium adsorbed by clay minerals in the presence of active bacteria, adsorption by the bacteria contributed 0.07 wt% of the total. The additional amount of cesium adsorbed by the bacterial culture suggests that the presence of a bacterial consortium in and around a repository would be advantageous in that it would increase sorption and hence retard movement of cesium.

Relative humidity also played an important role in the chemical environment of Cs in the interlayer. The evidence of this role is noted in the difference in the peak positions and spectra of ^{133}Cs MAS NMR of

montmorillonite conducted during the winter and summer. With increased amount of water in clay samples due to higher RH during the summer, the peak positions of shifted towards 0 ppm or hydrated Cs^+ cation, and in some cases resulted in motional averaging.

The ^{29}Si MAS NMR of montmorillonite showed a systematic shift from before exchange (peak at -93.7 ppm), after exchange at room temperature and pressure (peak at -93.7 ppm) through exchange at 80°C (peak at -94.0 ppm) to exchange at 107°C and 1.5 bars (peak at -94.1 ppm). These incremental shifts from -0.2 to -0.6 ppm towards more shielding showed that as the clay is heated, Cs becomes more tightly bonded and hence more shielding.

In the ^{29}Si MAS NMR spectrum of vermiculite, the sites assigned to $Q^3(2Al)$ and $Q^3(1Al)$ adsorbed Cs compared to the site assigned to $Q^3(0Al)$ which has no Cs adsorbed at the site hence no additional shielding and no shift in peak position. Cs is probably adsorbed close to the Al site to balance the overall negative charge.

CHAPTER 7 CONCLUSIONS

A deep geological repository for used nuclear fuel waste would be likely to contain sealing materials that include large amounts of montmorillonite. The fracture zones of crystalline rocks in the Canadian Shield, in which a repository could be constructed, are likely to contain kaolinite, illite, vermiculite and possibly montmorillonite. These clay minerals have been shown to adsorb varying amounts of cesium. In the adsorption experiment conducted for this study, montmorillonite adsorbed cesium more effectively than vermiculite, illite, and kaolinite. Bentonites, which contain large amounts of montmorillonite were also used in this study and adsorbed cesium effectively.

The presence of bacteria in solution increases the adsorption of cesium indicating that the presence of a bacterial consortium in and around the repository environment could enhance sorption and retard movement of cesium by adsorbing the cation. Therefore, it can be concluded from this study that the presence of bacterial consortium in the repository would help prevent radionuclide migration. Biofilms produced by the bacteria consortium will also help to plug pore spaces in the clay mineral and thereby effectively prevent the migration of radionuclides (Stroes-Gascoyne and West, 1997).

Cesium adsorption onto clay minerals is rapid and takes less than one minute. After the initial rapid uptake, the concentration of cesium in clay minerals increases after one hour as the cesium cation penetrates into the inner sphere of the interlayer and then remains relatively constant. The adsorption of

cesium seems to occur in two stages. The first stage involves a rapid or instantaneous adsorption that takes place mostly at the outer sphere of the interlayer, and the second stage is the continued slower process in which the cesium penetrates into the inner sphere of the interlayer of 2:1 layer clays.

The ^{133}Cs MAS NMR results show that cesium is adsorbed in several sites in the clay minerals. It occurs on the surface in kaolinite and in the interlayer of 2:1 clay minerals. Cesium is tightly bonded on the basal oxygen (CS1) in the interlayer, and is also loosely bonded on the basal oxygen (CS2) also in the interlayer. On the average, about 76% of the cesium adsorbed by montmorillonite clay is adsorbed in the CS1 (Stern layer) in the interlayer, whereas only about 24% is adsorbed in the CS2 (Gouy layer) also in the interlayer. ^{133}Cs spectra peaks occurring at 213 and 211 ppm in the kaolinite and montmorillonite respectively were proven to be a solid CsCl precipitation from residual solution onto clay surface.

Washing the samples with large amounts of water after Cs exchange affects the Cs environment, and in some cases removes the surface precipitation of solid CsCl.

Elevated temperature, pressure and extended adsorption time do not appear to affect the quantitative amount of cesium adsorbed by clay minerals. However, these factors do affect the site at which the Cs^+ is adsorbed, as shown by the NMR spectra.

High relative humidity during the summer is shown to affect the cesium environment in the clay mineral structure. At ambient relative humidity, the ^{133}Cs

spectrum of montmorillonite exhibited two peaks, however, at 100% relative humidity, the same sample exhibited only one peak that is better resolved and less shielded. The single peak may be due to motional averaging. The difference in the peak positions between the winter and summer runs are explained by the difference in relative humidity between the two periods.

The ^{27}Al and ^{29}Si MAS NMR study of clay minerals enables researchers to directly observe the distribution of the aluminum cation between the tetrahedral and octahedral sites in a given clay mineral. However, presence of iron (Fe_2O_3) causes some broadening, hindering collection of reliable data. In kaolinite and montmorillonite, ^{27}Al occur mostly in the octahedral sites, though there maybe a small presence in the tetrahedral site. Vermiculite on the other hand, has most of its aluminum in the tetrahedral site with a very small amount in the octahedral site.

The ^{29}Si MAS NMR provides information about the clay structure especially about the Si/Al substitution in the aluminosilicate. The ^{29}Si peaks for montmorillonite and kaolinite occurring in the -91.1 to -93.5 ppm range are assigned to $Q^3(0AL)$, whereas the three peaks in vermiculite are assigned to $Q^3(2Al)$, $Q^3(1Al)$ and $Q^3(0Al)$ respectively. ^{29}Si MAS NMR of montmorillonite under different conditions shows a systematic shift from exchange at room temperature and pressure through exchange at 80°C to exchange at 107°C and 1.5 bars. This shows an incremental shift towards more shielding from -0.2 to -0.6 ppm with increased temperature and pressure due to the fact that when the

clay is heated up the Cs^+ is more tightly bonded, hence more shielded (Figure 17).

This Si/Al substitution in some vermiculite sites produces less positive charge compared to the other sites; therefore more Cs^+ is adsorbed at Si sites adjacent to Al compared to the other sites with less or no neighboring substitutions. Two sites showed more shielding after Cs ion exchange indicating that Cs cation is adsorbed close to the Al site to balance the overall negative charge. The site giving the peak at -92.8 ppm has no adjacent Al, no charge and no Cs^+ adsorption therefore no change in peak position before and after Cs exchange. It is possible that Cs is attracted to the Al-rich sites in vermiculite.

REFERENCES

* Unrestricted, unpublished report, available from SDD0, Atomic Energy of Canada Ltd. Company, Chalk River, Ont. K1J 1J0.

AECL. 1994. Environmental Impact Statement (EIS) on the concept for disposal of Canada's nuclear fuel waste. Atomic Energy of Canada Limited Report, AECL-10721*, 496p.

Bailey, S.W. 1980. Structure of layer silicates. In: (Brindley G.W. and Brown G eds),: Crystal Structures of Clay Minerals and their X-ray Identification. Mineralogical Society Monograph No. 5, Mineralogical Society, London, pp 1-124.

Becker, E.D. 1980. High Resolution NMR. 2nd edition. Academic Press, New York, 354p.

Brindley, G.W. 1980. Order-disorder in clay mineral structure. In: (Brindley G.W. and Brown G, eds.), Crystal Structures of Clay Minerals and their X-ray Identification, Mineralogical Society Monograph No. 5. Mineralogical Society, London, pp.125-195.

Brown, A., Soonawala, N.M., Everitt, R.A. and Kaminen,i D.C. 1989. Geology and geophysics of the Underground Research Laboratory Site, Lac du Bonnet Batholith, Manitoba. Canadian Journal of Earth Sciences, **26**: 404-425.

Brown, D.A. and Sherriff, B.L. 1999. Evaluation of the effect of microbial subsurface ecosystems on spent nuclear fuel repositories. Environmental Technology, **20**: 469-477.

Brown, D.A., Kamineni, D.C., Sawicki, J.A. and Beveridge, T.J. 1994. Mineral associated with biofilm occurring on exposed rock in a granite underground research laboratory. Applied and Environmental Microbiology, **60**: 3182-3191.

Brown, D.A., Gross, G.A. and Sawicki, J.A. 1995. A review of the microbial geochemistry and banded iron formation. Canadian Mineralogist, **33**: 1321-1333.

Brown, D.A., Beveridge, T.J., Keevil, C.W. and Sherriff, B.L. 1998. Evaluation of microscopic techniques to observe iron precipitation in a natural microbial biofilm. FEMS Microbiology Ecology, **26**: 297-310.

Comans, R.N.J., Haller, M. and De Preter, P. 1991. Sorption of cesium on Illite: Non-equilibrum behaviour and reversibility. Geochimica et Cosmochimica Acta., **55**: 433-440.

Davis, D.W., Corfu, F. and Krogh, T.E. 1986. High precision U-Pb geochronology and implications for the tectonic evolution of the Superior Province. In: (de Wit M.J. and Ashwal L.D. eds), Tectonic evolution of greenstone belts. Lunar and Planetary Science. Institute. Technical. Report, 80-81, pp 77-79.

Davis, J. A. and Kent, D. B. 1990. Surface complexation modeling in aqueous geochemistry. In: (M. F. Hochella Jr. and A. F. White.eds) Mineral-Water Interface geochemistry. Mineralogical Society of America Reviews in Mineralogy, **23**: pp177-260.

Davison, C.C., Brown, A., Everitt, R.E., Gascoyne, M., Kozak, E.T., Lodha, G.S., Martin, C.D., Soonawala, N.M., Stevenson, D.R. Thorne, G.A. and Whitaker, S.H. 1994a. The disposal of Canada's nuclear fuel waste: site screen and site evaluation technology. Atomic Energy of Canada Limited Report, AECL-10713, COG-93-3*, 255p.

Davison, C.C., Chan, T., Brown, A., Gascoyne, M., Kamineni, D.C., Lodha, G.S., Melnyk, T.W., Nakka, B.W., O'Connor, P.A., Ophori, D.U., Scheier, N.W., Soonawala, N.M., Stanchell, F.W., Stevenson, D.R., Thorne, G.A., Vandergraaf, T.T., Vilks, P. and Whitaker, S.H. 1994b. The disposal of Canada's nuclear fuel waste: The Geosphere Model of Postclosure Assessment. Atomic Energy of Canada Limited Report, AECL-10719, COG-93-9*. 497p.

Deer, W.A., Howie, R.A. and Zussman, J. 1998. An introduction to the Rock-Forming Minerals. 2nd Edition, Longman Scientific and Technical Press,.Hong Kong, pp 279-387.

de la Calle C. and Suquet H. 1988. Vermiculite. In: (Bailey S.W, ed.) Hydrous Phyllosilicates (Exclusive of Micas). Mineralogical Society of America Reviews in Mineralogy, **19**: 455-492.

Dixon, D.A. 1994. Na-Bentonite of Canada, United States and Mexico: Source, reserve and properties. In: (Crawford A., Radhakrishna H., Goulania M. and Lau K.,eds), Engineering materials for waste isolation. Canadian Society for Civil Engineering Special Publication, Toronto, pp. 37-65.

Dixon, D.A. 1995. Towards an understanding of water structure and water movement through dense clays. PhD. Thesis, University of Manitoba, pp. 12-40.

Ejeckam, R.B., Stone, D. and Kamineni, D.C. 1990. Surface and subsurface geology of Permit Area 'D' in Lac du Bonnet batholith, Manitoba. Atomic Energy of Canada Limited Technical Record, TR-490*, 167p.

Engelhardt, G. and Michel, D. 1987. High-resolution solid-state NMR of silicates and Zeolites. John Wiley and Sons. Toronto, 485p.

Everitt, R.A. and Brown, A. 1995. Geological mapping of AECL Research Underground Research Laboratory. A cross section of thrust faults and associated fractures in the roof zone of an Archean batholith. In: (Myer L.R., Cook N.G.W., Goodman R.E. and Tsang C-F.,eds), Proceedings of Fractured and Jointed Rock Masses, International Society for Rock Mechanics. Balkema, Lake Tahoe, California, USA, p. 3-12.

Everitt, R., Brown, A., Ejeckam, R.B., Sikorsky, R. and Woodcock, D. 1998. Litho-structural layering within the Archean Lac du Bonnet Batholith, at AECL's Underground Research Laboratory, southeastern Manitoba. Journal of Structural Geology, **20**: 1291-1304.

Faure, G. 1998. Principles and Applications of Geochemistry 2nd Ed. Prentice Hall, New Jersey, 625p.

Fyfe, C.A., Kennedy, G.J. and Strobl, H. 1986. Characterization of synthetic and naturally occurring clays by ^{27}Al and ^{29}Si magic-angle spinning NMR Spectroscopy. Journal of American Ceramic Society, **69**: c45-c47.

Gascoyne, M. 2000. Hydrogechemistry of the Whiteshell Research Area. Report prepared by Gascoyne Geoprojects Inc. for Ontario Power Generation. OPG, Nuclear Waste Management Division Report, 06819-REP-01200-10033-R00. Toronto, Ontario, 120p,

Gascoyne, M. 2001. Paleohydrogeological studies of the Whiteshell Research Areas using the isotopic composition of fracture minerals. Ontario Power Generation Technical Memorandum, 06819(UF)-03781-T10, Toronto, Ontario, 40p.

Gascoyne, M. and Cramer, J.J. 1987. History of actinide and minor element mobility in an Archean granitic batholith in Manitoba. Applied Geochemistry, **2**: 37-53.

Gascoyne, M. and. Kamineni, D.C. 1990. Groundwater chemistry and fracture mineralogy in the Whiteshell Research Area: Supporting data for the geosphere and biosphere transport models. Atomic Energy of Canada Limited Technical Record, TR-516*, 28p.

Gascoyne, M., Brown, A., Ejeckam, R.B. and Everitt, R.A. 1997. Dating fractures and fracture movement in the Lac du Bonnet batholith. Atomic Energy of Canada Limited Report, AECL-11725*, COG-96-634-1, 41p.

Griffault, L.Y., Gascoyne, M., Kamineni, D.C. and Vandergraaf, T.T. 1992. A study of the migration of radionuclides, major, trace and rare-earth elements along deep fractures in the Lac du Bonnet batholith, Manitoba. Atomic Energy of Canada Limited Technical Record, TR-545*, 60p.

Hammond, C. R. 1993. The Elements. In (Lide, D. R., ed) CRC Handbook of Chemistry and Physics 73rd Edition. CRC Press Ann Arbor, pp. 4-1 to 4-8.

Hartman, J.S., Vance, E.R., Power, W.P. and Hanna, J.V. 1998. A ^{133}Cs magic angle spinning nuclear magnetic resonance study of cesium environments in barium hollandites and SYNROC. Journal of Material Research, **13**: 22-27.

Johnson L.H., Tait J.C., Shoesmith D.W., Crosthwaite J.L. and Gray M.N. (1994) The disposal of Canada's nuclear fuel waste: Engineered barriers alteratives. Atomic Energy of Canada Limited Report, AECL-10718, COG-93-8., 418p.

Kamineni, D.C. 1992. The anatomy and evolution of thrust faults in Lac du Bonnet Batholith, MB, Canada. Unpublished Internal report, 30p. Available from Applied Geoscience Branch, AECL, Whiteshell Laboratories, Pinawa, MB. R0E 1L0.

Kamineni, D.C., Stone, D. and Peterman, Z.E. 1990. Early Proterozoic deformation in the Western Superior Province, Canadian Shield. Geological Society of America Bulletin, **102**: 1623-1634.

Kamineni, D.C., Ticknor, K.V. and Vandergraaf, T.T. 1986. Occurrence, composition and radionuclide sorption characteristics of illite from a fractured granite pluton, southern Manitoba, Canada. Clay Minerals, **21**: 909-924.

Kamineni, D.C., Vandergraaf, T.T. and Ticknor, K.V. 1983. Characteristics of radionuclide sorption on fractures-filling minerals in the Eye-Dashwa Pluton, Atikokan, Ontario. Canadian Mineralogist, **21**: 625-636.

Karger, B.L., Snyder, L.R. and Horvath, C. 1973. An Introduction to separation science. John Wiley and Sons New York, 608p.

Kemner, K.M., Hunter, C.B., Bertsch, P.M., Kirkland, J.P and Elam, W.T. 1997. Determination of site-specific binding environments of surface sorbed cesium on clay-minerals by Cs-EXAFS (English). Journal de Physique IV **7**: 777-779.

Kim, Y. and Kirkpatrick, R.J. 1998. NMR T1 relaxation study of ^{133}Cs, ^{23}Na adsorbed on Illite. American Mineralogist, **83**: 661-665.

Kim, Y., Cygan, R.T. and Kirkpatrick, R.J. 1996a. ^{133}Cs NMR and XPS investigation of cesium adsorbed on clay minerals and related phases. Geochimica et Cosmochimica Acta., **60**: 1041-1052.

Kim, Y., Kirkpatrick, R.J. and Cygan, R.T. 1996b. ^{133}Cs NMR study of cesium on the surface of kaolinite and illite. Geochimica et Cosmochimica Acta, **60**: 4059-4074.

Kim, Y., Kirkpatrick, R.J. and Cygan, R.T. 1995. ^{133}Cs NMR study of Cs reaction with clay mineral. In: (Jain V. and Palmer R., eds), Environmental Issues in Waste Management Technologies in the Ceramic and Nuclear Industries. Ceramic Transaction Series, **61**: 629-636. Journal of American Ceramic Society. Columbus, Ohio.

Kirkpartick, R.J. 1988. MAS NMR spectroscopy of minerals and glasses. In: (Frank. C. Hawthorne,ed.), Spectroscopic Methods in Mineralogy and Geology. Mineralogical Society of America, Reviews in Mineralogy, **18:** 341-395.

Kirkpatrick, R.J. and Phillips, B.J. 1993. ^{27}Al NMR spectroscopy of minerals and related materials. Applied Magnetic Resonance, **4**: 213-236.

Klein, C. and Hurlbut, Jr. C.S., 1985. Manual of Mineralogy; 20th edition. John Wiley and Sons, New York., pp. 240-249.

Kozak, E.T., Frost, L.H., Gascoyne, M., Ejeckam, R.B., Vandergraaf, T.T., Scheier, N.W., Ticknor, K.V. and Davison, C.C. 1997. SA7-Moderately Fractured Rock (MFR) Solute Transport Experiment 1997 Annual Report. Ontario Hydro Report, No: 06819-REP-01200-0035-R00, 24p.

Krogh, T.E., Davis, G.L., Ermanovics, I and Harris, N.B.W. 1976. U-Pb isotopic ages of zircon from the Berens block and English River gneiss belt. Proceedings of 1976 Geotraverse Conference, University of Toronto **12-1**, 46.

Last, W. M. 2001. Mineralogical Analysis of Lake Sediments in (W. M. Last and Smol, J. P ,eds.). Tracking Environmental Change Using Lake Sediments. **2**: 143-187. Physical and Geochemical Methods. Kluwer Academic Publishers, Dordrecht, The Netherlands.

Liang, J 1992. Lead exchange into zeolite and clay minerals. M. Sc. Thesis, Department of Geological Sciences, University of Manitoba, Winnipeg, 116p.

Lippmaa, E., Magi, M., Samoson, A., Tarmak, M and Engelhardt, G. 1981. Investigation of the structure of zeolites by solid-state high resolution ^{29}Si NMR spectroscopy. Journal of American Chemical Society, **103**: 4992-4996.

Maiti, T.C., Smith, M.R. and Laul, J.C. 1989. Colloid formation study of uranium, thorium, radium, lead, polonium, strontium, rubidium, and cesium in briny (high ionic strength) groundwater: Analog study for waste disposal. Nucl. Technology, **84**: 82-87.

McBride, M. B. 1994. Environmental Chemistry of Soils. Oxford University Press New York, pp. 63-120.

McMurry, J. and Ejeckam, R. B., 2002. Paleohydrogeological study of fracture mineralogy in the Whiteshell research area. Prepared by Atomic Energy of Canada Limited for Ontario Power Generation. Ontario Power Generation, Nuclear Waste Management Division Report 06819-REP-01200-10082-R00. Toronto, Ontario, 81p.

Motamedi M. (1999) The survival and activity of bacteria in compacted bentonite clay in conditions relevant to high level radioactive waste (HLW) repositories. PhD. Thesis Department of Cell and Molecular Biology Microbiology, Goteborg University Sweden, pp. 1-49.

Mortimer C.E. (1975) Chemistry: A conceptual Approach 3rd Ed. D. Van Nostrand Company, New York, 756p.

Oscarson, D.W., Watson, R.L. and Miller, H.G. 1987. The interaction of trace levels of cesium with montmorillonite and Illite clays. Applied Clay Science, **2**: 290-39.

Oscarson, D.W., Hume, H.B. and King, F. 1994. Sorption of cesium on compacted bentonite. Clays and Clay Minerals, **42**: 731-736.

Quigley, R.M. 1984. Quantitative mineralogy and preliminary pore-water chemistry of candidate buffer and backfill materials for nuclear fuel waste disposal vault. Atomic Energy of Canada Limited Report, AECL-7827*, 41p.

Rzepa H. 1996. NMR Spectroscopy Principles and Application. 6th second year lectures Department of Chemistry, Imperial College UK, by Henry Rzepa (http://www.ch.ic.ac.uk/local/organic/nmr.html).

Sanders J.K.M. and Hunter B.K. 1989. Modern NMR Spectroscopy: A Guide for Chemists. Oxford University Press, Toronto, 281p.

Sawhney, B.L. 1972. Selective sorption and fixation of cations by clay minerals: A Review. Clays and Clay Minerals, **20**: 93-100.

Silverstein, R.M., Bassler G.C. and Morrill T.C. 1991. Spectrometric identification of organic compounds, 5th Ed. Wiley and Sons. London, 419p.

Simmons, G.R. and Baumgartner, P. 1994. The disposal of Canada's nuclear fuel waste: Engineering for a disposal facility. Atomic Energy of Canada Limited Report, AECL-10715*, COG-93-5, 331p.

Sposito, G. 1984. The Surface Chemistry of Soils. Oxford University Press. New York, 234p.

Stone, D., Kamineni, D.C. and Brown, A., 1984. Geology and fracture characteristics of the Underground Research Laboratory lease near Lac du Bonnet Manitoba. Atomic Energy of Canada Limited Technical Record, TR-243*, 50p.

Stroes-Gascoyne, S., Haveman,S. A., Hamon, C.J. and Ticknor, K.V. 2000. Analysis of Biofilms Grown In Situ At Aecl's Underground Research Laboratory On Granite, Titanium And Copper Coupons, Atomic Energy of Canada Limited Report, AECL-12098*, 82p.

Stroes-Gascoyne, S. and Sargen,t F.P. 1998. The Canadian approach to microbial studies in nuclear waste management and disposal. Journal of Contaminant Hydrology, **35**: 175-190.

Stroes-Gascoyne, S. and West, J.M. 1997. Microbial studies in the Canadian nuclear fuel waste management program. FEMS Microbial Reviews, **20**: 573-590.

Stroes-Gascoyne S. and West J.M. 1996. An overview of microbial research related to high-level nuclear waste disposal with emphasis on the Canadian concept for disposal of nuclear fuel waste. Canadian Journal of Microbiology, **42**: 349-366.

Stroes-Gascoyne, S and West, J.M. 1994. Microbial issues pertaining to the Canadian concept for the disposal of nuclear fuel waste. Atomic Energy of Canada Limited Report, AECL-10808*, COG-93-54, 43p.

Stroes-Gascoyne, S., Tait, J.C., Garisto, N.C, Porth, R.J., Ross, J.P.M., Glowa, G.A and Barnsdale, T.R. 1992. Instant release of ^{14}C, 99Tc, ^{90}Sr and ^{137}Cs from used CANDU fuel at 25°C in distilled deionized water. Atomic Energy of Canada Limited Report, AECL-10526*, 8p

Sullivan, D.J., Shore, J.S. and Rice, J.A. 1998. Assessment of cation-binding to clay-minerals using solid-state NMR. Clays and Clay Minerals, **46**: 349-354.

Tait, J.C., Gauld, I.C. and Wilkin, G.B. 1989. Derivation of initial radionuclide inventories for the safety assessment of the disposal of used CANDU fuel. Atomic Energy of Canada Limited Report, AECL-9881*, 155p..

Tamura, T. and Jacobs, D.G. 1960. Structural implications in cesium sorption. Health Physics, Pergamon Press, **2**: 391-398.

Tarbuck, E.J. and Lutgens, F.K. 2000. Earth Science 9th edition. Prentice Hall, New Jersey, pp. 407-418.

Thompson, J.G. 1984. ^{29}Si and ^{27}Al nuclear magnetic resonance spectroscopy of 2:1 clay minerals. Clay Minerals, **19**: 229-236.

Ticknor, K.V., Kamineni, D.C. and Vandergraaf, T.T. 1991. Flow path mineralogy: Its effect on radionuclide retardation in the geosphere. Materials Research Society Proceedings, **212**: 661-668.

Ticknor, K.V., Kamineni, D.C. and Vandergraaf, T.T. 1989. Radionuclide sorption on primary and fracture-filling minerals from the East Bull Lake pluton, Massey, Ontario, Canada. Applied Geochemistry, **4**: 163-176.

Weiss, Jr. C.A., Kirkpatrick, R.J. and Altaner, S.P. 1990a. The structural environments of cations adsorbed onto clays: ^{133}Cs variable-temperature MAS NMR spectroscopic study of hectorite. Geochimica et Cosmochimica Acta., **54**: 1655-1669.

Weiss, Jr. C.A., Kirkpatrick, R.J. and Altaner, S.P. 1990b. Variations in interlayer cation sites of clay minerals as studied by ^{133}Cs MAS nuclear magnetic resonance spectroscopy. American. Mineralogist, **75**: 970-982.

Westritch H.R., Brady P.V., Cygan R.T., Gruenhagen S.E., Anderson H.L. and Nagy K.L. 1998. Characterization of retardation mechanism in soil. NUREG/CR-6603 SAND98-0419, 23p.

* Unrestricted, unpublished report, available from SDD0, Atomic Energy of Canada Ltd. Company, Chalk River, Ont. K1J 1J0.

APPENDIX A: SOLID STATE NMR PRINCIPLES

Nuclear Magnetic Resonance (NMR) is a useful tool to study or probe the molecular structure and dynamic behaviour of solids. It is used to examine the properties of specific elements; this ability sets it apart from other techniques such as diffraction method. NMR spectroscopy is also capable of examining the structures of amorphous or poorly crystalline material, gels or crystalline materials that are too fine grained to be examined by crystal diffraction methods.

Every element carries a charge in its nucleus, and when the spins of the proton and neutron that make up the nuclei are not paired, the overall spin of the charged nucleus generates a magnetic dipole along its spin axis (Rzepa 1996). The nuclear spin of a proton is associated with a magnetic moment that will interact with an applied magnetic field. Depending on the spin number of the proton, when placed in a magnetic field, it undergoes a precession about the field. The frequency of the precession is the observed frequency, called the Larmor precession frequency (ν) and is expressed as:

$$\nu = \gamma B_o/2\pi \text{ or } \omega = \gamma B_o \qquad \textbf{(A.1)}$$

where γ is the magnetogyric ratio, B_o is the magnitude of the applied static magnetic field,. ω is the resonant frequency in radians/seconds and γ is the resonant frequency in Hertz.

The magnetogyric ratio is a proportionality constant that is different for each nuclei. The Larmor precession frequency is directly proportional to the applied magnetic field and is dependent on γ. It also depends on the chemical environment of the nuclei. The intensity of the signal for a given nuclear isotope is proportional to the number of nuclei contributing to the signal.

The nuclei are classified according to their nuclear spin number. Some nuclei such as those with even mass numbers and even charge numbers (e.g. ^{12}C, ^{16}O, and ^{32}S) have nuclear spin number $I = 0$. These possess no angular momentum; however, many nuclei have spin number $I \neq 0$. Nuclides with odd mass numbers (e.g. ^{29}Si, ^{27}Al, ^{133}Cs) have half-integer spin numbers. Others, such as ^{2}H, and ^{14}N, with even mass numbers but odd charge numbers have integer spin numbers but are usually difficult to study in solids (Kirkpatrick 1988). Each nuclide has $2I + 1$ energy levels. If there is no magnetic field present, the energy levels have the same energy, but when a magnetic field is applied, there is interaction between the nuclides and the magnetic field. This interaction is called Zeeman interaction. This Zeeman interaction lifts the same energy levels to a value ΔE, that is proportional to the magnetic field at the nucleus. Figure AP-A1 shows the Zeeman interaction and first order quadruple interaction of two nuclei, one with a spin I=1/2 and the other with a spin of I=5/2.

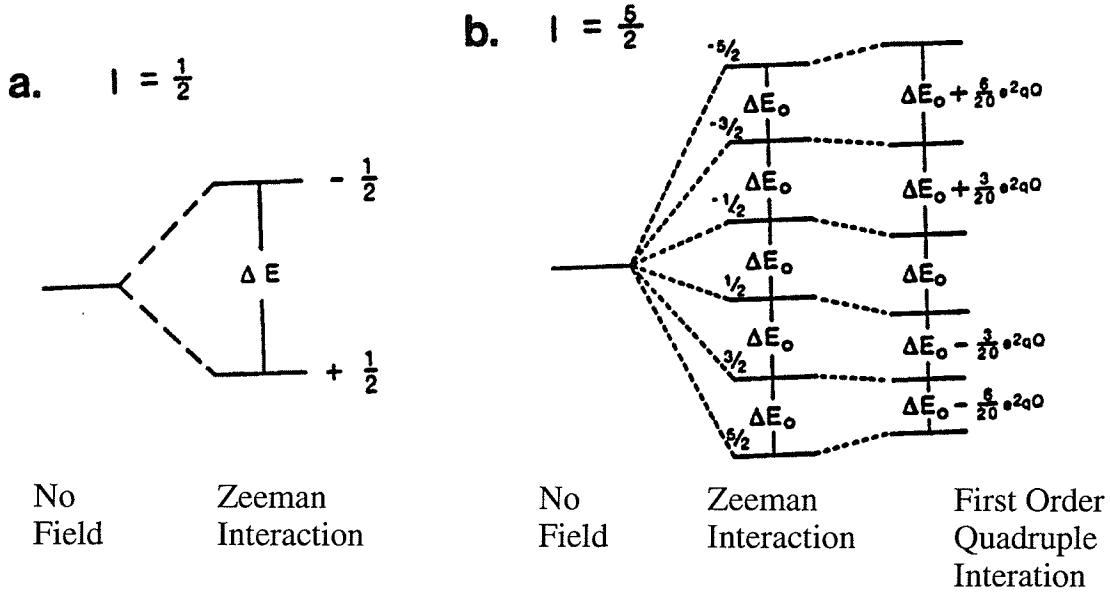

Figure AP-A1: Diagram showing nuclear spin energy levels for (a) a spin I = ½ nuclide, and (b) a spin I = 5/2 nuclide. The energy levels are split by Zeeman interaction and further split by first order quadrupole interactions (from Kirkpatrick 1988).

A nucleus can increase or decrease its energy by emitting or adsorbing a photon. The transition between energy levels are limited to adjacent energy levels; it is the frequency of the radiation during this transition that is measured in NMR experiments.

The nucleus of a sample does not directly experience the effect of the applied magnetic field because the screening or shielding of the cloud of electrons surrounding the nucleus alters this. Electrons are magnetic particles whose motion is affected by the presence of an external magnetic field. This motion is induced by the applied field in such a way that the direction is opposite that of the applied field. Therefore the magnetic field of the nucleus is expressed as:

$$H_{(nucleus)} = H_o - \sigma H_o = H_o(1-\sigma) \qquad \textbf{(A.2)}$$

where σ is the screening or shielding factor. The magnitude of the shielding depends on the orientation of the molecules relative to the applied field (Becker 1980, Kirkpatrick 1988). When the shielding factor **(σ)** is included in the Larmor equation, that relates the resonance frequency and the applied magnetic field (Ho) to give:

$$\nu_o = (\gamma/2\pi)H_o(1-\sigma) \qquad \textbf{(A.3)}$$

If the field is fixed at H_o while varying the frequency, the resonance frequency of the sample (ν_s) and reference (ν_R) are:

$$\nu_s = (\gamma/2\pi)H_o(1-\sigma_s) \quad \textbf{(A.4)}$$

and

$$\nu_R = (\gamma/2\pi)H_o(1-\sigma_R) \quad \textbf{(A.5)}$$

Chemical shift (δ) is reported in ppm and is referenced as a dimensionless scale by Becker (1980). It is given by:

$$\delta \equiv (\nu_s - \nu_R)/\nu_{R\,x}10^6 \quad \textbf{(A.6)}$$

where δ is the chemical shift, and ν_s, and ν_R are the resonant frequencies of the sample and the reference, respectively.

In the NMR experiments, a ν pulse excites the sample to generate a small magnetic field, and when the excitement is removed, the nucleus releases some absorbed energy and returns to its original ground state. This return to ground state is called relaxation. Quadrupolar nuclei such as ^{27}Al have a short relaxation time compared to nuclei with spin ½ such as ^{29}Si that have longer relaxation times. The radiation emitted during relaxation is detected and recorded as a function of time. This irradiation of sample is repeated many hundreds or thousands of times, and the recorded amplitude is added together, thereby enhancing the signal to noise ratio (signal/noise ratio is proportional to

the number of pulses) that provides an observable spectrum with reduced noise. Different nuclei have different sensitivities to the applied magnetic field and their detection vary due to their different natural abundance. NMR principles and application have been reviewed in details by several authors (Kirkpatrick 1988, Becker 1980, Silverstein et al. 1991, Sanders and Hunter 1989, and others).

APPENDIX B: RELATIVE HUMIDITY

Humidity is defined as the amount of water vapour in the air. In a closed environment, when the amount of water molecules evaporating from water surface equals the amount of water molecule returning to the water surface, the air is considered saturated. However, if the temperature in the environment is increased, more water vapour will evaporate. At warmer temperatures, therefore, the capacity of air to hold water vapour is increased compared to a cold environment. This means that the water vapour capacity of air during the warmer (summer) months of the year is greater than the water vapour capacity of air during the colder (winter) months of the year. Table AP-B1 from Tarbuck and Lutgens (2000) indicates the amount of water vapour required to saturate 1kg of air at various temperatures.

However, air is not always saturated, therefore, a method was devised to measure the amount of moisture in the air at any given temperature, which is expressed as relative humidity (RH). At any given temperature, relative humidity is defined as the ratio of the actual amount of water vapour content of the air to the potential amount of water vapour the air could hold (Tarbuck and Lutgens 2000). As the temperature changes, the amount of water vapor needed to saturate the air also changes.

Table AP-B1: Amounts of water vapour in grams required to saturate 1 kg of air at various temperatures (from Tarbuck and Lutgens 2000)

Temperature °C	Grams of water vapour/1kg of air
-40	0.1
-30	0.3
-20	0.75
-10	2
0	3.5
5	5
10	7
15	10
20	14
25	20
30	26.5
35	35
40	47

In some cases, at different temperatures, there can be less water in humid air than in dry air. Tarbuck and Lutgens (2000) compared a typical January day in Winnipeg, Manitoba to a typical day in Phoenix, Arizona. In Winnipeg, if the temperature is -10°C with a relative humidity of 100%, 2g of water vapour is all that is required to completely saturate 1kg of air (Table AP-B1). In contrast, in Phoenix, if the temperature is 25°C, 25g of water vapour is required to saturate 1kg of air. In both cases, the relative humidity at saturation would be 100%. However, if the air in Phoenix, Arizona has a relative humidity of 20%, then the water vapour content of the air is calculated to be 4g/kg of air. This shows that even with a lower relative humidity (20%), a warmer, dry air in Phoenix contains more water vapour/kg of air than air in Winnipeg that has a higher relative humidity (100%) and a humid air. In Winnipeg, at -20°C there is a maximum of 0.75g/kg of water vapour in the air and at 25°C, 20g/kg of water vapour is needed to saturate the air. Therefore, bringing -20°C of air inside the laboratory in the winter gives 3.8% relative humidity. At 25°C during the summer, there can be 20g of water vapour in the air. The increase in the amount of water in the air in the laboratory from winter to summer can be about 19.25g/kg. Therefore in summer, clay samples will not loose water to the atmosphere and may even adsorb water from the atmosphere and stay wet. However, in the winter, water in the clay will be sucked out of the clay minerals into the atmosphere leaving the clay dryer.

APPENDIX C: ANALYTICAL DATA

Table AP-C1: Cs concentration in different types of clay minerals. Apart from the first exchange rate experiment, all the other experiments were done at RTP unless indicated and adsorption time is 6 hours.

Mineral		Sample	Wt % of Cs		Avg Cs%	STD DEV
Montmorillonite at RTP first exchange rate xp.		STx-1-1m	5.83			
		STx-1-30m	6.32			
		STx-1-1h	6.40			
		Stx-1-2h	6.35			
		STx-1-3h	5.91		6.1	0.25
		STx-1-4h	5.99			
		STx-1-5h	5.90			
		STx-1-6h	6.10			
		STx-1-24h	4.60			
Montmorillonite at 80°C		STx-1-CsT(1)	6.58			
		STx-1-CsT(2)	6.54		6.6	0.03
		STx-1-CsT(3)	6.60			
Montmorillonite at 107°C & 1.5 bars		STx-1-CsTP(1)	6.20			
		STx-1-CsTP(2)	6.37		6.2	0.2
		STx-1-CsTP(3)	6.05			
Kunigel Bentonite at RTP		JP-KN-Cs(1)	6.31			
		JP-KN-Cs(2)	6.64		6.3	0.3
		JP-KN-Cs(3)	6.06			

Continued...

Mineral		Sample	Wt % of Cs		Avg Cs%	STD DEV
Wyoming Bentonite at RTP		WYOB-1-Cs(1)	4.91			
		WYOB-1-Cs(2)	4.79		4.9	0.1
		WYOB-1-Cs(3)	4.90			
Vermiculite (CMS) at RTP		VTx-1-Hp-cs	3.81		3.8	0
Vermiculite (WARD) at RTP		Ver-46-Ecs(1)	4.9			
		Ver-46-Ecs(2)	4.93		4.9	0.02
		Ver-46-Ecs(3)	4.87			
SealBond Illite at RTP		ILL-SB-ECs(1)	1.08			
		ILL-SB-ECs(2)	0.86		0.9	0.13
		ILL-SB-ECs(3)	0.86			
Kaolinite at RTP		Kga-1-1-Cs(1)	0.80		0.8	0.3
		Kga-1-1-Cs(2)	0.85			
		Kga-1-1-Cs(3)	0.81			

Table AP-C2: Bulk chemistry of clay minerals before (A) and after (B) ion exchange (n/d = not determined)

	Vermiculite (WARD)				Vermiculite (CMS)	
	1A	1B			2A	2B
	Ver 46-E	VER-46-Ecs(1)	VER-46-Ecs(2)	VER-46-Ecs(3)	VTx-1HP	VTx-1-HP-Cs
	wt%	wt%	wt%	wt%	wt%	wt%
SiO2	35.59	43.16	39.68	40.29	62.88	62.95
Al2O3	5.80	5.90	5.14	5.37	6.85	4.18
TiO2	0.89	0.90	0.88	0.91	0.25	0.25
Fe2O3	6.41	6.40	6.25	6.20	0.01	0.01
MnO	0.04	0.03	0.03	0.03	0.00	0.00
MgO	21.01	17.20	16.97	17.09	1.04	0.87
CaO	0.22	0.43	0.46	0.42	0.99	0.33
Na2O	0.36	0.01	0.01	0.01	1.55	1.24
K2O	5.43	5.20	5.15	5.22	0.10	0.06
P2O5	0.36	0.06	0.08	0.10	0.01	0.01
Cs	0.00	4.90	4.93	4.87	0.03	3.81
Total	76.11	84.19	79.58	80.51	73.70	73.70

Continued...

	Kaolinite				Montmorillonite			
	Before exchange (3A)	After exchange (B)			Before exchange (4A)	After Exchange (B)		
	KGa-1-1 wt%	KGa-1-cs(1) wt%	KGa-1-Cs(2) wt%	KGa-1-Cs(3) wt%	STx-1-1 wt%	STx-1-1-Cs(1) wt%	STx-1-1-Cs(2) wt%	STx-1-1-Cs(3) wt%
SiO2	38.24	35.77	36.55	35.87	51.38	49.68	50.71	51.69
Al2O3	42.61	42.49	43.00	43.45	15.75	15.64	15.03	15.83
TiO2	n/d	n/d	n/d	n/d	n/d	n/d	n/d	n/d
Fe2O3	0.04	0.07	0.09	0.05	0.53	0.52	0.41	0.53
MnO	n/d	n/d	n/d	n/d	n/d	n/d	n/d	n/d
MgO	0.02	0.01	0.01	0.00	2.46	2.04	1.99	2.00
CaO	0.02	0.00	0.00	0.01	1.49	0.13	0.11	0.18
Na2O	0.09	0.09	0.08	0.07	0.37	0.09	0.11	0.09
K2O	0.04	0.03	0.04	0.03	0.10	0.07	0.08	0.08
P2O5	n/a	n/a	n/a	n/a	n/a	n/a	n/a	n/a
Cs	0.00	0.80	0.85	0.81	0.00	6.10	6.10	6.10
Total	81.05	79.26	80.61	80.28	72.09	74.27	74.53	76.49

Continued...

	Wyoming Bentonite				Kunigel (Japanese Bentonite)			
	Before Exchange (5A)	After exchange (5B)			Before exchange (6A)	After Exchange (6B)		
	WYOB-1-1	WYOB-1-Cs(1)	WYOB-1-Cs(2)	WYOB-1-Cs(3)	JP-KN-1	JP-KN-Cs(1)	JP-KN-Cs(2)	JP-KN-Cs(3)
Cs	0.00	4.91	4.79	4.90	0.00	6.31	6.64	6.06
	Sealbond Illite							
	Before Exchange (7A)	After Exchange (7B)						
	ILL-SB-E	ILL-SB-ECs(1)	ILL-SB-ECs(2)	ILL-SB-ECs(3)				
Cs	0.00	1.08	0.86	0.86				

Ver 46-E	Vermiculite (WARD)
VTx-1-1-HP	Vermiculite (CMS)
KGa-1-1	Kaolinite (CMS)
STx-1-1	Montmorillonite CMS)
WYOB-1-1	Wyoming Bentonite (AECL)
JP-KN-1	Kunigel bentonite (Japanese bentonite)(AECL)
ILL-SB-E	Sealbond Illite (AECL)

Table AP-C3: Cs concentration in montmorillonite used in second exchange rate experiment done in triplicate at RTP (refer to Table 10, M1 is the same as M1-1-Cs)

Sample	Time (hours)	CLAY			SOLUTION		
		M0(1)	M0(2)	M0(3)	M0(1)	M0(2)	M0(3)
M1	0.02	4.06	4.42	4.59	0.01	0.02	0.02
M10	0.2	3.70	4.03	3.81	0.01	0.02	0.01
M20	0.3	3.63	4.11	4.11	0.01	0.02	0.02
M30	0.5	3.81	3.77	4.31	0.01	0.02	0.02
M40	0.7	4.04	4.31	3.82	0.01	0.02	0.01
M50	0.8	3.62	3.60	3.20	0.01	0.01	0.01
M60	1	4.17	4.19	3.61	0.01	0	0.02
M2h	2	5.83	6.41	6.40	0.06	0.05	0.08
M3h	3	6.50	6.39	5.52	0.04	0.05	0.05
M4h	4	5.78	5.46	5.64	0.03	0.05	0.05
M5h	5	6.54	6.34	5.84	0.05	0.07	0.05
M6h	6	6.29	6.88	5.86	0.1	0.08	0.05
M1d	24	5.56	6.02	5.48	0.05	0.04	0.05
M2d	48	6.10	5.88	6.79	0.05	0.05	0.05
M3d	72	5.98	6.29	6.31	0.05	0.05	0.05
M4d	96	6.22	5.32	6.52	0.05	0.05	0.05
M5d	120	5.83	5.92	5.95	0.05	0.05	0.05
M6d	144	6.04	5.62	5.62	0.05	0.04	0.05
M7d	168	6.04	6.45	6.46	0.05	0.05	0.07

Table AP-C4: Cesium concentration in montmorillonite and kaolinite after ion exchange in bacterial culture. All experiments were conducted at RTP. Adsorption time is 6 hours (refer to Table 11).

	Sample	Cs in wt%	Average	Std. Dev.
Montmorillonite	Cy + Cs + B (1)	7.96		
	Cy + Cs + B (2)	7.09	7.5	0.4
	Cy + Cs + B (3)	7.45		
	Cy + Cs + Bst (1)	6.66		
	Cy + Cs + Bst (2)	7.14	7.0	0.3
	Cy + Cs + Bst (3)	7.18		
	Cy + Cs (1)	6.81		
	Cy + Cs (2)	7.21	6.9	0.2
	Cy + Cs (3)	6.77		
	montst + B + Cs (1)	7.55		
	montst + B + Cs (2)	6.02	6.8	0.8
	montst + B + Cs (3)	6.87		
Kaolinite	Cy + Cs + B (1)	0.46		
	Cy + Cs + B (2)	0.44	0.4	0.1
	Cy + Cs + B (3)	0.34		
	Cy + Cs + Bst (1)	0.29		
	Cy + Cs + Bst (2)	0.36	0.3	0.1
	Cy + Cs + Bst (3)	0.28		
	Cy + Cs (1)	0.35		
	Cy + Cs (2)	0.44	0.4	0.04
	Cy + Cs (3)	0.4		
	kaolst + B + Cs (1)	0.4		
	kaolst + B + Cs (2)	0.44	0.4	0.05
	kaolst + B + Cs (3)	0.42		
Bacterial Culture + 0.1M CsCl solution				
	Pellets (1)	0.06		
	Pellets (2)	0.07		
	Pellets (3)	0.06	0.07	0.01
	Supernatant (1)	0.66		
	Supernatant (2)	0.64	0.64	0.03
	Supernatant (3)	0.61		

Cy = Clay mineral
Bst = Sterilized bacterial culture
montst = montmorillonite clay sterilized
B = Bacterial culture
Cs= 0.1M Cesium Chloride solution;
kaolst = kaolinite clay, sterilized

Table AP-C5A: Calculated values based on the weights of areas under peaks 1 and 2 in M2 and M3 series of the second exchange rate experiments

M2 SERIES

Sample	Weight of Peak1 area (g) M2	Weight of Peak2 area (g) M2	Cs Adsorbed by mont wt% M2	Total No. of moles	Amt of Cs Adsorbed in PK1	Amt of Cs Adsorbed in PK2	Amt of Cs No. of moles in peak 1	Amt of Cs No. of moles in peak 2
M1	0.1066	0.0482	4.42	0.033	3.04	1.38	0.02	0.01
M10	0.3568	0.1968	4.03	0.03	2.6	1.43	0.02	0.01
M20	0.3449	0.1969	4.11	0.031	2.62	1.49	0.02	0.01
M30		-	3.77	0.028				
M40	0.3684	0.1294	4.31	0.032	3.19	1.12	0.02	0.01
M50	0.2651	0.1056	3.60	0.027	2.57	1.03	0.02	0.01
M60	-	-	4.19	0.032	-	-	-	-
M2h	-	-	6.41	0.048	-	-	-	-
M3h	0.1839	0.0332	6.39	0.048	5.41	0.98	0.04	0.01
M4h	0.1402	0.0168	5.46	0.041	4.88	0.58	0.04	0.00
M5h	-	-	6.34	0.048	5.52	0.82	0.04	0.01
M6h	0.2851	0.092	6.88	0.052	5.21	1.68	0.04	0.01
Md1	0.1434	0.0491	6.02	0.045	4.48	1.53	0.03	0.01
Md2	-	-	5.88	0.044	5.08	0.79	0.04	0.01
Md3			6.29	0.047	-	-	-	-
Md4	-	-	5.32	0.04	-	-	-	-
Md5	-	-	5.92	0.045	-	-	-	-
Md6	-	-	5.62	0.042	-	-	-	-
Md7	0.2706	0.1991	6.45	0.048	3.71	2.73	0.03	0.02

Table AP-C5B: Calculated values based on the weights of areas under peaks 1 and 2 in M2 and M3 series of the second exchange rate experiments

M3 SERIES

Sample	Weight of Peak1 area (g) M3	Weight of Peak2 area (g) M3	Cs Adsorbed by mont wt% M3	Total No. Of moles	Amt of Cs Adsorbed in PK1	Amt of Cs Adsorbed inPK2	Amt of Cs, No. of moles in peak 1	Amt of Cs No. of moles in peak 2
M1	0.1316	0.0422	4.59	0.03	3.47	1.11	0.03	0.01
M10	0.2604	0.1418	3.81	0.03	2.47	1.34	0.02	0.01
M20	0.1529	0.0883	4.11	0.03	2.60	1.50	0.02	0.01
M30	-	-	4.31	0.03	-	-	-	-
M40	-	-	3.82	0.03				
M50	0.3766	0.1697	3.20	0.02	2.21	0.99	0.02	0.01
M60	-	-	3.61	0.03	-	-	-	-
M2h	0.3461	0.0641	6.40	0.05	5.40	1.00	0.04	0.01
M3h	0.236	0.0351	5.52	0.04	4.81	0.71	0.04	0.01
M4h	0.1658	0.0348	5.64	0.04	4.66	0.98	0.04	0.01
M5h	-	-	5.84	0.04	-	-	-	-
M6h	0.339	0.0542	5.86	0.04	5.06	0.81	0.04	0.01
Md1	0.1827	0.039	5.48	0.04	4.51	0.96	0.03	0.01
Md2	-	-	6.79	0.05	-	-	-	-
Md3	0.3426	0.0555	6.31	0.05	5.43	0.88	0.04	0.01
Md4	0.309	0.0471	6.52	0.05	5.66	0.86	0.04	0.01
Md5	-	-	5.95	0.04	-	-	-	-
Md6	0.2643	0.055	5.62	0.04	4.65	0.97	0.03	0.01
Md7	0.3136	0.0623	6.46	0.05	5.39	1.07	0.04	0.01

Table AP-C5C: Calculated average values based on the weights of areas under peaks 1 and 2 in M2 and M3 series of the second exchange rate experiments

AVERAGE OF M2 AND M3

Sample	M2 & M3 in PK1	M2 & M3 in PK2	Cs Adsorbed M2 & M2	No. of moles	Amt of Cs wt% in Peak 1	Amt of Cs wt% in Peak 2	# of moles of Cs in peak 1	Amt of Cs No. of moles in peak 2
M1	0.12	0.05	4.50	0.034	3.26	1.24	0.02	0.01
M10	0.31	0.17	3.92	0.029	2.53	1.39	0.02	0.01
M20	0.25	0.14	4.11	0.031	2.61	1.50	0.02	0.01
M30	-	-	4.04	0.030	-	-	-	-
M40	0.37	0.13	4.07	0.031	3.01	1.06	0.02	0.01
M50	0.32	0.14	3.40	0.026	2.38	1.02	0.02	0.01
M60	-	-	3.90	0.029	-	-	-	-
M2h	0.35	0.06	6.40	0.048	5.40	1.00	0.04	0.01
M3h	0.21	0.03	5.96	0.045	5.12	0.83	0.04	0.01
M4h	0.15	0.03	5.55	0.042	4.75	0.80	0.04	0.01
M5h	-	-	6.09	0.046	-	-	-	-
M6h	0.31	0.07	6.37	0.048	5.16	1.21	0.04	0.01
Md1	0.16	0.04	5.75	0.043	4.53	1.22	0.03	0.01
Md2	-	-	6.33	0.048	-	-	-	-
Md3	0.34	0.06	6.30	0.047	5.42	0.88	0.04	0.01
Md4	0.31	0.05	5.92	0.045	5.14	0.78	0.04	0.01
Md5	-	-	5.93	0.045	-	-	-	-
Md6	0.26	0.06	5.62	0.042	4.65	0.97	0.04	0.01
Md7	0.29	0.13	6.45	0.049	4.46	1.99	0.03	0.01